Chapter 1

Introduction

Chapter 1

1.1 The Hydrogen Bond

Intermolecular interactions play a vital role in our life. In 1923, H. E. Armstrong talked about the structure of water.[1] Since 1930's, various descriptions of interactions between the hydrogen atom and the electronegative atoms to which hydrogen were not bonded covalently started appearing in the literature. This topic attracted attention of researchers after 1939 when Linus Pauling in his book entitled "The nature of chemical bond" included a chapter about hydrogen bonding.[2] Since 1939, to date, numerous research groups are constantly publishing their work on various types of hydrogen bonding. The role of intermolecular and intramolecular hydrogen bond is so diverse that this field has attracted a large number of research groups across the oceans in their exploration and utilization for various types of applications.

Pauling, in his book, explained the hydrogen bonds to be "*Under certain conditions an atom of hydrogen is attracted by rather strong forces to two atoms instead of only one, so that it may be considered to be acting as a bond between them.*" This definition was given for an interaction of kind X–H···A, and Pauling assumed that only if X and A are highly electronegative, then H will be deshielded and the electrostatic interaction between

H and A be sufficiently high to be termed as a hydrogen bond. Thus, the hydrogen bonding was restricted to only the highly electronegative atoms like F, O, Cl, N, Br and I. This definition was later modified in 1960 by Pimentel and McClellan, who re-defined the hydrogen bonds as "*A hydrogen bond is said to exist when (a) there is evidence of a bond, and (b) there is evidence that this bond sterically involves a hydrogen atom already bonded to another atom X.*"[3] This definition did not mention the nature of X and A and therefore enables the hydrogen bonding potential for P–H, As–H and C–H etc. But as the single electron of hydrogen is already involved in a covalent bond X–H, so H is always deshielded in the forward direction irrespective to the nature of A. So does that mean the X–H group to be always a potential hydrogen bond donor? This question resulted in further modification in the definition of hydrogen bonds. Later, in 1993, Steiner and Saenger proposed the definition for hydrogen bonds as "*Any cohesive interaction for X–H···A, where H carries a positive charge and A a negative charge (partial or full) and the charge on H is more positive than on X*".[4] But this definition does not enclose different type of hydrogen bonds and was further modified by a committee appointed by IUPAC. This committee has stated that hydrogen bond is "*an attractive interaction between a hydrogen atom from a molecule or a molecular fragment X-H in which X is more electronegative than H, and an atom or group of atoms in the same or a different molecule, in which there is an evidence of bond formation."*[5] This definition is very broad and encloses all the different kinds of hydrogen bonds within its limit.

The hydrogen bonds can be intermolecular (between two molecules) and intra molecular (within the same molecule). The intermolecular interactions present between the molecules are responsible for their physical and chemical properties. Intermolecular hydrogen bonds can be divided into strong (40-15 kcal/mol)(eg. N–H···N, N–H···O, O–H···O, O–H···N, N–H···F, O–H···F, O–H···N, $[F–H···F]^-$, $[OH_3···OH_2]^+$,

$[NH_4\cdots NH_3]^+$ etc.), moderate (15-4 kcal/mol) (like C–H···N, Cl–H···OH_2, $H_2O\cdots OH_2$, C–H···O, S–H···N, S–H···N etc.) and weak (<4 kcal/mol) (like Cl–H···SeH_2, H–C≡C–H···C≡C–H, $CH_4\cdots SH_2$, $CH_4\cdots FCH_3$ etc.) hydrogen bonds on the basis of their strength of interaction energy.[6] The strong hydrogen bonds have been studied extensively and their characteristics and implications have been illustrated in the literature. There are various examples in the literature that shows the importance of strong hydrogen bonds, like HF exist as liquid at ambient temperature and pressure whereas other halogen acid like HCl, HBr and HI exist as gas. This is because of very strong hydrogen bonding in HF (···H–F···H–F···). Similarly, H_2O is liquid because of strong O–H···O hydrogen bonds present between the water molecules and the same hydrogen bonds is so weak in H_2S, H_2Se and H_2Te etc that they exist as gases under the ambient conditions. The strength of intermolecular hydrogen bonding plays a significant role in the melting and boiling points of various compounds. Strong hydrogen bond in ammonia makes it higher boiling compound compared to PH_3.

The moderate and weak hydrogen bonds also play crucial roles in packing and physical properties of crystalline molecular compounds. These electrostatic forces are directional to some extent and the directionality of these bonds can be altered by the presence of some other interactions in the crystal lattice. Owing to this flexibility, a lot of studies are being carried out to understand the nature and explore the utilization of these hydrogen bonds in the field of crystal engineering. Among these weak interactions, a few interactions like C–H···N and C–H···O are studied extensively in the literature and are reported in great detail.[7-9]

1.2 **Fluorine mediated Hydrogen Bond**

In addition to the weak hydrogen bonds offered by O and N, the intermolecular interactions involving Fluorine has also been in the centre of attraction for a long time.

Among N, O and F, fluorine being the highest electronegative element is supposed to offer the strongest hydrogen bonds when bonded to any other element. But it has been observed that when F is bound to a carbon atom then it becomes a poor hydrogen bond acceptor. In the early 1980s and 1990s, the role of C–F as hydrogen bond acceptor was refuted by many authors. Dunitz termed C–F as "organic fluorine" and ignored this group as an acceptor for hydrogen bond.[10] The organic fluorine has later emerged as one among the weak acceptor for hydrogen bonds[11] and its acceptor capabilities have been debated over the years.[12-31] Fluorine being the most electronegative atom in the periodic table should be the strongest hydrogen bond acceptor as per the hydrogen bond definition. But when fluorine is bonded to carbon, it acts as a very weak proton acceptor. Such behaviour of fluorine was pointed out by Dunitz *et al.* in their study.[15] Many studies have been conducted to understand the impact and influence of the organic-fluorine mediated interactions in crystal engineering. The intermolecular interactions involving fluorine has been in the forefront of structural studies since 1990s. Rust *et al.* observed in 1983, that the C–F group is capable of significant interactions with alkali metal cations and proton donors, but these interactions are generally weaker compared to the one involving C–N and C–O groups.[32] Shimoni and Glusker in 1994 through their CSD analysis based on a handful number of crystal structures of fluorinated molecules inferred that X–H···F–C interactions are very weak and hence insignificant, compared to the X–H···O=C interactions.[33] Dunitz and Taylor in 1997 also intended to ignore these interactions in crystal packing based on their combined CSD and *ab-initio* studies and claimed that "Organic Fluorine Hardly Ever Accepts Hydrogen Bonds".[34] In 1998, for the first time, C–H···F–C hydrogen bond received due recognition in crystal packing through the report by Thalladi *et al*., based on their systematic structural study on fluorobenzenes.[11] They had recognized that the C–H···F–C interactions can be as important as the C–H···O–C or

C–H···N–C hydrogen bonds for structure directing abilities to pack molecules in a particular array in its crystal structure. Their study on halogenated benzenes had opened up a new horizon in the area of intermolecular interactions involving "organic fluorine". In their report, they for the first time demonstrated the use of *in*-situ cryo-crystallization as a method of structure determination of compounds which were liquid at room temperature. This new technique was also used by many research groups for structural studies of various small organic compounds and mixture of compounds.[35] Motivated by this report of Thalladi *et al.*, several systematic studies were conducted on different types of fluorinated model systems like indole derivatives,[36] isoquinolines derivatives,[37-40] halogenated benzamides,[41-43] and also with trifluoromethyl group as a substituent,[44,45] aromatic azo compounds,[46] *N*-benzylideneanilines[47-50] and many more to elucidate the importance of fluorine mediated interactions in crystal packing.[51] A few research activities in this area were purely based on computations[48,49]and database analysis[46] as well. Through all these studies, it was indicated that C–H···F–C interactions should be considered as weak hydrogen bonds and these can be utilized for building a supramolecular architecture.

The organic fluorine mediated intermolecular interactions have attracted considerable attention. Fluorine has been defined as odd man out,[52] the little atom that could,[53] atom with many faces,[54] and the chameleon of non-covalent interactions.[55] The nature of organic fluorine mediated interactions has been debated. Some groups suggest its little influence on molecular packing, others postulates its significant role in small-molecule crystal structure and some authors comment on its subtle role in protein-ligand binding.[56]

If H is replaced by F in a molecule, it is considered to be isosteric, through which the electronic and the conformational changes in the molecule can be brought with minor

changes in the steric effect.[57] But, in one of the review articles, Smart[58] has denied the generalized statement about the similarity of size of H and F in terms of steric effects. Smart plotted the energies of non-bonding interactions *versus* the distance between two hydrogen atoms, two fluorine atoms and a hydrogen and a fluorine atom. From this study it was observed that at an interatomic separation of 2.0 Å, the steric repulsion energy for two hydrogens is 0.1 kcal/mol whereas for two fluorine atoms it is 6.2 kcal/mol. This indicates a "*significant fluorine steric effect*". The organic fluorine mediated interactions are not only useful in context of crystal engineering but also in the systematic design of functional materials. Because of the strength of the C-F bond, fluorine containing compounds, compared to hydrocarbons, exhibit high thermal and oxidative stability, small surface tension, weak intermolecular interactions and low polarity.[59] The C–F···H hydrogen bond is classified into two categories as per Desiraju,[60] the C–F···H–X hydrogen bond with a strong donor (X= N, O), and a weak donor (X = C). Hydrogen bond is a complex conglomerate of at least four component interaction type i.e electrostatic (Acid/base), polarization (hard/soft), van der Waals (dispersion/repulsion) and covalency (charge transfer). Organic fluorine accepts a hydrogen bond with great difficulty despite the electro-negativity of fluorine because of its hardness (lack of polarizability). C–F···H–C hydrogen bond is a soft donor-hard acceptor kind of hydrogen bond.[60] D'Oria and Novoa exhaustively investigated the nature of C–H···F interactions in molecular crystals taking two cases, one where both the interacting fragments are neutral and the other when at least one of the interacting fragment is charged.[61] Selecting the complexes from CSD with short C–H···F interactions, the investigation was conducted on their strength, directionality, property of H···F bond critical points and energetic components of the interaction energy. From these observations, it was found that C–H···F interactions behave as weak hydrogen bonds when both the fragments are neutral and

have an interaction energy around -0.4 kcal/mol. These are dominated by electrostatic and dispersion components where dispersion component is stronger than the former. Whereas, when at least one of the fragments of charged, the interaction energy is calculated to be between -164 and 50 kcal/mol. The electrostatic energetic component is the strongest one. For both charged and neutral systems, the angular dependence is similar with maximum around 120° for C–H···F angles. The strength-length correlation fails in the charged fragments as the shortest interactions are not the strongest ones.

1.3 Halogen···Halogen interaction

While demonstrating the role of C–H···X–C (X = F, Cl, Br and I) hydrogen bonds in crystal packing, short C–X···X–C (X = F, Cl, Br and I) interactions were also encountered. Researchers were dragged in the in-depth analysis of these interaction where two highly electronegative elements were found to come close in crystal packing of small organic molecules. The importance of C–X···X–C (X = Cl, Br, I) were soon recognized and such interactions were classified as Type I and Type II interactions (Figure 1.3.1). The halogen···halogen interactions of the type C–X_1···X_2–C, was divided into three types based on the two angles θ_1 and θ_2, where θ_1 = ∠C–X_1···X_2 and θ_2 = ∠X_1···X_2–C by Ramasubbu *et al.*[62]

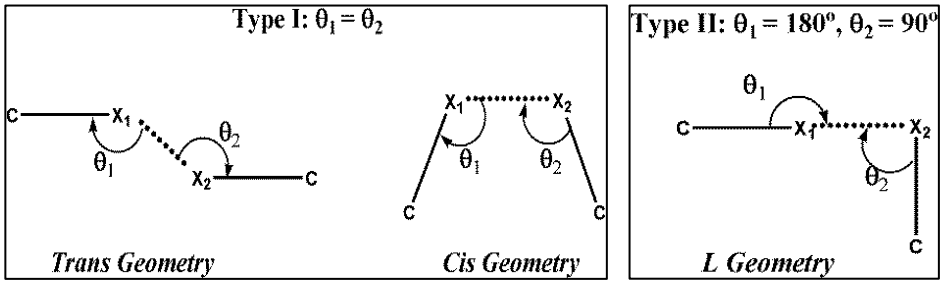

Figure 1.3.1 Types of halogen···halogen interactions based on the classification done by Ramasubbu *et al.*

- *Type I* inter halogen interactions, $\theta_1 = \theta_2$ and the two halogen atoms are related by crystallographic center of inversion,
- *Type II* inter halogen interactions, θ_1 or $\theta_2 = 90°$, and
- *Type II* inter halogen interactions, θ_1 or $\theta_2 = 180°$.

Subsequently, the interactions of the type C–X···Y–C (X = Cl, Br, I, Y = Cl, Br, I but X ≠ Y) were also investigated in depth. The statistical survey by Desiraju and Partasarathy have claimed that X···X interactions are attractive in nature except the F···F interactions.[63,64] Generally these contacts were stated to be the consequence of close packing, and hence they were ignored while considering their contribution to the crystal packing.[65-68] Choudhury *et al*. has emphasized the importance of F···F contacts in the structural analysis of a series of fluorine substituted Isoquinolines.[37-40] Prasanna and Guru Row has established the impact of C–F···π interactions in determining the molecular conformation and its role in the crystal packing through their CSD analysis in 2000.[69] In the past decade, various research groups across the globe have contributed in the development of the area related to fluorine mediated interactions in the solid state. A recent highlight by Chopra and Guru Row[70] and a perspective by Chopra[71] have summarized the developments in this area. Shukla and Chopra reported the structural variations due to fluorine mediated interactions in terms of the hybridization of the C atoms associated with C–H···F–C hydrogen bonds using CSD and a combination of computational methods.[72] Based on their result they concluded that C–H···F–C interactions should be considered as hydrogen bonds based on Koch and Popelier[73] criteria for hydrogen bonds. Kaur and Choudhury demonstrated that when a non-interactive fluorine is replace by Cl or Br to make a new molecule the crystal structure

remains unchanged while the replacement of an interactive fluorine by Cl or Br completely changes the crystal packing.[47-50]

Recently, Thotadi *et al*., proposed homohalogen (X···X) contacts to be of three types based on their CSD analysis on such contacts.[74] Their new classification criterion is based on the difference between angles θ_1 and θ_2.

- $0° \leq |\theta_1 - \theta_2| \leq 15°$ -contacts will be classified as *type I*,
- $30° \leq |\theta_1 - \theta_2|$ -contacts will be classified as *type II*,
- $15° \leq |\theta_1 - \theta_2| \leq 30°$-contacts will be classified as *quasi type I/type II* interactions.

Based on this recent classification, the interactions between homohalogen involving fluorine is studied.

In a tutorial review, O'Hagen explored the rationale for the geometry conformation and reactivity of fluorinated organic compounds and explained the fundamental aspects related to the C–F bond.[75] The high electronegativity of fluorine leads to the polarization of the C–F bond thereby making it more electrostatic and less covalent in nature. In fluorinated organic compounds, this offers relatively large dipole-dipole interaction and hence these can be interprets as electrostatic interactions. As the three lone pairs of electrons on fluorine are tightly held because of high electronegativity of F, unexpectedly the polarised C–F bond does not have good donor ability. The lone pairs of F are reluctant to participate in resonance unlike O and N, and act as hydrogen bond acceptor. O'Hagen also pointed out in 2008 that the X–H···F–C (X = O, N) hydrogen bonds are less frequent and are about 75% weaker in strength compared to the corresponding X–H···X–C (X = O, N) hydrogen bonds. Schlosser, in his article,[76] commented about the unusual nature of fluorine when introduced in a compound as:

"*Fluorine leaves nobody indifferent; it inflames emotions be that affections or aversions. As a substituent, it is rarely boring, always good for a surprise, but often completely unpredictable*."

1.4 Methods of studying hydrogen bonds

Various experimental and computational methods have been used to study and understand the nature, strength, and directionality of moderate and weak hydrogen bonds.

1.4.1 Crystal Structure Analysis

X-ray diffraction analysis and the neutron diffraction analysis are widely used for studying the crystal structure and intermolecular phenomenon in crystalline system. The moderate and weak hydrogen bonding interactions cannot be studied by spectroscopic methods. X-ray diffraction has therefore become very important to the researchers in exploring the weak hydrogen bonds as by using this method, with the advent of advanced X-ray sources and detectors and sophisticated software for accurate data reduction, structure solution, and refinement, one can totally understand the forces involved in the packing of molecules in the observed crystalline lattice. Structural data enables us to analyse the intermolecular as well as intra-molecular interactions in crystalline compounds.

1.4.2 Crystallographic Databases

The large amount of crystal structure data generated all over the world is systematically archived in various databases so that researchers can study and utilize the information that are already reported. Crystal structure database offers a reliable source to study the moderate and the weak intermolecular interactions in small organic molecules

and in macromolecules as well. A few routinely utilized crystal structure databases include Cambridge Structural Database (CSD),[77] the Protein Data Bank (PDB),[78] the Nucleic Acid Data Bank (NDB),[79] Biological Macromolecule Crystallization Database (BMCD),[80] Crystallogrpahic Open Database (COD),[81] The Pauling File,[82] Powder Diffraction File for International Centre for diffracted data (ICDD)[83] and Inorganic Crystal Structure Database (ICSD).[84]

Cambridge Structural Database (CSD) is the database of all kinds of small organic compounds, organic salts, and organometallic complexes maintained by Cambridge Crystallographic Data Centre (CCDC). CSD enables us to explore whether the crystal structure of any compound is already reported or not. Conquest[85] is a software package, which is linked to this database is used to search and visualize the crystal structures of desired molecules, salts and complexes. Various functionalities of Conquest are widely used to study the geometric parameters of various intermolecular interactions observed among the structures deposited in the database. A careful analysis of CSD on any particular type of intermolecular interactions offers wonderful insights about the concerned interaction. The regular patterns observed in these interactions are important in determining the basis of a stable crystal packing, which are called supramolecular synthons.[86]

As we are interested in the analysis of weak interactions involving a C–F, our targeted search of CSD indicated the existence of various supramolecular synthons involving weak C–H···F–C hydrogen bonds as shown in the Figure 1.4.1.

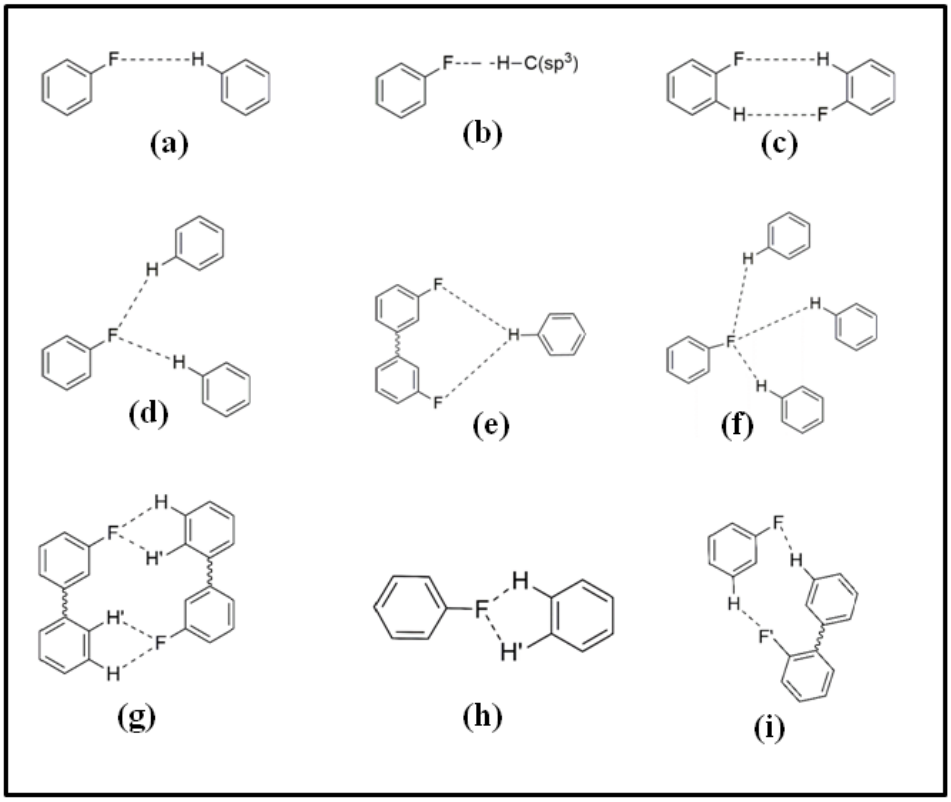

Figure 1.4.1: Commonly observed synthons

1.4.3 Computational Methods

Quantum chemical computation is a complimentary tool in spectroscopy and crystallography related research for the moderate and weak intermolecular interactions. Computational quantum chemistry provides tools for intermolecular energy calculations without complicating the effects of solid state or the solution environment.[87] With the easy accessibility of computers with advanced capabilities, it has become affordable to utilise the knowledge of theoretical chemistry in calculating various molecular and supramolecular properties using various computational packages like Gaussian09, Amber, Crystal14 etc. The amalgamation of the inputs from the database analysis with computational methods have resulted in a large number of significant research publications.[88] About more than a decade ago, semi-empirical methods were used to study the intermolecular interactions but these are no longer used as they could not account to many intermolecular factors. Currently *ab initio* methods are used instead of semi-

empirical methods. The former gives reliable interaction energies to various degrees of approximations in most of the cases. The computational methods enable us to calculate the interaction energies and understand the contribution of various hydrogen bonds and other interactions in the system under study.

1.5 *Ab initio* methods

Ab initio is a Latin term that means "from the beginning". Without taking the experimental data into account, it computes directly from the theoretical principals. This quantum chemical method is used as a computational chemistry tool for gas phase calculations. It is based on the most fundamental equation of physics and chemistry, the Schrödinger equation.[89] The Schrödinger equation is solved using the *ab initio* method for a molecule and gives the energy and wave function of the molecule. Due to the presence of electron-electron interaction terms, the Schrödinger equation cannot be solved exactly and a variety of approximations are adapted with reasonable basis sets to obtain an approximate solution. The approximations that are adapted are mathematical, such as using simpler functions to escape negative value for a positive quantity or ending a calculation to an approximate solution of a differential equation.[90] The more the approximations are adapted for a solution, the more is the deviation of result from the actual value. *Ab initio* methods are mainly used to calculate the molecular geometries, energies, vibrational frequencies, ionization potential, spectra and properties like dipole moment which are connected with electron distribution. The methods that are extensively used to solve the Schrödinger equation are Hartree-Fock method and post Hartree-Fock methods like the density functional theory (DFT), Møller-Plesset **(**MP2) method etc.

1.5.1 Hartree Fock Method

The Hartree-Fock (HF) method is the most common type of *ab initio* approximation method used to solve the Schrödinger equation with the main approximation taken into account being the central field approximation.[91] It is also known as self-consistent field method (SCF). Many-electron Schrödinger equation is broken into many one-electron equation in this method. Each one-electron equation is solved to get a single-electron wave function which is known as the orbital and the energy associated is called the orbital energy. In the central field approximation method, the electron-electron repulsion between each pair of electrons in the molecule is approximated to an average field of all the electron on a single electron. So, this gives the average effect of repulsion and not the explicit repulsion interaction. This is a variational calculation and therefore, the energies of the HF calculations are all greater than the exact energy and it tends to reach the Hartree-Fock limit with improvement in the basis set. There is another approximation in the HF calculation which is that the wave functions must be described by some mathematical functions, which is known exactly for only a few one-electron systems. The mathematical functions that are used are linear combinations of GTO or Gaussian-type orbitals. This helps in breaking the Schrödinger equation in many one-electron equations. These orbitals or the single electron wave functions determine the behaviour of electron in average field of other electrons. The main drawback of the HF method is exclusion of electron correlation,[92] but the HF solution is the central starting point for most methods, that define the many-electron system more accurately, for both atoms and molecules.

1.5.2 DFT method

In the density functional theory, the exact exchange (in HF) for a single determinant is replaced by a more general expression, the exchange-correlation functional, which can include terms accounting for both the exchange and the electron correlation energies, the latter not being present in Hartree-Fock theory. A DFT calculation adds an additional step to the major phase of a Hartree-Fock calculation. The step includes numerical integration of a functional or various derivative of a functional. A self-consistent reaction field (SCRF) can be used with the DFT energies, optimisations, and frequency calculations to model the systems. In addition to the sources of numerical errors in Hartree-Fock calculations, the accuracy of DFT calculations also depend upon the number of points used in numerical calculations.

1.5.3 Møller-Plesset Method

Møller-Plesset method is post Hartree Fock method. By using Møller-Plesset perturbation theory, electron correlation can be added to the system. Christian Møller and Milton S. Plesset, in 1934, published the idea of Møller-Plesset method.[93] When this theory is introduced to the calculation, HF becomes the first order perturbation and higher order perturbation is added as second order or MP2 method. The third order (MP3)[94] and the fourth order (MP4)[95] calculations are also common. The effect of these perturbed systems on the electronic distribution is determined after mixing the electronic states with the higher order states. MP2 accounts for inter-electronic repulsions. The higher orders like MP5[96] are seldom used because of the high computational cost that it adds.

1.5.4 Basis Set

The basis set is an approximate representation of the atomic orbitals (AOs) using the mathematical functions. The linear combinations of basis set are taken to generate the molecular orbitals. Choice of basis set for a given type of calculation decides the accuracy of the results. Initially the Slater-type-orbitals (STOs) were used for molecular calculations. In these type of basis sets, the long range overlap between the atoms, the atomic orbitals, the charge and the spin at the nucleus are well defined. But, it was found that STOs are computationally difficult to use. Therefore, the Slater type orbitals are approximated as linear combinations of the Gaussian orbitals.[97] With the Gaussian type orbitals, it is easier to calculate the overlap and other integrals as compared to the Slater type orbitals. Gaussian type orbitals are easy to use computationally and today, most functions are composed of Gaussian type orbitals (GTOs).

1.6 Atoms in molecule Study (AIM)

Bader's Quantum Theory of Atoms in Molecule (QTAIM), generally referred as Atoms in Molecule (AIM)[98] is a quantum mechanical application useful to understand the hydrogen bonding. This is very important tool for quantitative estimation of various molecular properties. QTAIM defines the structure of chemical system and chemical bonding based on the topology of the electron density. According to this theory, an atom in a molecule is an open system which can freely exchange charge and momentum with the neighbouring atoms.[99] This quantum description of an open system recovers the molecular system hypothesis which states that

"*A molecule is a collection of atoms each with a characteristic set of properties, that are linked by a network of bonds."*

The AIM approach is used to compute the bond paths and the bond critical paths between the interacting atoms. Bond Critical Point (BCP) is a point at which the first derivative of the electron density is zero. The two nuclei, which are connected with either covalent or non covalent interaction, are joined by a single line which follows the path of maximum electron density is known as the Bond Path. The bond path for any interaction need not necessarily be a straight line. The critical point on the bond path is known as BCP. A point, within a ring, where electron density is minimum is called the Ring Critical Point (RCP). In symmetric systems, like benzene, RCP is at the centre of the ring. Nuclear Critical Point (NCP) and Cage Critical Point (CCP) also fall under the categories of critical points. In general, a Critical Point (CP) is labelled by giving both its rank and signature. The number of non zero curvatures of the Hessian matrix defines the rank and the sum of the signs curvatures depicts the signature. In a stable molecule, the rank for all CPs is 3. On this basis of the rank and signature, CPs can be classifies into four categories:

(3, -3) Peaks: all the curvatures are negative and this represent a NCP

(3, -1) Passes: this has two negative and one positive curvature, this is found between every pair of nuclei that is linked by a chemical bond and represents a BCP

(3, +1) Pales: this has two positive and one negative curvature, found at the centre of ring of the bonded atoms and represents a RCP

(3, +3) Pits: all the curvature points are positive in this and represents CCP.

The bond order, or strength of the bond is defined by the magnitude of electron density at the BCP, $\rho_b(r)$. The second derivative of $\rho_b(r)$ is Laplacian ($\nabla^2\rho(r)$), a very important scalar quantity. It represents the area of local charge concentration and depletion. If $\nabla^2\rho(r) > 0$, the electron density is depleted and the interaction is a closed shell kind of

interaction. If $\nabla^2\rho(r) < 0$, the density is locally concentrated representing a shared interaction.

1.7 Experimental Charge Density Analysis

In the molecules, the distance between the atom is of the order of 0.1nm to 10nm and therefore, X-rays are best suited to probe the arrangement of atoms in the molecule as the wavelength of X-ray is in the same range. This helps us to visualize the molecular structure, shape and the interactions within the molecular crystal. The electrons in the atom scatter X-rays and the electron density can be plotted in the crystal space. "Charge Density" is a better term than electron density[100] because the chemically useful properties like electric field gradient, electrostatic potential, and molecular moments along with the electron distribution are contained in the X-ray diffraction experiment, which utilizes both the positive and the negative charges. Charge density analysis allow to probe the intermolecular interactions. Although charge density analysis is crucial to understand the intermolecular interactions, the data collection techniques and strategies for the same are equally important. Pinkerton *et al.* highlight the significance of extremely accurate data in the charge density analysis.[101,102] Zuo *et al.* with the help of charge density analysis, were able to provide the direct evidence of *d-s* hybridization for Cu(I) with production of *d* holes, and an accumulation of charge between the Cu(I) ions associated with Cu–Cu bonding.[103]

The basis of X-ray structure analysis is the spherical atom approximation which assumes that the atomic electron density is essentially the spherically average density of an isolated atom. This implies that a molecular crystal is build up by spherical independent atoms that bond together into a molecule and then re-arrange following the allowed symmetry of the crystal lattice. The major drawback for this assumption is that

the position of nuclei is at the maxima of electron density and the deformation of the electron density of an atom is not accounted. This Independent Atom Model (IAM) assumes atoms to be neutral in the crystal system, whereas there are evidences that the atoms in the molecule carry partial charges.[104] The spherical atom approximation is, to some extent, appropriate for heavy atoms, where the core scattering is quite effective but for the lighter atoms, the valence electrons are more deformed and this approximation becomes inappropriate for high-resolution studies. The first extension to the spherical atom approximation is the separation of scattering contributions of valence and the core shells. Coppen *et al.*[105] called it *kappa formalism (kappa, κ)*. This assumes that the electrons in the core shells are unperturbed and the atomic density is defined as:

$$\rho_{at}(\mathrm{r}) = \rho_{core}(\mathrm{r}) + P_v\kappa^3\rho_{valence}(\kappa\mathrm{r})$$

The expansion and the contraction of the atomic valence shells and the charge-transfer between the atoms is allowed by valence population P_v and the radial parameter, κ. Some improvements were further made to account for the non-spherical density function, which is accounted for the multipole-modelling.[105]

The multipole refinement is then performed using the program XD2006,[106] which uses Hansen-Coppens multipole formalism.[107] As per this model, the electron density of the atom(s) is given by $\rho_{atom}(\mathrm{r})$, which is given in the following equation:

$$\rho_{atom}(\mathrm{r}) = P_c\rho_{core}(\mathrm{r}) + P_{val}\kappa^3\rho_{val}(\kappa\mathrm{r}) + \sum_{l=0}^{l_{max}} \kappa'^3 \mathrm{R}_l(\kappa'\mathrm{r}) \sum_{m=0}^{l} P_{lm} y_{lm}(\theta,\phi)$$

Where the first two terms are spherical averaged core and valence electron densities of the atom and the last term corresponds to the non-spherical valence density, which is described in terms of real spherical harmonic functions. P_c, P_{val} and P_{lm} are the core, valance and multipole population parameters respectively and y_{lm} is the deformation density represented in terms of normalized spherical harmonics. The coefficient κ and κ′

describe the contraction/expansion for the spherical and multipolar valences densities respectively.

The topological analysis carried out using charge density analysis gives the information related to the Bond Critical Points (BCPs) and the parameters at BCPs can be related to the local energy densities of the electron by the following equation

$$E(\boldsymbol{r}_{cp}) = G(\boldsymbol{r}_{cp}) + V(\boldsymbol{r}_{cp})$$

Where, $E(\mathbf{r}_{cp})$ is the local energy density, $G(\mathbf{r}_{cp})$ is the local kinetic energy density and $V(\mathbf{r}_{cp})$ represents local potential energy density.

1.8 Foreword:

The non-covalent interactions directly influence the nucleation process and also determine the crystal packing. The knowledge of these intermolecular non-covalent interactions is necessary to design a targeted supramolecular assembly in solid state. Though the literature has significant reports of moderate and weak hydrogen bonds building desired crystalline lattice but the prediction of the result of crystallization experiment to achieve a control on the intermolecular interaction is not possible. There is a lot more to explore in this dimension and we are enthusiastic to gain knowledge about the nature and ability of fluorine to alter and control the packing of molecules in crystal lattice in different environments. We would want to see if other intermolecular interactions (either strong or weak) effect the organic fluorine mediated interactions or vice versa.

To widen our knowledge in this area i.e. fluorine mediated interactions in small organic molecules in presence and absence of other interactions, a systematic study is performed in the following chapters. The number of fluorine atoms on the studied system is also varied to know the effect of variation of number and position of organic fluorine

on the crystal system. The organic fluorine mediated interactions are found to be of extreme importance.

Chapter 2 comprises of 18 bridge-flipped isomers of diamides having one and two fluoro substitutions (Scheme 1.1). These molecules have a strong hydrogen bond donor, N–H group as well as a strong hydrogen bond acceptor, C=O group. In this, we have structurally and computationally analysed these compounds for various intermolecular interactions and have shown the influence the weak interactions have on the strong hydrogen bonds. A detailed computational analysis for the studied compounds shows the influence of position of fluorine on the other strong interactions present in the compounds.

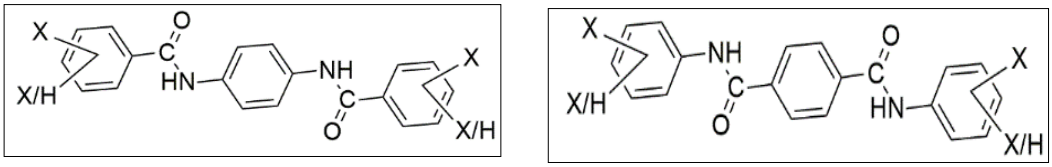

Scheme 1.1

Chapter 3 highlights the computational features arising due to the presence of four C–F groups in the presence of strong hydrogen bond acceptor C=O group but absence of any strong donor group like N–H in *tetrafluoro* substituted *benzamides*. The molecular representation for the compound is given in Scheme 1.2. In these compounds too, no hydrogen bond donor like N–H group is present. These structures have intermolecular interactions like C–H···F–C interaction, C–F···F–C interaction, C–H···O–C interaction and C–H···O=C interactions. All these interactions are studied in the further chapter and the energies of these interactions are computationally analyzed. These interactions are found to be directional in nature.

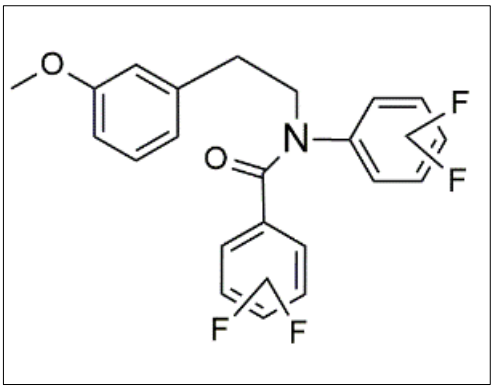

Scheme 1.2

Chapter 4 describes, computationally the strength of C–H···F–C interactions in *tetrafluoro* derivatives of *diphenyl tetrahydroisoquinolines* (Scheme 1.3). These molecules neither have strong hydrogen bond donors like N–H group, nor do these have strong hydrogen bond acceptors like C=O group. The only interactions observed in these set of compounds is C–H···F–C interaction, C–F···F–C interaction and C–H···O–C interactions. Based on the Gaussian calculations, the energies of these interactions are computed and a statistical analysis of C–H···F–C interaction against the distance and angle are also analysed.

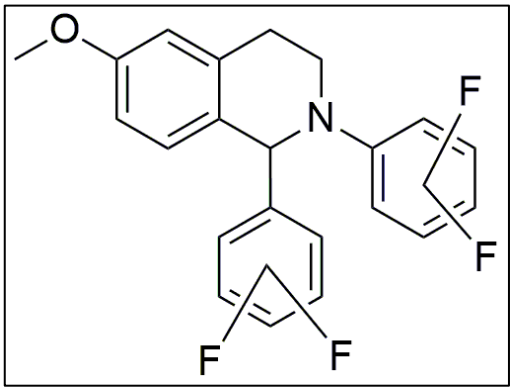

Scheme 1.3

Chapter 5 deals with understanding the different types of C–F···F–C interactions and C–H···F–C interaction with the help of experimental charge density analysis on tetrafluorinated benzamides (Scheme 1.4). The experimental charge density analyses is performed on the high resolution X-ray data collected at Liverpool. The topological parameters for these interactions is analysed using the AIM approach.

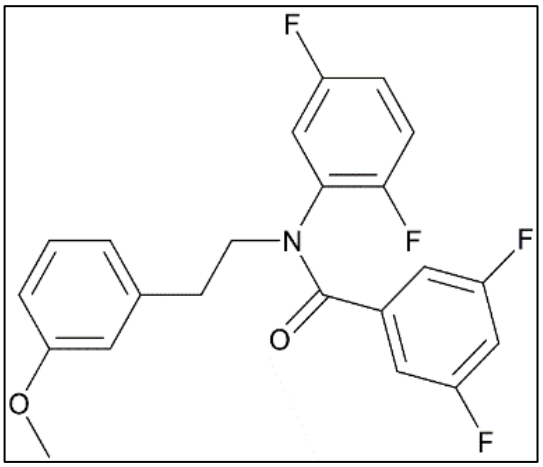

Scheme 1.4

Chapter 2

The influence of fluorine mediated interactions on the strong hydrogen bonds in a series of "bridge flipped" N,N'-(1,4-phenylene)dibenzamides and N,N'-diphenylterephthalamides

Chapter 2

2.1 Introduction

Intermolecular interactions offered by a C–F group in altering the crystal packing of molecules has always fascinated the researchers over the last few decades.[10,27,33,108,109] While many researchers indicated that organic fluorine[25] hardly participates in intermolecular interactions and alters crystal packing;[11,14,110,111] several others have demonstrated the importance of organic fluorine in crystal packing.[29-31,44,47] Computational,[38,40,50] experimental[37,112-116] and database based analysis[58,76,117,118] of fluorine mediated interactions and its significance in crystal packing have been reported in the literature. Many systematic studies have highlighted the role of organic fluorine in altering the crystal packing of small organic molecules. Some of them were conducted in the presence of other stronger hydrogen bonds involving N and O as acceptors[29,37,47,40,50,112] while others considered molecules where no other strong or weak hydrogen bonds involving N or O were expected.[30,31,38,113] The significance of fluorine in small organic compounds is evident in the drug and pharmaceutical industry as 70% of the drug molecules contain one or more fluorine atom while their non-fluorinated analogues do not display any biological activity.[119] The introduction of fluorine in a small

organic molecule can heavily alter the physical and the chemical properties of the molecule because of its high electronegativity, low polarisation and high bond strength.[120]

Our group have been especially interested in the investigation of the importance of intermolecular interactions offered by the C–X (X = F, Cl, Br) group in various small organic molecules, both in the presence and in the absence of other stronger interactions like the classical hydrogen bonds.[29-31,37-38,40,47,50,112-113] The C–X (X = F, Cl, Br) bonds are expected to be reasonably polar because of the high electronegativity of the halogens. Heavier halogens (Cl, Br and I) are seen to form short intermolecular contacts with electron donating as well as electron accepting groups.[11] It has been accepted that interactions involving halogens are significant in the crystal packing both in the absence as well as in the presence of other relatively stronger intermolecular interactions.[29-31,37-38,40,47,50,112-113,119] Among the halogens, apparently, fluorine has been recognized to behave differently in solution and in the solid state. The low polarizability and small size of fluorine compared to other halogens is believed to be responsible for this different behaviour. While other halogens mostly preferred to interact through $C–X_1\cdots X_2–C$ interactions or R–X···Y (X = Cl, Br, I; Y = O, N, S) halogen bond[114] but F preferably interacts through C–H···F–C hydrogen bond.[58,76] Hence, the interactions involving F are treated separately in the literature.

In this chapter, we aim to demonstrate the importance of fluorine mediated interactions on strong hydrogen bonds using a model system of a series of substituted aromatic amides [N,N′-(p-phenylene)dibenzamide (PPDB) and N,N′-diphenylterephthalamide (DPTP)], which comprise of three aromatic rings bridged by amide functionality in two different orientations (Scheme 2.1). The amide bridge is flipped to synthesis the bridge-flipped isomer. Different fluorine substitutions were introduced and the structures of all the compounds were analyzed. The intermolecular interactions offered by these molecules

in their crystal structures were also studied and analyzed computationally using Gaussian09.

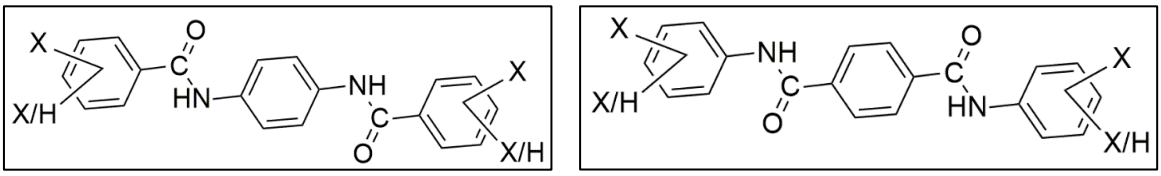

N, N'-(p-phenylene)dibenzamide (PPDB) N,N'-diphenylterephthalamide (DPTP)

Scheme 2.1: Molecular representation of the studied molecules

2.2 Experimental

2.2.1 Synthesis and Characterization

All the starting materials, substituted benzoyl chlorides and aniline derivatives were purchased from Sigma-Aldrich, India and were used without further purification. The synthesis of compounds 1-19 were carried out in a single step using a reported procedure by Cheng *et al*.[119] (Scheme 2.2.1 and Scheme 2.2.2).

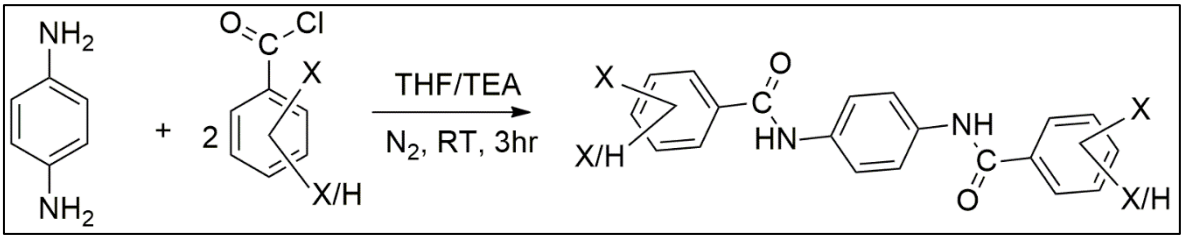

Scheme 2.2.1: Synthesis of N, N'-(p-phenylene)dibenzamide (PPDB)

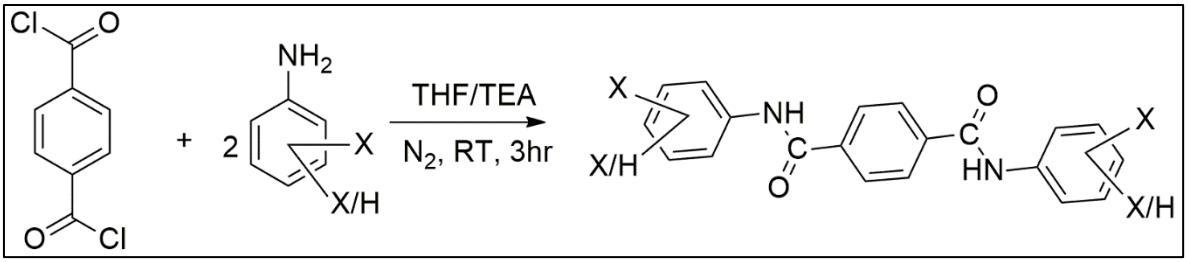

Scheme 2.2.2: Synthesis of N,N'-diphenylterephthalamide (DPTP), where, X=F

The PPDB compounds were synthesized from their corresponding mono- or di-fluorinated benzoyl chloride (4 mmol) and benzene-1,4-diamine (2 mmol) in the solution of dry Triethylamine (TEA) as a base and Tetrahydrofuran (THF) a solvent. The DPTP compounds were synthesized from their corresponding mono- or di- fluorinated anilines (4 mmol) and terephthaloyl chloride (2 mmol) in the solution of dry TEA as a base and THF as a solvent. The addition of aniline to terephthaloyl chloride was carried out at 0 ˚C. The suspension was stirred for 2-3 hours at room temperature (25 ˚C) under nitrogen atmosphere. The precipitated product was filtered, washed with acetone and was dried in vacuum to obtain the desired compound. No further purification was done.

All the new compounds were characterised using FTIR, ^{1}H, ^{13}C and ^{19}F NMR, and Powder X-ray Diffraction (PXRD). Single Crystal X-ray Diffraction (SCXRD) data were collected for the compounds for which suitable crystals were obtained after the crystallization experiment. The Powder patterns of the bulk samples were compared with that of the simulated patterns from the SCXRD for polymorph screening. The data for all the NMR and PXRD are given in the SI. All the bulk samples (as synthesised) were found to have the same structure as was determined by SCXRD. The crystal structures of the compounds were solved at 100K and none of them is isostructural. The compounds are crystallised in different space groups giving rise to various supramolecular synthons. The numbering scheme of the molecules used in the chapter is mentioned in Scheme 2.2.3 and scheme 2.2.4.

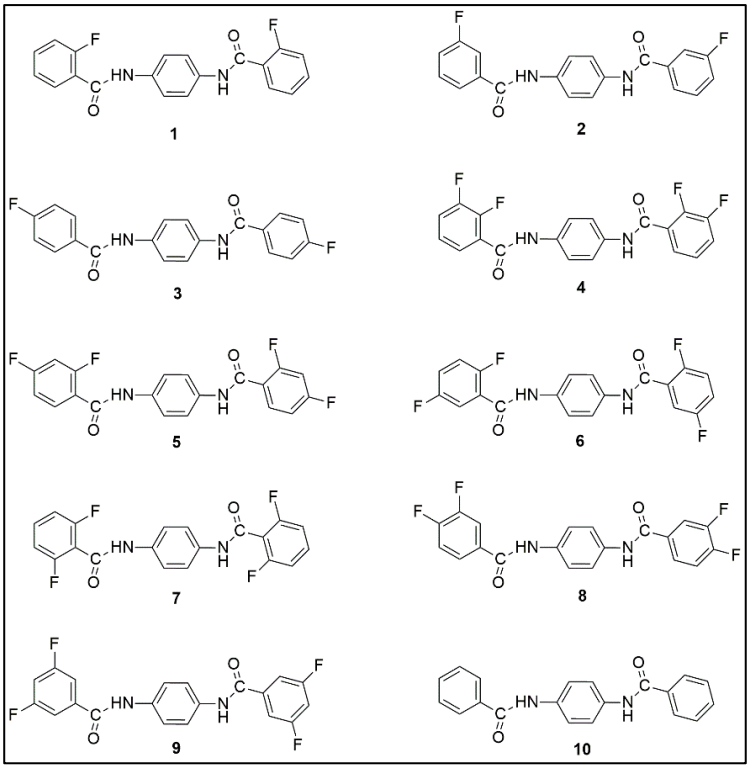

Scheme 2.2.3: Numbering scheme for Mono and di fluorinated PPDBs.

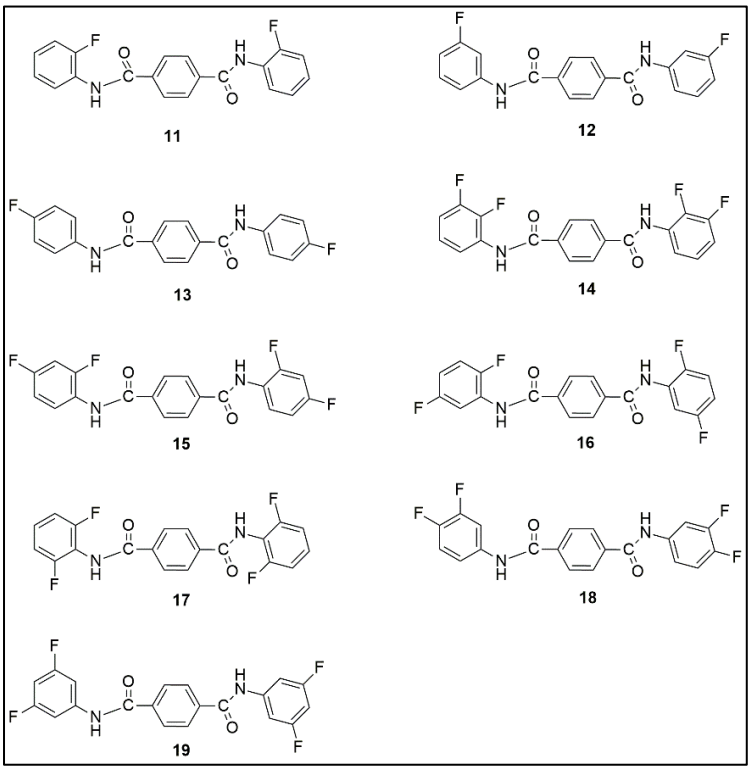

Scheme 2.2.4: Numbering scheme for Mono and di fluorinated DPTPs.

2.2.2 Powder X-ray Diffraction (PXRD) Analysis

PXRD patterns of all the pure compounds were recorded on a Rigaku Ultima IV X-ray diffractometer using parallel beam geometry equipped with a Cu – Kα radiation, 2.5° Primary and secondary solar slits, 0.5° divergence slit with 10 mm height limit slit, sample rotation stage (120 rpm) attachment and DTex Ultra detector. The tube voltage and current applied were 40 kV and 40 mA. The data were collected over an angle range 5 to 50° with a scanning speed of 2° per minute with 0.02° step. The observed PXRD patterns have been compared (using WINPLOTR[120]) with the simulated PXRD patterns generated from the crystal coordinates using Mercury.[121] The PXRD patterns or all the compounds are given in the figure below (Figure 2.2.2.1 and figure 2.2.2.2)

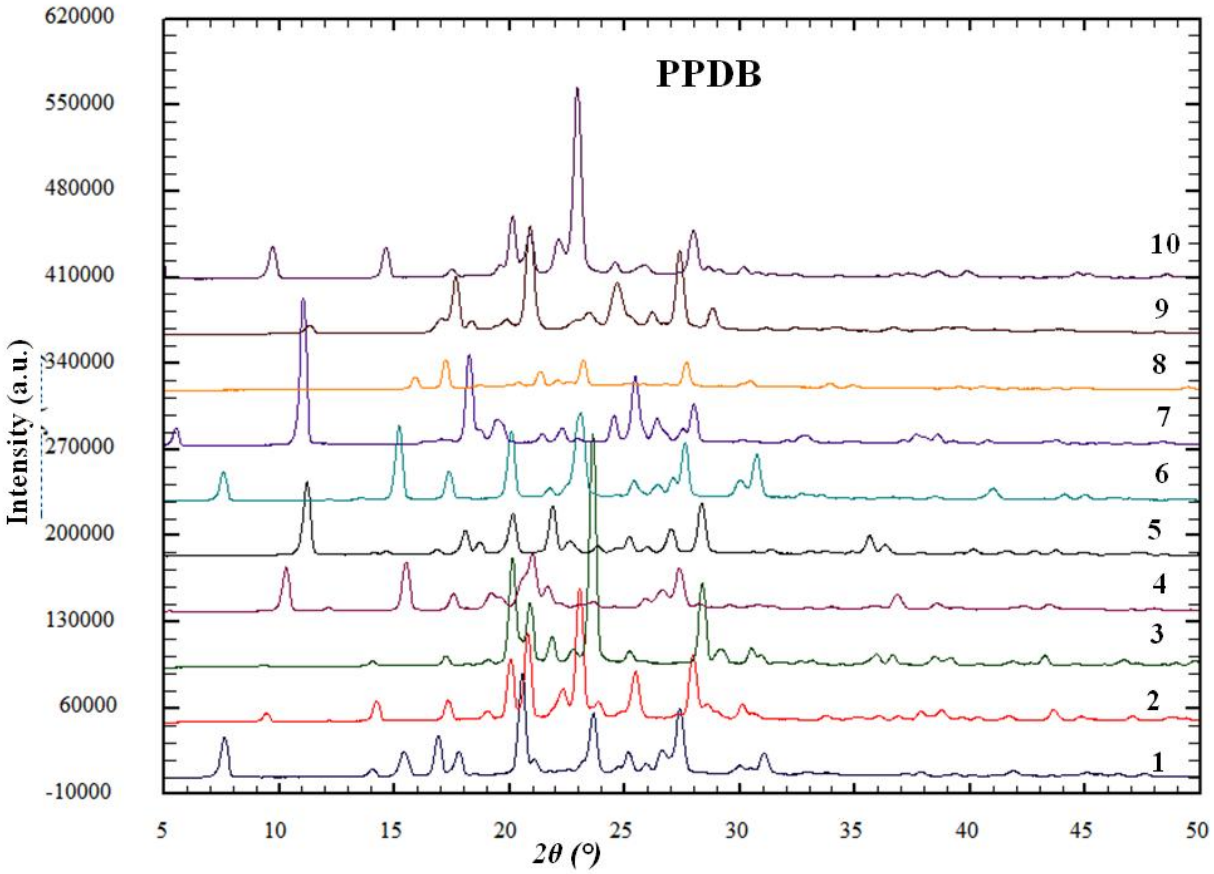

Figure 2.2.2.1: PXRD patterns for all the PPDBs

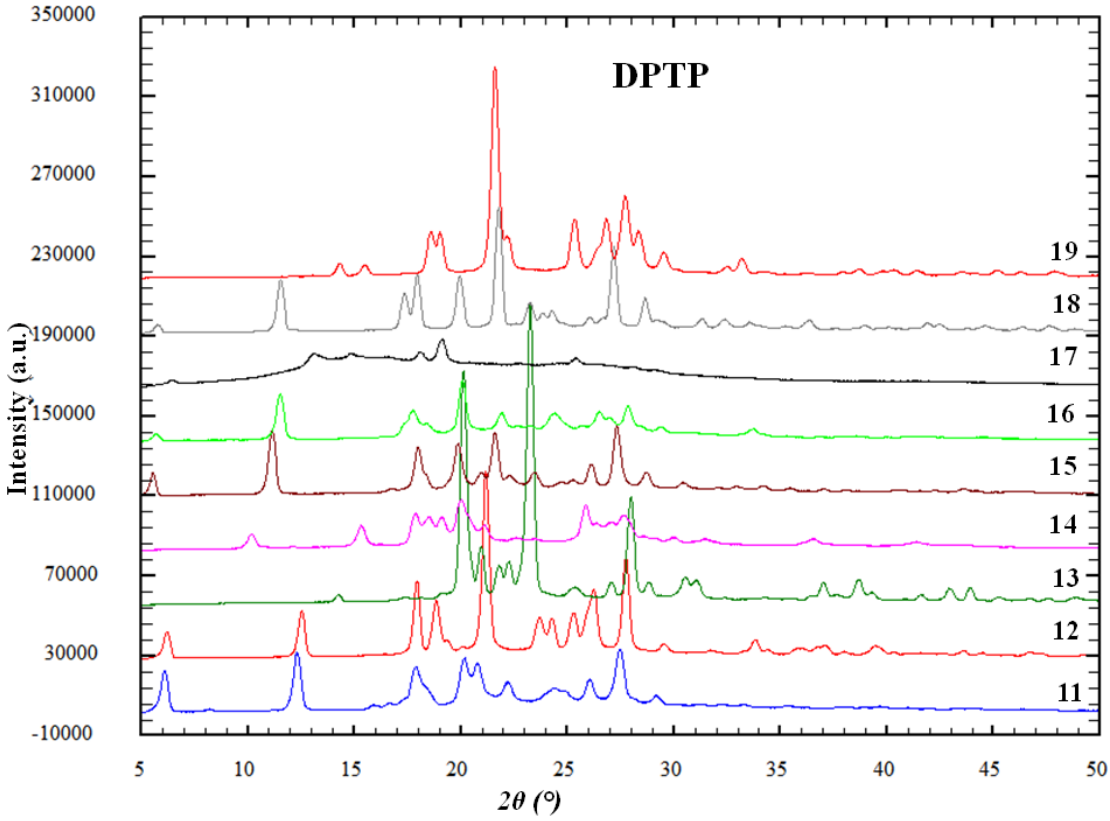

Figure 2.2.2.2: PXRD patterns for all the DPTPs

2.2.3 Crystal Growth, Single Crystal Data Collection, Structure Solution and Refinement

Single crystals of desired size and quality were grown by slow evaporation by dissolving the compound in DMF, DMSO or a mixture of solvents such as DFM/ACN, DMF/hexane, DMSO/hexane, and DMF/acetone etc.

Single crystal X-ray diffraction data (Table 2.2.3.1, 2.2.3.2, 2.2.3.3) were collected using a Rigaku XtaLABmini X-ray diffractometer equipped with Mercury CCD detector with graphite monochromatic Mo-Kα radiation (λ = 0.71073 Å) at 100.0(2) K using ω scans. The data were reduced using CrysAlisPro[122] and the space group determination was done using Olex2.[123] The crystal structures were solved by using one of Olex2.solve,[123] XT[124] and SHELXT[125] and were refined using SHELXL97[126] through

Olex2 suite. All the hydrogen atoms were geometrically fixed and refined using the riding model. Absorption correction was performed by multi-scan method. Data collection, crystal structure solution and refinement details for all the compounds are listed in the tables below. All the packing and interaction diagrams have been generated using Mercury 3.5.[109] Geometric calculations have been carried out using PARST[127] and PLATON.[128]

2.2.4 Computational

The fluorinated molecules were found to crystallize through various fluorine mediated interactions (C–H···F–C, and C–F···F–C) using five different synthons (Scheme 2.2.4.1) forming different types of dimers and strong N–H···O hydrogen bonds. The stabilization energies of these dimers were calculated using Gaussian09[129] using MP2/6-31+G(d) level of theory. Gauss view[130] was used as a graphical interface for Gaussian09. Experimental CIFs were used for the primary coordinates of the molecules under study. Monomers of the dimers formed by C–H···F–C, C–F···F–C, and N–H···O interactions were first identified and the energy of each individual monomer was calculated ($E_{monomer}$). Similarly, the single point energy of the dimer formed by C–H···F–C, C–F···F–C, and N–H···O interactions was calculated (E_{dimer}). The energy of the dimers was corrected for basis set superposition error (BSSE) using the counterpoise method. The stabilization energy (ΔE_{dimer}) of the dimeric motifs were then calculated using the following equations (Table 2.3.1).

$$\Delta E_{dimer} = E_{dimer} - 2 \times E_{monomer} \quad \text{.....1}$$

Equation 1 provides the stabilization energy of the dimer involving C–H···F–C hydrogen bond.[30]

Table 2.2.3.1: SCXRD data for the crystals obtained and the data for unsubstituted compounds from literature[119]

Identification code	**1**	**2**	**3**	**4**	**5**
CCDC number	**2194723**	**2194724**	**2194726**	**2194714**	**2194713**
Formula	$C_{20}H_{14}F_2N_2O_2$	$C_{20}H_{14}F_2N_2O_2$	$C_{20}H_{14}F_2N_2O_2$	$C_{20}H_{12}F_4N_2O_2$	$C_{20}H_{12}F_4N_2O_2$
Formula Weight	352.33	352.33	352.33	388.32	388.32
Temperature (K)	100.0(2)	100.0(2)	100.0(2)	100.0(2)	100.0(2)
Space group	$P2_1/n$	$P2_1/c$	$P2_1/c$	$P2_1/n$	$P2_1/n$
Solvent Used	DMF	DMF	DMF/ACN	DMF	DMF
***a* (Å)**	5.3125(3)	18.6383(14)	18.7926(8)	5.0406(2)	4.9571(6)
***b* (Å)**	6.4121(4)	5.3118(4)	5.3114(2)	4.6074(2)	5.2260(4)
***c* (Å)**	22.4263(13)	7.7528(6)	7.6237(3)	33.8212(18)	30.887(4)
***α* (°)**	90	90	90	90	90
***β* (°)**	94.569(5)	94.959(6)	95.167(2)	92.512(4)	90.387(11)
***γ* (°)**	90	90	90	90	90
***V* (Å^3)**	761.51(8)	764.68(10)	757.87(5)	784.71(6)	800.13(16)
Z	2	2	2	2	2
Z'	0.5	0.5	0.5	0.5	0.5
ρ_{calc} (g/cm^3)	1.537	1.530	1.544	1.643	1.612
μ/mm^{-1}	0.117	0.117	0.118	0.140	0.137
F(000)	364.0	364.0	364.0	396.0	396.0
2*θ* (°) ranges for data collection	6.61 to 65.594	6.582 to 65.46	2.176 to 50.054	7.236 to 65.578	5.276 to 65.584
Index ranges	-8,7; -9,9; -32,33	-27,28; -7,7; -10,11	-20,22; -6,6; -9,9	-7,6; -7,6; -46,43	-6,7; -7,7; -42,47
Total reflections	16102	8885	4716	8330	9497
R_{int}	7.24	7.46	1.43	2.68	5.43
No. of unique reflections	2762	2729	1341	2711	2842
R_1 [I > 2σ(I)]	6.83	8.35	3.01	5.52	5.66
wR_2 (all data)	20.60	27.11	7.97	16.89	15.40
GooF	1.042	1.042	1.043	1.079	1.020
Largest diff. Peak/Hole/e Å^{-3}	0.64/-0.40	1.02/-0.54	0.21/-0.23	0.61/-0.37	0.29/-0.30

Table 2.2.3.2: SCXRD data

Identification code	**6**	**8**	**9**	**Unsubstituted PPDB (literature)[119]**
CCDC number	**2194718**	**2194715**	**2194716**	**942458**
Formula	$C_{20}H_{12}F_4N_2O_2$	$C_{20}H_{12}F_4N_2O_2, C_6H_{14}N_2O_2$	$C_{20}H_{12}F_4N_2O_2$	$C_{20}H_{16}N_2O_2$
Formula Weight	388.32	534.51	388.32	316.35
Temperature (K)	100.0(2)	100.0(2)	100.0(2)	173(2)
Space group	$P2_1/n$	$P\bar{1}$	$P\bar{1}$	$P2_1/c$
Solvent Used	DMF	DMF	DMF	*
***a* (Å)**	5.1065(4)	7.2562(7)	5.2248(3)	18.047(4)
***b* (Å)**	6.7462(5)	10.4571(7)	6.9466(5)	5.2394(10)
***c* (Å)**	22.8647(17)	17.3771(10)	11.7610(8)	7.8799(16)
***α* (°)**	90	105.618(6)	94.350(6)	90.00
***β* (°)**	96.313(8)	95.817(6)	101.228(5)	94.25(3)
***γ* (°)**	90	103.293(7)	107.027(6)	90.00
***V* (Å^3)**	782.90(10)	1216.96(17)	396.30(5)	743.1(3)
Z	2	2	1	2
Z'	0.5	0.5	0.5	0.5
ρ_{calc} (g/cm^3)	1.647	1.459	1.627	*
μ/mm^{-1}	0.140	0.120	0.138	*
F(000)	396.0	556.0	198.0	*
2*θ* (°) ranges for data collection	5.378 to 65.468	5.434 to 49.998	6.196 to 65.622	*
Index ranges	-6,6; -9,10; -29,34	-8,8; -10,12; -20,20	-7,7; -10,10; -17,17	*
Total reflections	7407	13025	8203	1345
R_{int}	3.87	5.58	3.87	0.0000
No. of unique reflections	2742	4298	2781	1345
R_1 [I > 2σ(I)]	5.47	6.61	4.85	9.31
wR_2 (all data)	16.43	21.22	13.64	16.85
GooF	1.100	1.046	1.036	*
Largest diff. Peak/Hole/e Å^{-3}	0.48/-0.39	0.37/-0.35	0.40/-0.38	*

Table 2.2.3.3: SCXRD data

Identification code	12	13	14	16	18	19	Unsubstituted DPTP (Literature)[119]
CCDC number	**2194719**	**2194717**	**2194720**	**2194721**	**2194722**	**2194725**	**942462**
Formula	$C_{20}H_{14}F_2N_2O_2$	$C_{20}H_{14}F_2N_2O_2$	$C_{20}H_{12}F_4N_2O_2$	$C_{20}H_{12}F_4N_2O_2$	$C_{20}H_{12}F_4N_2O_2$	$C_{20}H_{12}F_4N_2O_2$	$C_{20}H_{16}N_2O_2$
Formula Weight	352.33	352.32	388.32	388.32	388.32	388.32	316.35
Temperature(K)	100.0(2)	100.0(2)	100.0(2)	100.0(2)	100.0(2)	100.0(2)	173(2)
Space group	$P2_1/n$	$P2_1/c$	$P2_1/c$	$P2_1/c$	$P\bar{1}$	$P2_1/n$	$P2_1/n$
Solvent Used	DMF/ACN	DMF/ACN	DMF	DMF	DMF/ACN	DMF	*
***a* (Å)**	5.6011(3)	18.551(4)	4.8889(3)	13.5185(19)	5.2433(2)	5.4300(3)	5.3070(11)
***b* (Å)**	4.9790(2)	5.2479(11)	4.7708(2)	4.9788(5)	8.6264(8)	5.0203(2)	21.226(4)
***c* (Å)**	27.4236(13)	7.8078(16)	33.7108(18)	12.7307(13)	9.0245(8)	29.4430(15)	6.8830(14)
***α* (°)**	90	90	90	90	84.730(7)	90	90
***β* (°)**	95.184(5)	96.983(3)	90.704(5)	112.501(14)	75.942(6)	94.964(4)	107.01(3)
***γ* (°)**	90	90	90	90	75.561(6)	90	90
***V* (Å^3)**	761.66(6)	754.5(3)	786.21(7)	791.62(18)	383.37(5)	796.05(8)	741.5(3)
Z	2	2	2	2	1	2	2
Z'	0.5	0.5	0.5	0.5	0.5	0.5	0.5
ρ_{calc} (g/cm^3)	1.536	1.542	1.640	1.629	1.682	1.6199	*
μ/mm^{-1}	0.117	0.118	0.139	0.138	0.143	0.138	*
F(000)	364.0	360.0	396.0	396.0	198.0	0.138	*
2*θ* (°) ranges for data collection	5.966 to 65.59	2.212 to 50.126	7.254 to 65.638	6.43 to 54.998	6.632 to 65.824	5.56 to 65.86	*
Index ranges	-8,8; -7,7; -38,41	-22,22; -6,6; -9,9	-6,7; -7,7; -50,50	-15,17; -6,6; -16,16	-7,7; -12,13; -12,13	-8,7; -7,7; -44,42	*
Total reflections	12389	7290	9466	7242	8467	16836	5228
R_{int}	4.91	2.43	4.53	5.82	4.74	3.42	5.22
No. of unique reflections	2946	1339	2818	1820	2716	2882	1683
R_1 [I > 2σ(I)]	10.14	3.08	5.70	7.71	6.68	5.14	6.40
wR_2 (all data)	39.59	7.79	17.89	22.55	21.17	14.21	13.08
GooF	1.674	1.061	1.055	1.112	1.087	1.052	*
Largest diff. Peak/Hole/e Å^{-3}	1.24/-0.95	0.21/-0.20	0.60/-0.35	0.82/-0.61	0.80/-0.56	0.56/-0.37	*

*This data were not mentioned in the reported cif

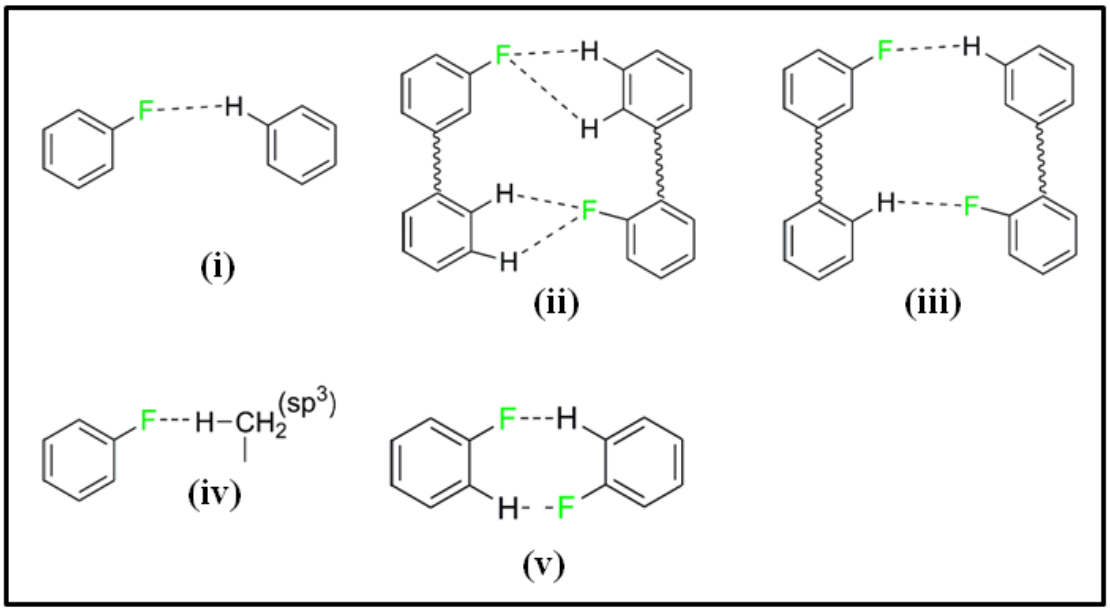

Scheme 2.2.4.1: Synthons involved in C–H···F–C interactions

2.3. Results & Discussions

Out of 19 compounds, we were able to crystallise 14 of them and carry out the SCXRD experiment. All these compounds are sparingly soluble in DMF and DMSO. We added anti-solvents like ACN, DCM etc. to the solution of compounds in DMF. In one of the compounds (compound 8), a solvent molecule (DMF) has crystallized along with the parent compound. This has not been observed for any other molecule. All the N–H···O hydrogen bonds are in parallel orientation.

The stabilization energies for all the observed interactions were calculated computationally and are mentioned in a tabulated form (Table 2.3.1)

Table 2.3.1: Computationally analysed energies for all the interactions

Interaction	Distance/ Å	Angle/Å	Stabilisation energy/ kcal/mol	Interaction diagram	Synthon number
1					
C4–H4···F1	2.476(1)	143.12(1)	-1.0	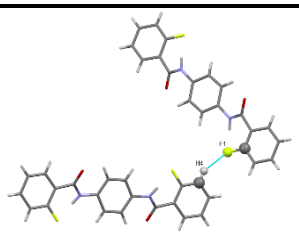	**I**
N1–H1···O1	2.316(1)	159.31(2)	**-13.7**	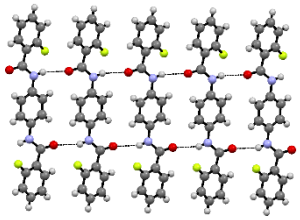	**Parallel**
2					
C6–H6···F1	2.623(2)	148.70(2)	-0.7	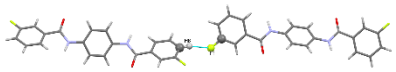	I
N1–H1···O1	2.311(1)	164.31(2)	**-17.7**	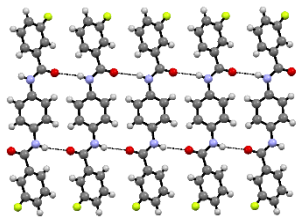	**Parallel**
C1–F1···F1–C1	2.856(1)	172.5(1) /172.5(1)	0.2	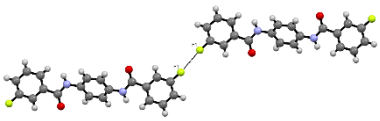	
3					
N1–H1···O1	2.314(2)	164.37(3)	**-17.7**	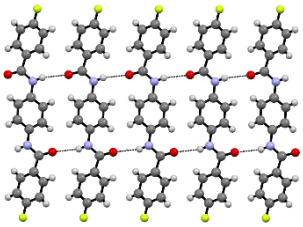	**Parallel**

C5–F1···F1–C5	2.94(2)	127.13(1) /101.11(1)	-0.8	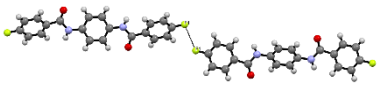	
4					
C6–H6···F1 C7–H7···F1	2.625(1) 2.551(1)	122.23(3) 125.80(3)	-6.7	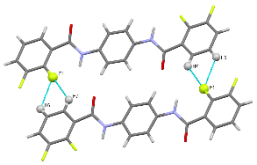	II
C5–H5···F2	2.646(2)	132.16(2)	-0.7	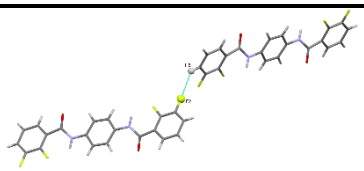	I
N1–H1···O1	2.317(2)	150.10(1)	**-16.5**	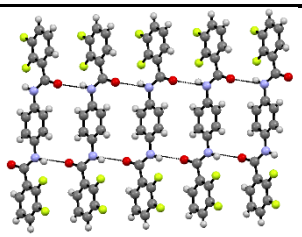	**Parallel**
5					
C6–H6B···F1A	2.448(1)	147.37(2)	-6.5	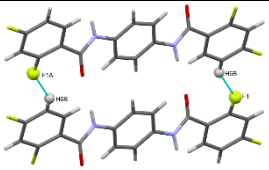	III
C4–H4B···F2B	2.658(2)	144.94(2)	-1.4	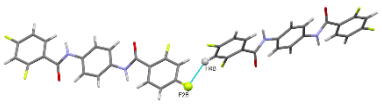	I
N1–H1···O1	2.065(1)	158.61(2)	**-20.6**	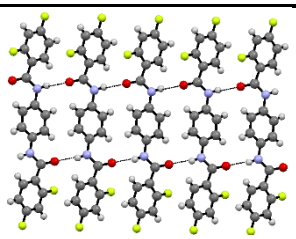	**Parallel**
6					
C4–H4···F1	2.588(1)	141.25(1)	-1.0	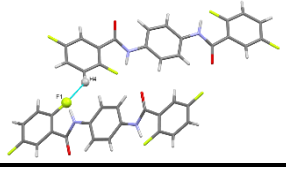	I

N1–H1···O1	2.179(2)	158.49(1)	**-15.9**	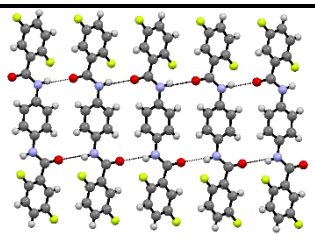	**Parallel**
8					
C26–H26A···F4B	2.429(1)	173.81(1)	-1.2	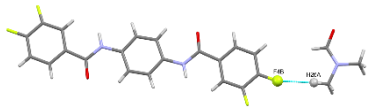	IV
C26–H26C···F4B	2.684(2)	116.05(2)	-0.5	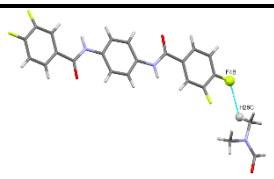	IV
N2–H2···O4	2.127(1) (with solvent)	163.64(1)	**-9.9**	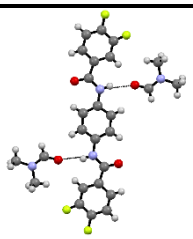	**With solvent**
9					
C4–H4···F1	2.640(2)	130.64(3)	-1.5	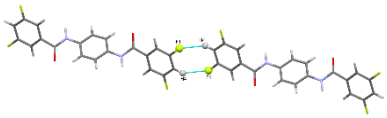	V
C4–H4···F2	2.660(2)	157.18(1)	-1.0	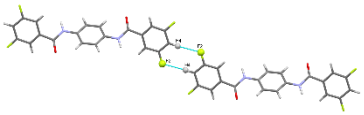	V
C3–F2···F2–C3	2.999(2)	125.66(1) /125.66(1)	-0.9	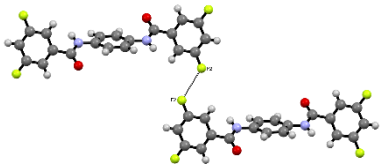	
N1–H1···O1	2.186(2)	156.86(2)	**-20.0**	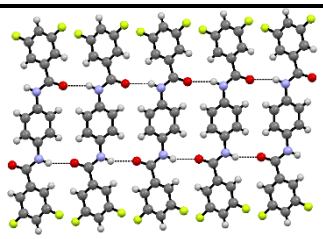	**Parallel**
Unsubstituted PPDB (taken from literature)[119]					
N1–H1···O1	2.241	163.72	**-17.7**	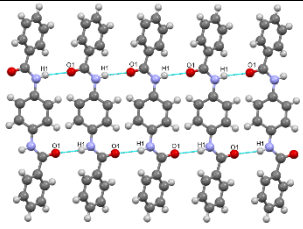	**Parallel**

12					
C6–H6···F1	2.481(1)	167.81(1)	-8.5	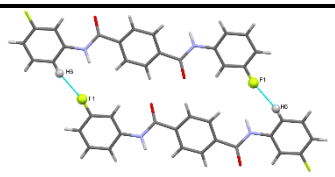	III
C4–H4···F1	2.678(1)	138.03(1)	-1.0	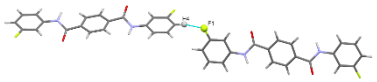	I
N1–H1···O1	2.147(1)	149.81(2)	**-17.1**	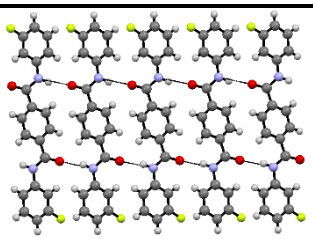	**Parallel**
13					
C2–H2···F1	2.591(1)	133.33(2)	-0.7	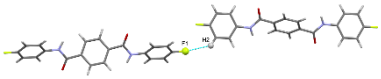	I
C1–F1···F1–C1	2.912(1)	107.18(2) /113.72(2)	-0.7	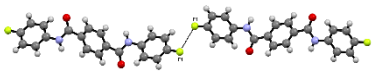	
N1–H1···O1	2.254(2)	164.06(1)	**-18.4**	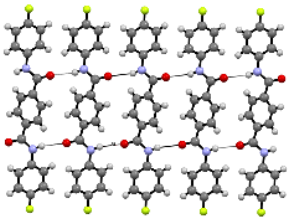	**Parallel**
14					
C5–H5···F2	2.63(1)	134.73(2)	-1.1	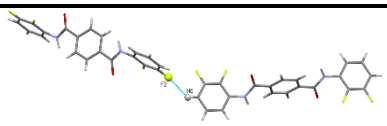	I
C6–H6···F1 C7–H7···F1	2.665(1) 2.554(1)	121.56(2) 126.51(2)	-5.9	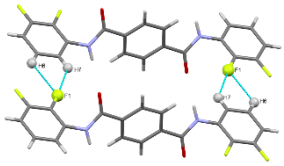	II
N1–H1···O1	2.101(2)	150.56(1)	**-20.5**	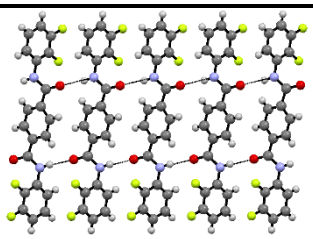	**Parallel**

16					
C4–H4···F1	2.673(1)	139.51(2)	-1.1	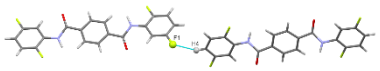	I
C3–H3···F2	2.443(2)	178.17(3)	-1.4	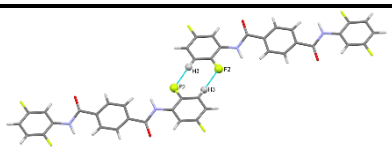	V
N1–H1···O1	2.068(2)	157.38(3)	**-17.1**	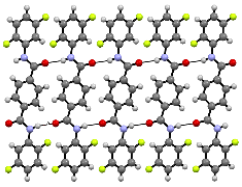	**Parallel**
18					
C5–H5···F1	2.608(1)	135.16(3)	-1.9	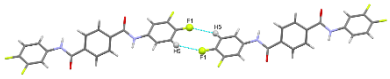	V
C2–H2···F2	2.538(1)	167.19(1)	-1.2	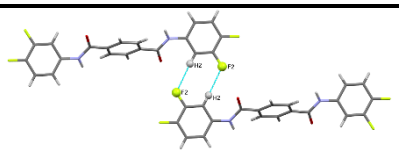	V
C4–F1···F1–C4 C4–F1···F2–C3	2.807(2) 2.970(2)	101.51(1) /101.51(1) 128.78(2) /97.72(2)	-0.4	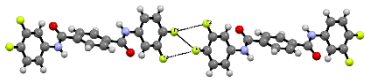	
N1–H1···O1	2.237(1)	157.10(1)	**-17.7**	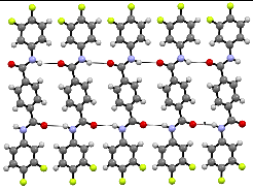	**Parallel**
19					
C2–H2···F2	2.347(1)	171.59(2)	-8.0	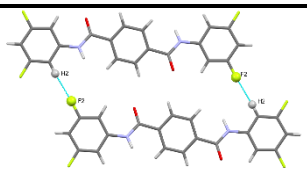	III
C4–H4···F1	2.477(2)	159.08(2)	-1.2	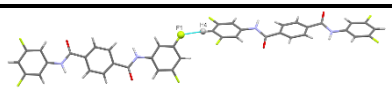	I

N1–H1···O1	2.152(2)	150.52(2)	**-18.7**	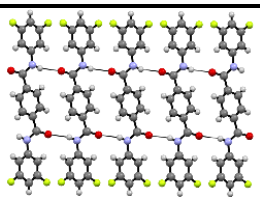	**Parallel**
Unsubstituted DPTP (Taken from literature)[119]					
N1–H1···O1	2.270	155.24	**-17.9**	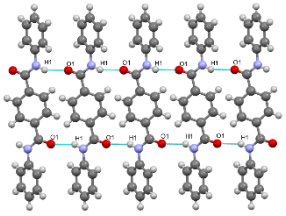	**Parallel**

It is observed that with the change in position of fluorine atom in the compounds, the angle, distance and stabilization energy of the strong hydrogen bond (N–H···O) is altered significantly (Table 2.3.2). For PPDB (N,N'-p-phenylene)dibenzamides, if fluorine is at meta position, the distance and angle for N–H···O hydrogen bond is at 2.311Å and 164.31˚ whereas these change to 2.147Å and 149.81˚ in it's brigde flipped isomer DPTP (N,N'-diphenylterephthalamide). Also, in 2,3 and 3,5 fluorine substituted PPDBs, the angle and distance for N–H···O hydrogen bond are 150.10˚/2.317Å and 156.86˚/2.186Å respectively. The same substitutions in DPTPs change the angle and distance to 150.56˚/2.101Å and 150.52˚/2.152Å respectively. The angle and the distance at which these strong hydrogen bonds are observed in the non-fluorinated analogues (data taken from literature) are different from the fluorinated analogues inferring the effect of fluorine substitution.

In these set of molecules, the C–H···F–C and C–F···F–C interactions are formed in the presence of strong hydrogen bond N–H···O. We have observed bifurcated C–F···F–C interactions. The computational calculations indicate the C–H···F–C interactions to be strongly stabilizing in nature even in the presence of other stronger bonds. In one of the

recent studies done by a previous lab member, the fluorinated interactions were studied in the presence of N–H···O=C strong hydrogen bonds in a system of substituted phenyl acetanilides.[131] A total of 10 compounds were synthesised and single crystal X-ray studies were done for 9 of them.

Table 2.3.2: Change in angle and distance for N–H···O interaction with respect to the position and interactions offered by organic fluorine

Compound name	**Position of F**	**N–H···O angle (˚)**	**N–H···O distance (Å)**	**No. of C–H···F–C present**	**No. of C–F···F–C present**
1	-2	159.31	2.316	1	-
2	-3	**164.31**	**2.311**	1	**1**
3	-4	164.37	2.314	-	1
4	-2,3	**150.10**	**2.317**	2	-
5	-2,4	158.61	2.065	2	-
6	-2,5	158.49	2.179	1	-
8	-3,4	163.64 (with solvent)	2.127 (with solvent)	2	-
9	-3,5	**156.86**	**2.186**	2	1
Unsubstituted PPDB	-	**163.72**	**2.241**		
12	-3	**149.81**	**2.147**	2	-
13	-4	164.04	2.254	1	1
14	-2,3	**150.56**	**2.101**	2	-
16	-2,5	157.38	2.068	2	-
18	-3,4	157.10	2.237	2	2 (Double bifurcated)
19	-3,5	**150.52**	**2.152**	2	-
Unsubstituted DPTP	-	**155.24**	**2.270**		

All the 9 compounds crystallised in monoclinic space group unlike in our set of compounds where we have crystals in both monoclinic as well as triclinic space groups. The stabilization energies for the 9 compounds was calculated and for the 2,5 substitution, the N–H···O=C stabilization energy was less than the other compounds (-12.1 kcal/mol for 2,5 substitution and for other compounds it was between -13.3 and -14.5 kcal/mol).

For the compounds discussed in this chapter, the isomers having 2,5 substitution too have lower values of stabilization energies for N–H···O hydrogen bonds as that of most of the compounds.

2.4 Conclusion

A detailed investigation is carried out for understanding the C–H···F–C and the C–F···F–C interaction in presence of strong N–H···O hydrogen bonds. Two sets of mono- and di- fluorinated molecules are chosen for this study which are bridge flipped isomers. The molecules are stable, and sparingly soluble only in DMF and DMSO. Among the 19 molecules synthesised, we were able to get single crystal X-ray diffraction data for 14 of them and the interactions among these molecules were studied computationally using Gaussian09 and Gauss View. All the molecules have strong N–H···O hydrogen bonds. These 14 molecules, using 5 different synthons gave 22 C–H···F–C interactions. These interactions were calculated for their stabilization energy and all the interactions are found to be stabilizing in nature. 17 of these 22 interactions are weak hydrogen bonds (have stabilization energy between 0 and -4 kcal/mol) and 5 of these C–H···F–C interactions are strong hydrogen bond (have stabilization energy between -4 and -15 kcal/mol). This categorization is carried out on the basis of classification done by Desiraju in his book.[6] In these 14 molecules, we have observed 5 C–F···F–C interactions among which 1 of the interactions has a positive value of stabilization energy (0.2345) and all other interactions have negative value for stabilization energy. An interesting observation is, the organic fluorine mediated interactions and the position of fluorine substitutions in the bridge flipped isomers alter the angle, distance and stabilization energy of the rather strong hydrogen bonds N–H···O. For two compounds, compound 1 and compound 8, the stabilization energy for N–H···O hydrogen bonds is calculated to be -13.7 kcal/mol and -9.9 kcal/mol respectively. For all

other compounds it is calculated to be more than -15 kcal/mol. This shows that the organic fluorine mediated interactions, are not only stabilizing in nature but also effect the strong hydrogen bonds present in the molecules. The fluorine substitutions in the synthesized compounds also alter the geometrical parameters for the N–H···O=C hydrogen bonds.

Chapter 3

How important are fluorine mediated interactions in controlling the crystal packing in the presence of C–H···O=C hydrogen bonds?

Chapter 3

3.1 Introduction:

The importance of fluorine mediated interactions on the strong hydrogen bonds in substituted aromatic amides using computational tools has been discussed in the previous chapter. Our observations from that study indicated that most of the interactions offered by organic fluorine are strongly stabilizing in nature. The organic fluorine mediated interactions effect the strong hydrogen bonds not only in their stabilization energy but also the geometry of the strong hydrogen bonds is altered in with change in position and number of fluorine substitutions; which in turn, altered the crystal packing which is evident from the variation in the unit cell dimensions of the compounds studied. C–H···F–C interactions play a significant role in crystal packing and are directional in nature, hence cannot be regarded as mere a van der Waals interaction. Among the structural studies in the previous chapter, we came across 5 different supramolecular synthons from 14 single crystal structures, offering 22 C–H···F–C interactions. Through this analysis of the concerned interactions, we have pointed out that the C–H···F–C interactions play a vital role in crystal engineering.

In this chapter, we intend to extend our analysis in another series of compounds, tetra fluorinated secondary amides, which provide us the opportunity to study the importance of fluorine mediated interactions in presence of C–H···O=C hydrogen bonds

and absence of other strong hydrogen bonds like N–H···O=C. The molecule is represented in scheme 3.1.1.

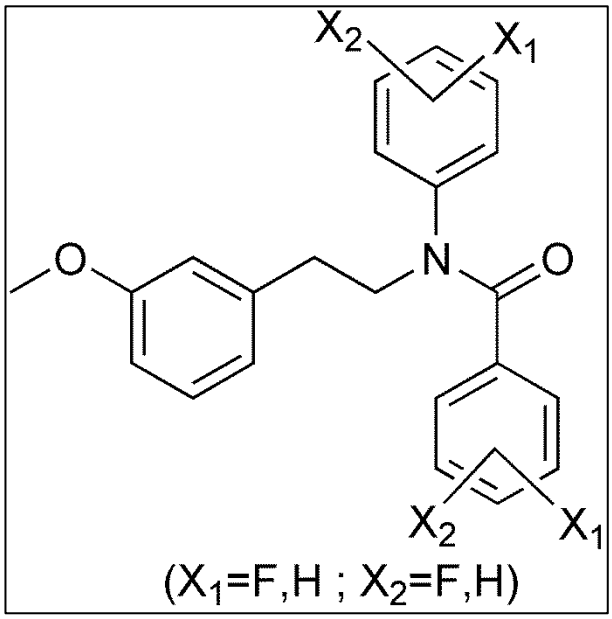

Scheme 3.1.1

Here, in these set of molecules, 4 fluorine atoms are substituted in two benzene rings and the position of fluorine substitution is varied. The intermolecular interactions possible in these molecules is either the organic fluorine mediated interaction or the interactions mediated by the methoxy and the C=O group. In this chapter, we aim at the stabilization energy calculations for the intermolecular interactions like C–H···F–C, C–H···O=C, C–H···O–C and C–F···F–C. Herein, we intend to study various supramolecular synthons offered by organic fluorine and aim to understand the strength and the directionality that the observed interactions offer.

3.2 Experimental

All the compounds studied in this chapter were synthesised by Dr. Hare Ram Yadav as per the synthetic procedure mentioned herein (Scheme 3.2.1). The following scheme (Scheme 3.2.2) represents the naming of the molecules used in the chapter.

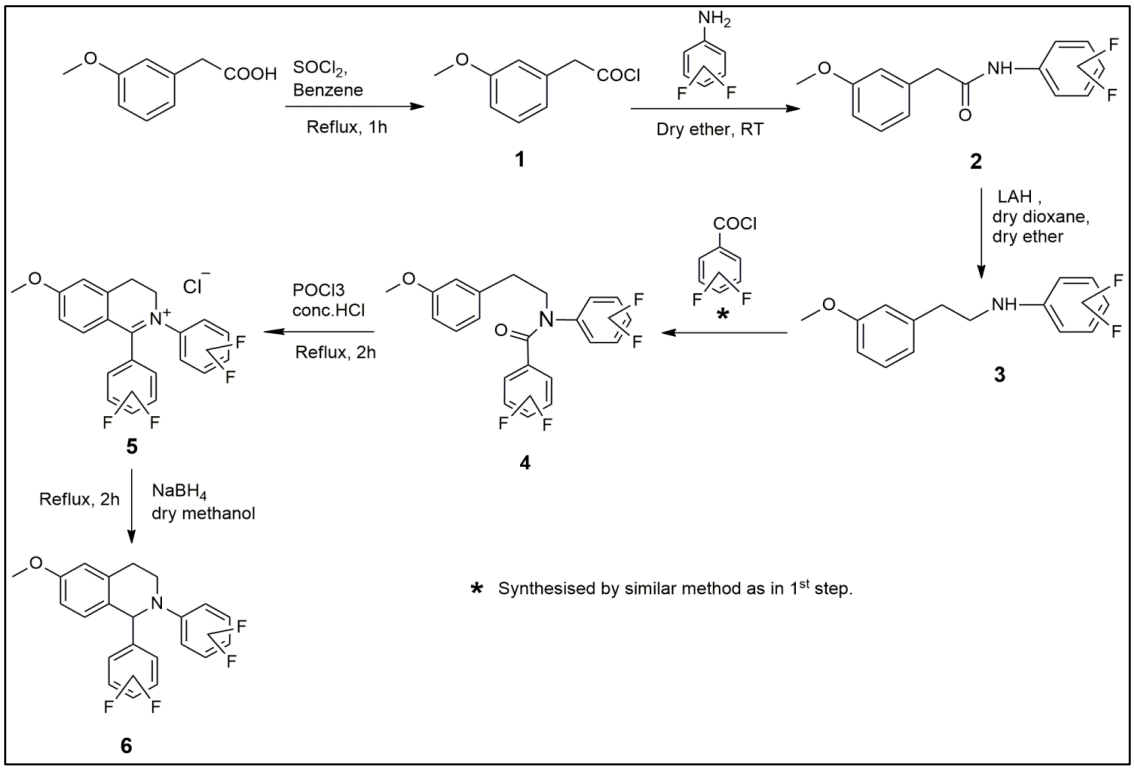

Scheme 3.2.1: Synthetic scheme for making the target molecules (4) (From Dr. Hare Ram Yadav Thesis[132])

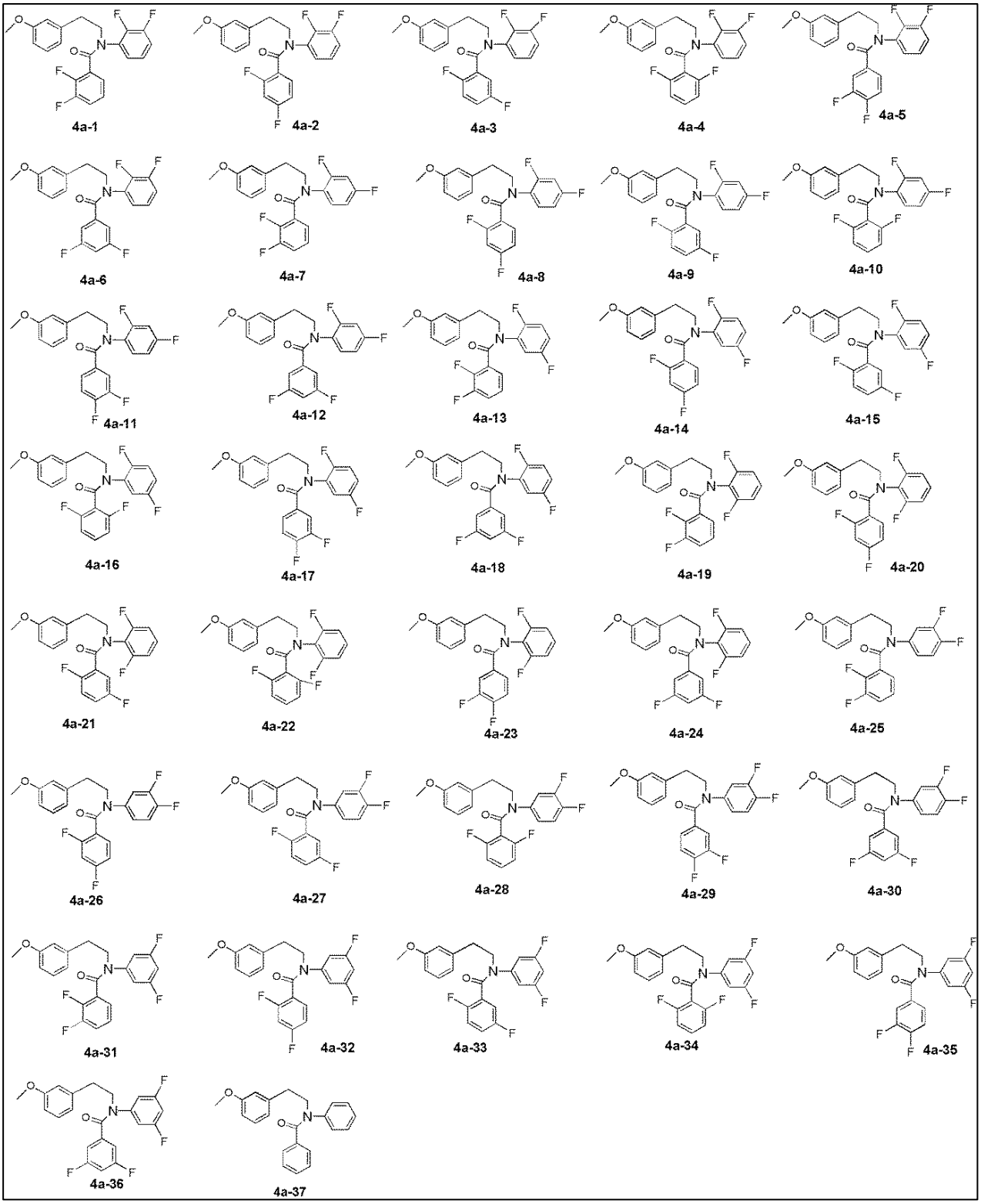

Scheme 3.2.2 : Naming scheme of molecules used in the chapter (Reproduced from the Ph. D. thesis of Dr. Hare Ram Yadav)

Among the 37 synthesised molecules, we were able to grow single crystals of 27 compounds. 26 of these are fluorinated derivatives and one is non-fluorinated analogue. Herein, in these tables (Table 3.2.1-3.2.4), we are presenting the crystal structure information for the 27 compounds.

Table 3.2.1: Single crystal X-ray diffraction data of compounds 4a-4 to 4a-11 (Reproduced from the Ph. D. thesis of Dr. Hare Ram Yadav)

Identification code	**4a-4**	**4a-5**	**4a-7**	**4a-8**	**4a-9**	**4a-10**	**4a-11**
CCDC No	1456822	1456823	1477818	1456811	1456814	1456812	1456813
Formula	$C_{22}H_{17}F_4NO_2$	$C_{22}H_{17}F_4NO_2$	$C_{22}H_{17}F_4NO_2$	$C_{22}H_{17}F_4NO_2$	$C_{22}H_{17}F_4NO_2$	$C_{22}H_{17}F_4NO_2$	$C_{22}H_{17}F_4NO_2$
Formula weight	403.36	403.36	403.37	403.37	403.37	403.36	403.36
Temperature (K)	100.0 (2)	100.0 (2)	100.0 (2)	100.0 (2)	100.0 (2)	100.0 (2)	100.0 (2)
Crystal system	Triclinic	Orthorhombic	Monoclinic	Monoclinic	Orthorhombic	Orthorhombic	Monoclinic
Space group	$P\ \bar{1}$	$P2_12_12_1$	$P2_1/c$	$P2_1$	$Pbca$	$P2_12_12_1$	$P2_1$
a (Å)	7.0928(7)	6.791(2)	8.3192(14)	11.2206(18)	19.630(4)	7.848(4)	11.3092(16)
b (Å)	11.30560(10)	14.041(4)	22.270(4)	6.7281(8)	12.640(3)	12.908(5)	6.6176(8)
c (Å)	12.4136(10)	19.036(4)	20.451(3)	12.6609(19)	15.195(3)	18.874(10)	12.6738(18)
α (°)	70.18(3)	90	90	90	90	90	90
β (°)	84.28(4)	90	97.292(8)	100.742(8)	90	90	100.290(7)
γ (°)	75.44(4)	90	90	90	90	90	90
V (Å^3)	906.29(12)	1815.1(9)	3758.2(11)	939.1(2)	3770.1(14)	1912.1(15)	933.2(2)
Z	2	4	8	2	8	4	2
Z′	1	2	2	1	1	1	1
ρ_{calc} (g cm^{-3})	1.478	1.476	1.426	1.427	1.421	1.401	1.435
μ/ mm^{-1}	0.122	0.122	0.118	0.118	0.118	0.116	0.119
F(000)	416	832	1664	416	1664	832	416

Table 3.2.2: Single crystal X-ray diffraction data of compounds 4a-12 to 4a-19.

(Reproduced from the Ph. D. thesis of Dr. Hare Ram Yadav)

Identification code	**4a-12**	**4a-13**	**4a-15**	**4a-16**	**4a-17**	**4a-18**	**4a-19**
CCDC No	1477817	1456815	1456804	1477815	1477814	1456807	1477816
Formula	$C_{22}H_{17}F_4NO_2$	$C_{22}H_{17}F_4NO_2$	$C_{22}H_{17}F_4NO_2$	$C_{22}H_{17}F_4NO_2$	$C_{22}H_{17}F_4NO_2$	$C_{22}H_{17}F_4NO_2$	$C_{22}H_{17}F_4NO_2$
Formula weight	403.36	403.36	403.36	403.37	403.36	403.36	403.36
Temperature (K)	100.0 (2)	100.0 (2)	100.0 (2)	100.0 (2)	100.0 (2)	100.0 (2)	100.0 (2)
Crystal system	Monoclinic	Triclinic	Triclinic	Triclinic	Monoclinic	Monoclinic	Monoclinic
Space group	$P2_1/c$	$P\bar{1}$	$P\bar{1}$	$P\bar{1}$	$P2_1/c$	$P2_1/c$	$P2_1/c$
a (Å)	14.054(3)	8.649(4)	8.661(3)	6.532(3)	7.699(8)	7.686(3)	10.3595(15)
b (Å)	18.823(4)	8.883(3)	10.069(3)	8.694(4)	14.711(14)	14.586(4)	12.9485(16)
c (Å)	15.625(4)	12.316(5)	11.400(3)	16.808(6)	19.52(2)	19.627(5)	14.705(2)
α (°)	90	91.08(2)	93.191(12)	94.99(2)	90	90	90
β (°)	115.509(8)	99.57(3)	100.573(9)	95.95(2)	123.47(4)	123.051(10)	106.947(6)
γ (°)	90	97.112(17)	106.933(7)	97.04(2)	90	90	90
V (Å^3)	3730.3(14)	925.1(7)	928.6(4)	937.3(7)	1844(3)	1844.2(10)	1886.9(5)
Z	8	2	2	2	4	4	4
Z′	2	1	1	1	1	1	1
ρ_{calc} (g cm^{-3})	1.436	1.448	1.443	1.429	1.453	1.453	1.420
μ/ mm^{-1}	0.119	0.120	0.119	0.118	0.120	0.120	0.117
F(000)	1664	416	416	416	832	832	832

Table 3.2.3: Single crystal X-ray diffraction data of compounds **4a-20** to **4a-30.**

(Reproduced from the Ph. D. thesis of Dr. Hare Ram Yadav)

Identification code	**4a-20**	**4a-22**	**4a-23**	**4a-25**	**4a-27**	**4a-28**	**4a-30**
CCDC No	1456805	1477813	1456798	1456799	1456800	1456801	1456802
Formula	$C_{22}H_{17}F_4NO_2$	$C_{22}H_{17}F_4NO_2$	$C_{22}H_{17}F_4NO_2$	$C_{22}H_{17}F_4NO_2$	$C_{22}H_{17}F_4NO_2$	$C_{22}H_{17}F_4NO_2$	$C_{22}H_{17}F_4NO_2$
Formula weight	403.36	403.36	403.36	403.36	403.36	403.36	403.36
Temperature (K)	100.0 (2)	100.0 (2)	100.0 (2)	100.0 (2)	100.0 (2)	100.0 (2)	100.0 (2)
Crystal system	Orthorhombic	Monoclinic	Orthorhombic	Monoclinic	Monoclinic	Orthorhombic	Triclinic
Space group	*Pbca*	$P2_1/c$	*Pbca*	$P2_1/c$	$P2_1/c$	$P2_12_12_1$	$P\bar{1}$
a (Å)	12.5050(16)	9.550(3)	12.646(2)	12.511(4)	12.9586(15)	8.1631(14)	8.062(4)
b (Å)	15.2686(19)	8.6078(19)	15.169(2)	8.430(3)	7.8587(7)	12.524(2)	9.592(5)
c (Å)	19.352(2)	25.576(7)	19.467(4)	18.189(5)	19.129(2)	18.705(3)	13.231(6)
α (°)	90	90	90	90	90	90	103.535(19)
β (°)	90	116.066(13)	90	102.301(12)	105.267(4)	90	91.312(6)
γ (°)	90	90	90	90	90	90	108.621(17)
V (Å^3)	3695.0(8)	1888.6(8)	3734.4(11)	1874.2(11)	1879.3(4)	1912.3(6)	937.4(8)
Z	8	4	8	4	4	4	2
Z′	1	1	1	1	1	1	1
ρ_{calc} (g cm^{-3})	1.450	1.419	1.435	1.430	1.426	1.401	1.429
μ/ mm^{-1}	0.120	0.117	0.119	0.118	0.118	0.116	0.118
F(000)	1664	832	1664	832	832	832	416

Table 3.2.4: Single crystal X-ray diffraction data of compounds 4a-31 to 4a-37.

(Reproduced from the Ph. D. thesis of Dr. Hare Ram Yadav)

Identification code	**4a-31**	**4a-33**	**4a-34**	**4a-35**	**4a-36**	**4a-37**
CCDC No	1456792	1456793	1456794	1477819	1456796	1456795
Formula	$C_{22}H_{17}F_4NO_2$	$C_{22}H_{17}F_4NO_2$	$C_{22}H_{17}F_4NO_2$	$C_{22}H_{17}F_4NO_2$	$C_{22}H_{17}F_4NO_2$	$C_{22}H_{21}NO_2$
Formula weight	403.36	403.36	403.36	403.36	403.36	331.40
Temperature (K)	100.0 (2)	100.0 (2)	100.0 (2)	100.0 (2)	100.0 (2)	100.0 (2)
Crystal system	Triclinic	Monoclinic	Monoclinic	Triclinic	Monoclinic	Monoclinic
Space group	$P\ \bar{1}$	$P2_1/c$	$P2_1/c$	$P\ \bar{1}$	$P2_1/c$	$C2/c$
a (Å)	7.1119(11)	14.7833(15)	15.170(5)	9.21160(10)	13.4004(19)	17.640(4)
b (Å)	9.5666(9)	8.5522(7)	8.022(2)	9.7778(15)	8.4135(10)	9.1027(14)
c (Å)	14.8367(18)	24.482(2)	15.485(5)	12.026(2)	26.011(3)	22.797(4)
α (°)	83.93(3)	90	90	89.67(5)	90	90
β (°)	76.68(3)	143.319(4)	90.823(16)	78.40(5)	138.825(4)	103.211(6)
γ (°)	73.34(3)	90	90	62.05(3)	90	90
V (Å^3)	940.2(3)	1849.0(3)	1884.2(10)	932.3(3)	1930.7(4)	3563.6(11)
Z	2	4	4	2	4	8
Z′	1	1	1	1	1	1
ρ_{calc} (g cm^{-3})	1.425	1.449	1.422	1.437	1.388	1.235
μ/ mm^{-1}	0.118	0.120	0.118	0.119	0.115	0.079
F(000)	416	832	832	416	832	1408

3.3 Computational Analysis

The fluorinated molecules were found to crystallize through various fluorine and oxygen mediated interactions (C–H···F–C, C–F···F–C, C–H···O–C and C–H···O=C) forming different types of dimers. The stabilization energies of these dimers were calculated using Gaussian09[129] using MP2/6-31+G(d) level of theory. Gauss view[130] was used as a graphical interface for Gaussian09. Experimental CIFs were used for the primary coordinates of the molecules under study. C–H···F–C, C–F···F–C, C–H···O–C and C–H···O=C mediated monomers were first identified and the energy of each individual molecule was calculated ($E_{monomer}$). Similarly, the energy of the dimer involving the interactions was calculated (E_{dimer}). The energy of the dimers was corrected for basis set superposition error (BSSE) using the counterpoise method. The stabilization energy (ΔE_{dimer}) of the dimeric motifs were then calculated using the following equations.

$$\Delta E^{F}_{dimer} = E_{dimer} - 2 \times E_{monomer} \quad \ldots\ldots\ldots\ldots\ldots\ldots 1$$

Equation 1 provides the stabilization energy of the dimer involving C–H···F–C hydrogen bond.

3.4 Results and Discussion

Only weak hydrogen bonds like C–H···F–C, C–H···O–C, C–F···F–C and C–H···π(C_g) interactions are possible in crystal packing of these molecules. The intermolecular interactions were analysed using PARST[127] and the stabilization energy calculations were performed using Gaussian09.

The structures of the Tetra fluoro substituted *N-[2-(3-methoxyphenyl)ethyl]-N-phenylbezamide* derivatives reported in this chapter display a library of supramolecular assemblies involving mostly the C–F group, which were historically refuted in stabilizing the crystal structures. It is noted that the crystal density of the non-fluorinated

analogue (**4a-37**) is the lowest (1.235 g/cm^3) among all the compounds reported here. The density of the fluorinated molecules is found to be between 1.388 g/cm^3 and 1.478 g/cm^3(Table 3.2.1-3.2.4). Fluorine mediated interactions are responsible for building different crystalline architecture in these molecules. The structures of these compounds revealed that the aromatic C–F acceptor groups not only form hydrogen bonds with aromatic C–H donors, but also form hydrogen bonds with –CH_2– groups present in the molecule.

We have observed 71 C–H···F–C interactions, 75 C–H···O interactions, among which, 47 are C–H···O=C interactions and only 28 interactions are of C–H···O–C type. In addition, we have observed 17 C–F···F–C interactions. Among the 17 C–F···F–C interactions, 8 are of Type I, 5 are Quasi Type I/II and 2 are Type II. The other two compounds (4a-17 and 4a-22) have 2 simultaneous C–F···F–C interactions. In 4a-17, we have observed a Type I interaction (C20A–F2···F2–C20B) and 2 Quasi Type I/ Type II kind of interactions (C20A–F2···F3–C11 and C19B–F1A···F3–C11). For the other compound, 4a-22, one interaction is Type I (C11–F4···F4–C11) and the other is a Type II kind of interaction (C22–F2···F4–C11). Aromatic organic fluorine (fluorine bonded with a carbon atom) forms dimers through 13 different synthons (Figure 3.4.1 and Table 3.4.1), which has generated 71 C–H···F–C intermolecular interactions among the 26 crystals. Some of these synthons involve fluorine and hydrogen in bifurcated interactions. The computationally calculated data along with the interactions is given in Table 3.4.2

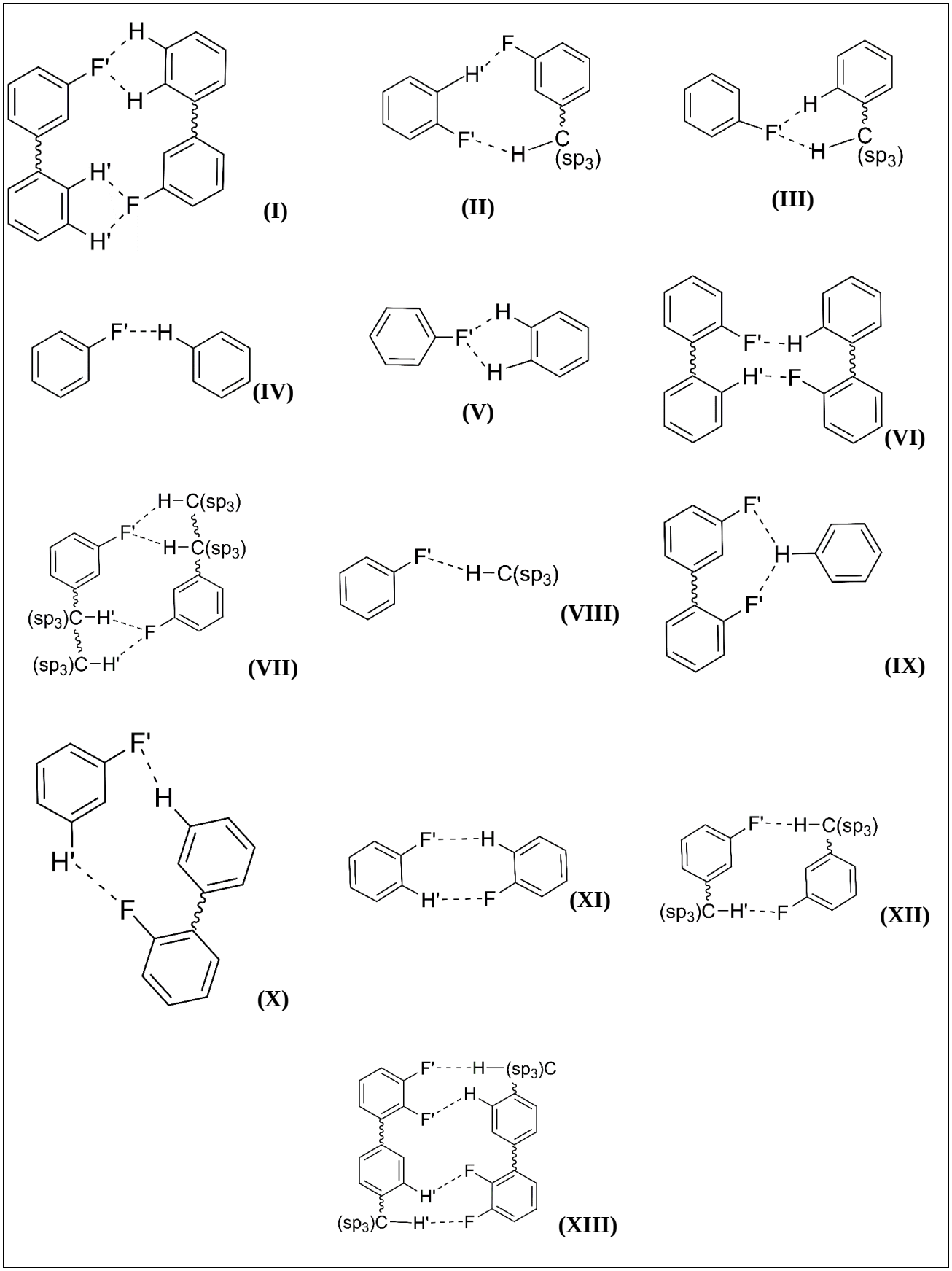

Figure 3.4.1: Synthons involved in C–H···F–C intermolecular interactions

Table 3.4.1: Synthons are their corresponding representative structures

Synthon	Representative Structure
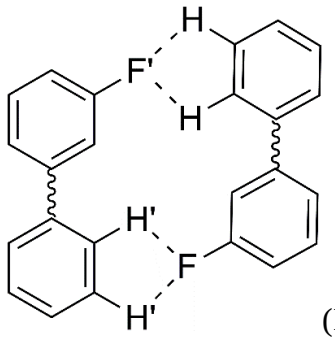 (I)	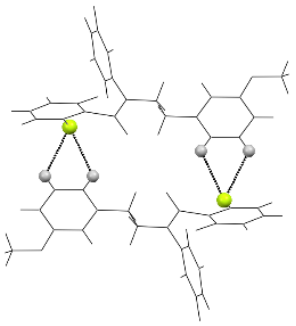 1a-4
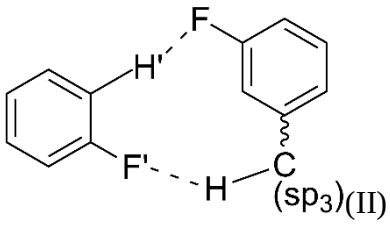 (II)	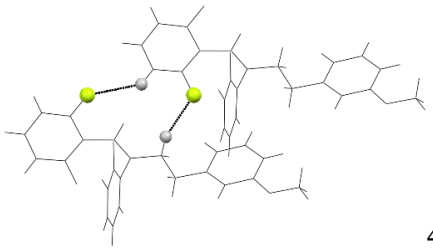 4a-4
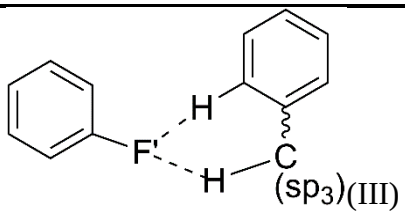 (III)	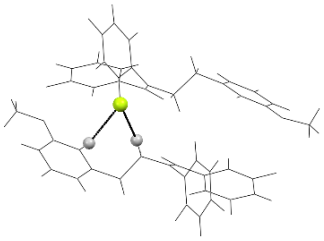 4a-5
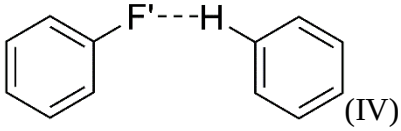 (IV)	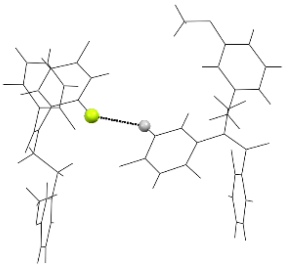 4a-8

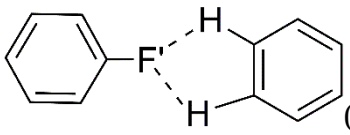 (V)	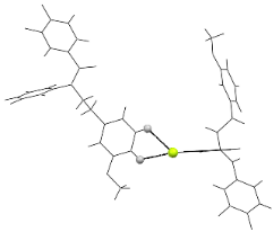 4a-5
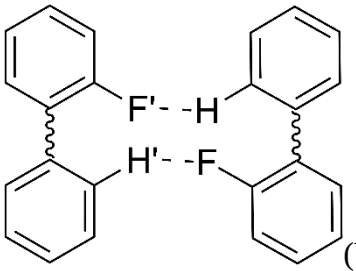 (VI)	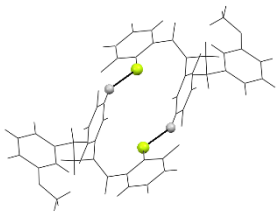 4a-7
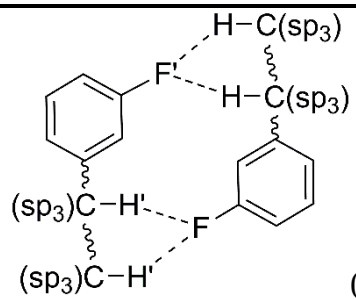 (VII)	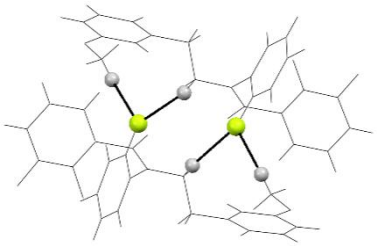 4a-7
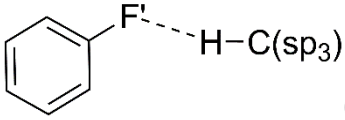 (VIII)	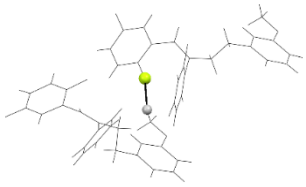 4a-12
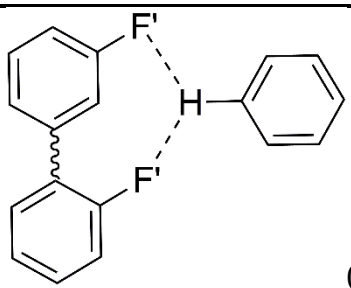 (IX)	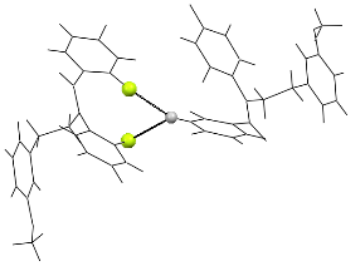 4a-8

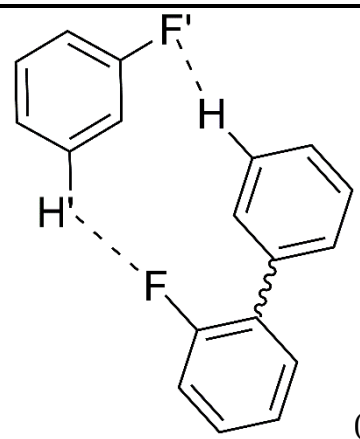 (X)	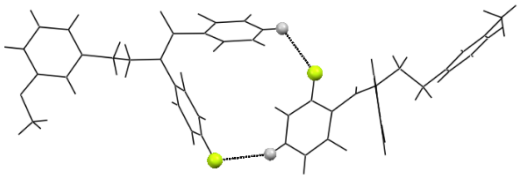 4a-10
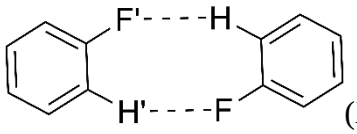 (XI)	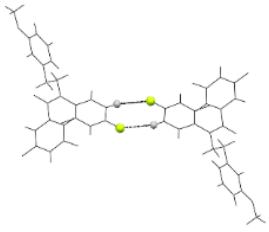 4a-12
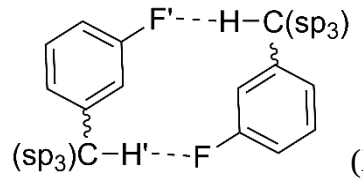 (XII)	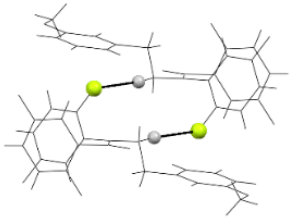 4a-15
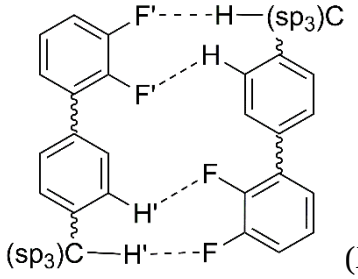 (XIII)	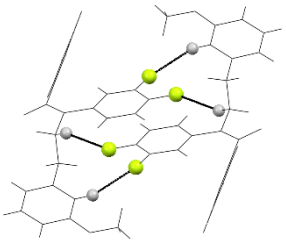 4a-30

Table 3.4.2: Geometric parameters of all the intermolecular interactions involved in crystal structures

D–B···X* (Synthon)	d(D···X) (Å)	d(B···X) (Å)	∠D-B···X (°)	ΔE (kcal mol^{-1})	Symmetry
4a-4					
C7–H7···F2′ and C8–H8···F2′ (I)	3.168(1) and 3.150(1)	2.683(1) and 2.651(1)	112.29(1) and 113.28 (1)	-5.9	2-x,1-y,2-z
C19–H19···F1′ and C1′–H1A′···F2 (II)	3.370 (1) and 3.266 (1)	2.685(1) and 2.391	129.55(6) and 146.96(2)	-9.0	x-1,y,z and x+1, -y,-z
C14–H14···O2′	3.531(1)	2.672(1)	150.74(3)	-5.3	-x+2,-y+1,-z+1
C19–H19···O1′=C16′	3.456(1)	2.552(1)	159.09(4)	-9.0	x-1,+y,+z
4a-5					
C2–H2A···F1′ and C4–H4···F1′ (III)	3.390(1) and 3.516(1)	2.49(1)1 and 2.690(1)	154.21(2) and 148.41(2)	-6.2	-x,+y+½,-z+ ½
C14–H14···F2′ (IV)	3.175(1)	2.507(1)	128.97(2)	-1.8	-x-1,+y+½,-z+½
C6–H6···F4′ and C7–H7···F4′ (V)	3.202 (1) and 3.247(1)	2.577(2) and 2.655(1)	124.99(2) and 122.14(2)	-1.3	-x+3/2,-y+1,+z+½
C21–H21···O1′=C16′ and C22–H22···O1′=C16′	3.244(1) and 3.140(1)	2.706(1) and 2.471(1)	117.64(1) and 128.99(1)	-4.4	x-½,-y+½,-z+1
C18–H18···O2′	3.472(1)	2.670(1)	144.82(1)	-4.5	-x+1,+y-½,-z+½
4a-7					
C14–H14B···F1B’ (VI)	3.221(1)	2.412(1)	145.50(1)	-5.4	-x+1,-y+1,-z+1
C9B–H9BB···F3A’ (VII)	3.604(1)	2.671(2)	163.98(1)	-12.7	-x+1,+y+½,-z+3/2
C2A–H2AB···F4A’ (VIII)	3.603(1)	2.678(2)	159.56(1)	-5.6	x+1,+y,+z
C2B–H2BA···F4B’ (VIII)	3.351(1)	2.537(2)	141.47(2)	-6.0	x+1,+y,+z
C20B–H20B···O1A’=C16A’	3.423(1)	2.495(2)	175.58(3)	-6.9	x,y,z
C12–H12B···O1B’=C16B’	3.241(1)	2.410(1)	148.63(1)	-6.0	x-1,+y,+z
C7B–H7B···O2A’	3.320(1)	2.405(2)	167.85(3)	-2.2	x,+y+1,+z
C21B–H21B···O2B’	3.199(1)	2.666(2)	117.10(1)	-1.7	-x+2,+y-½,-z+3/2
4a-8					
C4–H4···F4’ (IV)	3.496(1)	2.608(1)	155.72(1)	-5.2	-x+1,+y+½,-z+1
C19–H19···F3’ and C19–H19···F1’ (IX)	3.353(1) and 3.403(1)	2.670(1) and 2.504(2)	129.24(1) and 157.76(1)	-2.7	-x,+y-½,-z+1
C8–H8···O1’=C16’ and C22–H22···O1’=C16’	3.645(1) and 3.173(1)	2.732(1) and 2.351(1)	161.40(1) and 144.53(1)	-5.2	-x,+y+½,-z and -x,+y-½,-z
C21–H21···O1’=C16’	3.112(1)	2.597(1)	114.45(1)	-10.7	x,+y-1,+z
C12–H12···O2’	3.356(1)	2.410(1)	173.68(1)	-5.2	-x+1,+y-½,-z+1

4a-9					
C9–H9B···F1’ (VIII)	3.321(1)	2.370(2)	170.59(1)	-9.8	-x+½,+y+½,+z
C8–H8···F2’ (IV)	3.326(1)	2.462(1)	154.67(2)	-5.0	x,-y+½,+z-½
C20–H20···F4’ (IV)	3.313(2)	2.509(2)	144.95(1)	-1.2	-x+½,-y,+z+½
C6–H6···O1’=C16’	3.384(1)	2.599(2)	142.43(1)	-1.9	x,-y+3/2,+z-½
C19–H19···O1’=C16’	3.501(1)	2.667(2)	149.56(1)	-9.8	-x+½,+y-½,+z
C12–H12A···O2’	3.208(1)	2.476(2)	135.66(1)	-3.1	x,+y-1,+z
4a-10					
C8–H8···F1’ (IV)	3.343(1)	2.655(1)	131.33(2)	-8.2	-x+1,+y-½,-z+½
C20–H20···F1’ and C20’–H20’···F4 (X)	3.211(1) and 3.484(2)	2.612(1) and 2.647(1)	122.68(2) and 150.15(4)	-3.2	x-½,-y+3/2,-z
C14–H14B···F3A’ (IV)	3.306(1)	2.680(1)	125.27(2)	-1.1	-x,+y+½,-z+½
C14–H14A···O1’=C16’ and C15–H15A···O1’=C16’	3.188(1) and 3.177(1)	2.636(1) and 2.595(1)	118.62(2) and 121.17(2)	-8.2	-x+1,+y+½,-z+½
C2–H2A···O2’	3.531(1)	2.695(1)	144.59(2)	-7.2	x-½,-y+3/2,-z+1
C12–H12A···O1’=C16’	3.332(1)	2.432(1)	162.95(2)	-3.6	x-1,+y,+z
4a-11					
C18–H18···F1’ (IV)	3.330(2)	2.497(1)	149.10(1)	-2.8	-x+2,+y+½,-z+1
C4–H4···F4’ (IV)	3.463(1)	2.604(2)	153.78(1)	-5.2	-x+1,+y+½,-z+1
C21–H21···O1’=C16’	3.123(1)	2.747(2)	105.25(1)	-11.4	x,+y-1,+z
C22–H22···O1’=C16’	3.182(2)	2.412(1)	140.10(1)	-4.7	-x+2,+y-½,-z+2
C12–H12···O2’	3.345(1)	2.418(1)	174.81(1)	-5.1	-x+1,+y-½,-z+1
4a-12					
C4–H4B···F1A’ (IV)	3.250(1)	2.559(2)	129.84(1)	-2.9	-x+2,-y+1,-z+1
C9B–H9BB···F2A’ (VIII)	3.350(1)	2.539(2)	139.97(2)	-13.9	x,-y+½,+z-½
C9A–H9AC···F2B’ (VIII)	3.060(1)	2.385(1)	125.44(2)	-13.9	x,-y+½,+z+½
C4–H4B···F3A’ and C1B–H1BA···F3A’ (III)	3.347(1) and 3.576(1)	2.549(1) and 2.600(2)	141.67(1) and 168.65(2)	-13.6	x,-y+½,+z-½
C14–H14B···F4B’ (XI)	3.519(1)	2.678(1)	147.90(2)	-2.0	-x+1,-y,-z+1
C15–H15B···O1A’=C16A’	3.402(1)	2.571(2)	146.17(2)	-13.9	x,-y+½,+z-½
C7–H7B···O1A’=C16A’	3.475(1)	2.608(1)	151.87(1)	-5.0	-x+2,+y-½,-z+3/2
C20–H20B···O1A’=C16A’	3.297(1)	2.388(2)	160.07(2)	-3.8	-x+1,-y+1,-z+1
C20–H20A···O1B’=C16B’	3.449(1)	2.708(2)	135.33(2)	-2.9	-x+2,-y+1,-z+1
C12–H12B···O1B’=C16B’	3.420(1)	2.551(1)	152.04(1)	-4.0	x,-y+½,+z+½
C9–H9BA···O2B’	3.679(1)	2.740(1)	160.67(1)	-2.6	x+1,-y+½,+z-½
4a-13					
C9–H9B···F1’ (VIII)	3.205(1)	2.688(1)	113.29(4)	-9.7	-x,-y,-z+1
C9–H9C···F2’ (VIII)	3.482(2)	2.551(1)	158.65(5)	-1.8	x,+y,+z-1

C4–H4···F4' (XI)	3.430(1)	2.587(1)	148.09(4)	-6.3	-x+1,-y,-z+1
C12–H12···O1'=C16' and C13–H13···O1'=C16'	3.165(1) and 3.073(1)	2.640(1) and 2.452(1)	115.31(4) and 122.83(4)	-4.4	x,+y-1,+z
C21–H21···O2'	3.271(2)	2.550(1)	132.87(5)	-2.2	x+1,+y,+z+1
C6–H6···O2'	3.447(1)	2.618(1)	146.05(4)	-4.0	-x,-y+1,-z
4a-15					
C12–H12···F3' (XI)	3.418(1)	2.670(1)	137.94(2)	-2.3	-x+2,-y+1,-z+1
C1–H1A···F3' (XII)	3.556(1)	2.591(1)	173.57(2)	-10.3	-x+1,-y+1,-z+1
C12–H12···O1'=C16'	3.076(1)	2.308(1)	139.55(3)	-5.7	x+1,+y,+z
C1–H1B···O1'=C16'	3.510(1)	2.727(1)	138.20(2)	-10.2	-x+1,-y+1,-z+1
4a-16					
C21–H21···F1' (VI)	3.381(1)	2.585(1)	143.96(3)	-3.8	-x+1,-y+1,-z+2
C1–H1B···F2' (VIII)	3.562(1)	2.592(1)	177.66(4)	-9.2	x-1,+y,+z
C1–H1A···F4' (VIII)	3.465(1)	2.506(1)	169.76(4)	-9.2	x-1,+y,+z
C12–H12···O1'=C16' and C13–H13···O1'=C16'	3.019(1) and 3.157(1)	2.376(1) and 2.661(1)	126.14(3) and 114.17(3)	-5.1	x,+y-1,+z
C19–H19···O1'=C16'	3.286(1)	2.510(1)	140.99(4)	-9.2	x+1,+y,+z
C4–H4···O2'	3.612(1)	2.685(1)	174.58(4)	-4.4	-x,-y+1,-z+1
4a-17					
C21–H21A···F2' (XI)	3.401(3)	2.665(2)	136.50(8)	-2.0	-x-1,-y+1,-z+1
C8–H8···F4' (VI)	3.386(3)	2.521(2)	154.81(7)	-4.9	-x,-y+2,-z+1
C6–H6···O1'=C16' and C18–H18A···O2'	3.376(2) and 3.556(3)	2.524(2) and 2.735(2)	152.46(8) and 147.65(8)	-3.3	-x+3/2,+y+½,-z+3/2
C13–H13···O1'=C16'	3.162(4)	2.488(2)	129.53(6)	-5.3	x-½,-y+3/2,+z-½
4a-18					
C8–H8···F4' (VI)	3.396(1)	2.529(1)	155.27(2)	-5.0	-x+2,-y+2,-z+1
C6–H6···O1'=C16'	3.373(1)	2.524(1)	152.02(2)	-3.2	-x,+y+½,-z+½
C18–H18···O2'	3.538(1)	2.711(1)	148.61(3)	-3.2	-x,+y-½,-z+½
C13–H13···O1'=C16'	3.179(1)	2.499(1)	130.14(2)	-5.1	x+1,-y+3/2,+z+½
4a-19					
C9–H9B···F1' (VIII)	3.197(1)	2.551(1)	124.79(1)	-2.7	x,-y+½,+z+½
C12–H12···F1' (IV)	3.362(2)	2.669(1)	131.86(1)	-3.9	x,-y+3/2,+z+½
C9–H9A···F4' (VIII)	3.234(2)	2.631(2)	121.13(1)	-7.1	-x+1,+y-½,-z+½
C20–H20···O1'=C16' and C21–H21···O1'=C16'	3.127(1) and 3.052(2)	2.684(1) and 2.532(1)	110.03(1) and 115.63(1)	-5.5	-x+2,+y+½,-z+½
C12–H12···O2' and C13–H13···O2'	3.183(1) and 3.224(1)	2.566(1) and 2.638(2)	124.18(1) and 121.66(1)	-6.7	-x+1,-y+1,-z+1
4a-20					
C9–H9C···F1' (VIII)	3.387(1)	2.417(1)	170.04	-8.0	x-½,+y,-z+½

C13–H13···F2' (IV)	3.306(2)	2.556(2)	136.00(1)	-1.3	-x+1,+y+½,-z+½
C19–H19···O1'=C16'	3.334(2)	2.422(2)	160.74(1)	-8.0	x+½,+y,-z+½
C14–H14···O2'	3.178(2)	2.408(2)	137.96(1)	-3.0	x+1,+y,+z
4a-22					
C9–H9A···F2' (XII)	3.587(1)	2.650(1)	165.44(1)	-6.6	-x+1,-y+1,-z+1
C12–H12···O1'=C16'	3.167(1)	2.480(1)	130.81(1)	-6.0	x,+y+1,+z
C14–H14···O2'	3.282(1)	2.507(1)	140.90(2)	-2.9	x-1,+y+1,+z
4a-23					
C2–H2B···F1' and C8–H8···F1' (III)	3.383(1) and 3.324(1)	2.602(1) and 2.485(2)	137.81(1) and 150.26(1)	-6.9	-x+3/2,+y+1/2,+z
C13–H13···F2' (IV)	3.359(2)	2.558(1)	144.45(1)	-1.5	-x+2,+y+1/2,-z+1/2
C6–H6···O1'=C16'	3.505(2)	2.741(1)	140.00(1)	-1.8	-x+1/2,+y+1/2,+z
C21–H21···O1'=C16'	3.431(2)	2.590(1)	150.68(1)	-6.7	x+1/2,+y,-z+1/2
C14–H14···O2	3.185(1)	2.477(2)	133.03(1)	-3.2	x+1,+y,+z
4a-25					
C14A–H14A···F2A' (IV)	3.349(1)	2.642(1)	133.32(3)	-2.9	-x,+y-1/2,-z+1/2
C11A–H11A···O1'=C16'	3.204(1)	2.347(1)	152.99(3)	-11.1	-x+1,+y-1/2,-z+1/2
C9–H9A···O2'	3.517(1)	2.718(1)	141.08(2)	-3.0	-x+2,-y+1,-z+1
4a-27					
C14A–H14A···F1A' (IV)	3.332(1)	2.580(1)	138.36	-2.2	x,+y-1,+z
C1–H1A···F2A' (VIII)	3.428(2)	2.529(2)	154.24(1)	-4.0	x,-y+1/2,+z-1/2
C19A–H19A···F3A' (IV)	3.326(1)	2.507(1)	147.06(1)	-2.6	-x+2,+y+1/2,-z+3/2
C20A–H20A···F3A' (IV)	3.537(1)	2.637(1)	163.05(1)	-4.0	x,-y+1/2,+z+1/2
C15A–H15A···O1'=C16' and C2–H2B···O1'=C16'	3.304(2) and 3.449(2)	2.456(1) and 2.736(1)	151.62(1) and 130.79(1)	-9.3	-x+1,+y-1/2,-z+3/2
C9–H9B···O2'	3.520(1)	2.678(1)	146.78(1)	-3.0	-x,-y+1,-z+1
4a-28					
C8–H8···F2' (IV)	3.263(1)	2.663(1)	122.96(1)	-7.1	-x+1,+y-1/2,-z+3/2
C20–H20···F2' and C20'–H20'···F4 (X)	3.236(1) and 3.436(1)	2.684(1) and 2.611(1)	118.79(1) and 148.14(2)	-3.4	x+1/2,-y+3/2,-z+2
C15–H15···F3' (IV)	3.073(1)	2.558(1)	115.32(1)	-2.0	-x+2,+y-1/2,-z+3/2
C9–H9A···F3' (VIII)	3.545(2)	2.619(1)	162.22(1)	-0.6	-x+1/2+1,-y+2,+z-1/2
C6–H6···O1'=C16'	3.503(2)	2.670(1)	149.45(1)	-3.2	-x+1/2,-y+1,+z-1/2
C11–H11···O1'=C16'	3.235(2)	2.503(1)	135.71(1)	-7.1	-x+1,+y+1/2,-z+3/2
C14–H14···O1'=C16'	3.464(1)	2.572(2)	160.86(1)	-4.3	x+1,+y,+z
4a-30					
C9–H9C···F1' (VIII)	3.276(1)	2.661(1)	122.30(4)	-1.0	x,+y,+z-1
C6–H6···F2' (IV)	3.377(1)	2.817(1)	119.76(4)	-1.3	-x+1,-y+1,-z+1

C4–H4···F3' and C1–H1A···F4' (XIII)	3.477(2) and 3.541(1)	2.589(1) and 2.667(1)	159.94(4) and 150.05(4)	-8.7	-x+2,-y+1,-z+1
C1–H1B···F4' (VIII)	3.221(1)	2.616(1)	120.73(4)	-4.9	x-1,+y,+z
C14–H14···O1'=C16'	3.289(1)	2.398(1)	160.43(4)	-4.9	-x+1,-y+1,-z+1
C9–H9A···O2'	3.495(1)	2.732(1)	136.94(4)	-2.2	-x+1,-y,-z
C22–H22···O2'	3.447(2)	2.570(1)	157.44(5)	-15.4	-x+1,-y,-z+1
4a-31					
C11–H11···F2' (VI)	3.376(1)	2.518(1)	153.66(2)	-5.3	-x+1,-y+1,-z
C9–H9B···F3' (VIII)	3.145(1)	2.354(1)	139.34(3)	-0.5	x+1,+y+1,+z
C1–H1B···F3' (VIII)	3.439(1)	2.563(1)	150.29(4)	-10.0	x+1,+y,+z
C22–H22···F4' (IV)	3.161(1)	2.505(1)	127.73(2)	-1.6	x-1,+y+1,+z
C13–H13···O1'=C16'	3.392(1)	2.541(1)	152.34(3)	-3.6	x,+y-1,+z
C6–H6···O2'	3.506(1)	2.639(1)	155.40(3)	-0.6	-x+2,-y+2,-z+1
4a-33					
C22–H22···F1' (IV)	3.551(1)	2.689(1)	151.14	-9.1	-x+1,+y-1/2,-z+1/2
C13–H13···F2' (VI)	3.416(1)	2.642(1)	138.96	-4.4	-x,-y,-z
C20–H20···F3' (VI)	3.122(2)	2.597(1)	115.19	-3.5	-x,-y+1,-z
C1–H1B···F3' (VIII)	3.443(2)	2.527(1)	153.76(1)	-3.6	x+1,-y+1/2,+z+1/2
C15–H15···O1'=C16' and C22–H22···O1'=C16'	3.370(2) and 3.413(2)	2.557(1) and 2.724(1)	143.73 and 129.99	-9.1	-x+1,+y-1/2,-z+1/2
C20–H20···O2'	3.362(2)	2.431(1)	166.27(1)	-2.3	x-1,+y,+z
4a-34					
C1–H1A···F2' (XII)	3.165(1)	2.472(1)	128.11(2)	-4.1	-x+2,-y+1,-z+1
C13–H13···O1'=C16'	3.496(1)	2.644(1)	152.59(2)	-8.1	x,-y+1/2,+z+1/2
C20–H20···O1'=C16'	3.172(1)	2.441(1)	135.59(2)	-5.0	x,+y-1,+z
C19–H19···O2'	3.430(1)	2.511(1)	169.77(2)	-8.1	x,-y+1/2,+z-1/2
4a-35					
C4–H4···F1' (VI)	3.274(2)	2.358(1)	168.23(6)	-5.5	-x,-y+1,-z+1
C9–H9C···F2' (VIII)	3.302(1)	2.670(1)	123.86(4)	-1.4	x+1,+y-1,+z+1
C21–H21···F3' (VI)	3.035(2)	2.668(2)	104.29(3)	-3.6	-x+1,-y+1,-z
C7–H7···O1'=C16'	3.241(2)	2.387(1)	152.57(5)	-4.1	x+1,+y-1,+z
C11–H11···O1'=C16'	3.495(1)	2.612(1)	158.73(3)	-13.7	-x+1,-y+1,-z+1
C18–H18···O1'=C16'	3.346(1)	2.562(1)	142.15(4)	-5.5	-x,-y+1,-z+1
C9–H9B···O2'	3.218(2)	2.388(2)	144.56(3)	-3.9	-x+1,-y,-z+2
4a-36					
C1–H1A···F1' and C8–H8···F1' (III)	3.442(1) and 3.450(1)	2.638(2) and 2.684(2)	140.48(1) and 140.15(1)	-3.8	x+1,-y+3/2,+z+1/2
C18–H18···F3' (IV)	3.140(1)	2.655(2)	113.17	-1.5	x,+y-1,+z

C13–H13···F4' (IV)	3.414(1)	2.550(2)	154.82(1)	-1.5	-x+2,+y+1/2,-z+1/2
C11–H11···O1'=C16'	3.271(1)	2.416(2)	152.87(1)	-12.1	-x+1,+y+1/2,-z+1/2
C13–H13···O2'	3.222(1)	2.713(1)	115.28(1)	-2.5	x,-y+3/2,+z-1/2
C15–H15···O2'	3.318(1)	2.426(1)	160.69(1)	-12.2	-x+2,-y+1,-z+1
4a-37					
C7–H7···O1'=C16'	3.377(1)	2.598(1)	141.65(1)	-5.6	x,+y+1,+z
C18–H18···O1'=C16'	3.331(1)	2.676(1)	128.10(1)	-6.9	-x+1/2,-y+3/2,-z+1
C12–H12···O2'	3.441(1)	2.686(1)	138.85(1)	-11.7	-x+1/2,-y+ 5/2,-z+1

(* when X is O1, this represents the carbonyl oxygen in the crystal structure involved in the interaction and O2 represents the methoxy oxygen in the crystal structure involved in the interaction.)

We have performed a statistical analysis for all the compounds for C–H···F, C–H···O and C–H···O=C hydrogen bonds (Table 3.4.3). We have observed that the most probable distance (the distance where we have maximum number of given interactions) at which C–H···F interactions are occurring is between 2.5 Å and 2.6 Å and the most probable angle is observed between 150˚ and 160˚. C–H···O interactions are divided into two sub-categories which are C–H···O–C interactions and C–H···O=C type of interactions. C–H···O=C interactions are observed in every molecule, in some cases only one such interaction is present, in some cases multiple C–H···O=C are observed. Interestingly, for C–H···O=C interactions also, the most probable distance and the most probable angle is same as that for C–H···F interactions i.e. between 2.5Å and 2.6Å and 150˚ and 160˚. Whereas, for C–H···O–C interactions, we have observed a little deviation with the most probable distance being between 2.6 Å and 2.7 Å and the most probable angle for these interactions being between 140˚ and 150˚ respectively.

Table 3.4.3: Statistical Summary of C–H···F and C–H···O hydrogen bonds

Distance Range C–H···F/ C–H···O	**Number of C–H···F hydrogen bonds**	**Number of C–H···O–C hydrogen bonds**	**Number of C–H···O=C hydrogen bonds**
2.1≥d>2.0Å	0	0	0
2.2≥d>2.1Å	0	0	0
2.3≥d>2.2Å	0	0	0
2.4≥d>2.3Å	4	1	6
2.5≥d>2.4Å	6	8	11
2.6≥d>2.5Å	32	5	15
2.7≥d>2.6Å	29	9	9
2.8≥d>2.7Å	-	5	6
Angle Range ∠C–H···F/∠C–H···O	**Number of C–H···F hydrogen bonds**	**Number of C–H···O–C hydrogen bonds**	**Number of C–H···O=C hydrogen bonds**
110≥θ>100.0	0	0	1
120≥θ>110.0	6	2	5
130≥θ>120.0	15	1	3
140≥θ>130.0	11	6	7
150≥θ>140.0	12	8	11
160≥θ>150.0	17	3	13
170≥θ>160.0	8	5	6
180≥θ>170.0	3	3	1

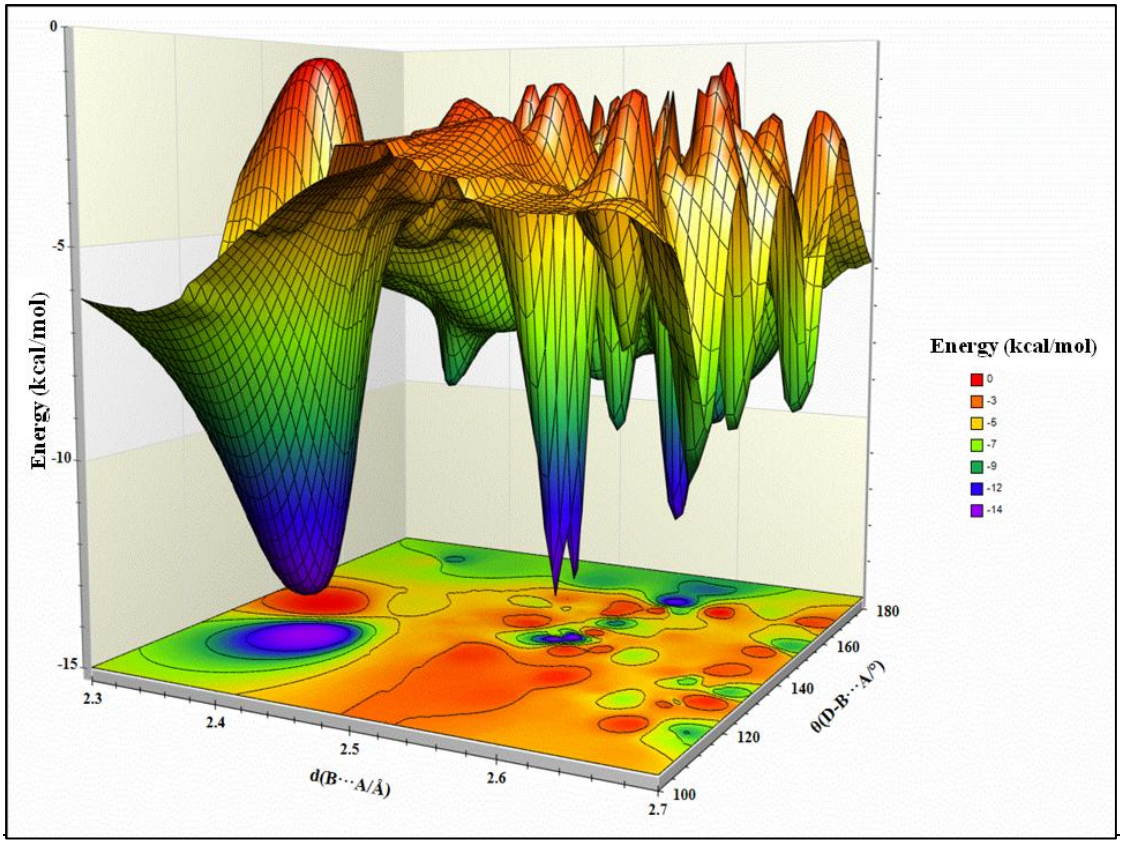

Figure 3.4.2: 3D graph representing the energies of various C–H···F–C interactions at their intermolecular distance and the angle.

We have plotted the energy values against the angle and the distance at which the interactions are taking place in a 3D graph (Figure 3.4.2). All the 71 C–H···F–C interactions are found to have negative value for the dimerization energy indicating the interactions to be stabilizing in nature. Among these 71 interactions, 35 interactions have the energy value between 0 and -4 kcal/mol and 36 interactions are found to have the energy values between -4 kcal/mol and -15 kcal/mol, which according to Desiraju and Steiner fall in the region of strong hydrogen bonds.[6]

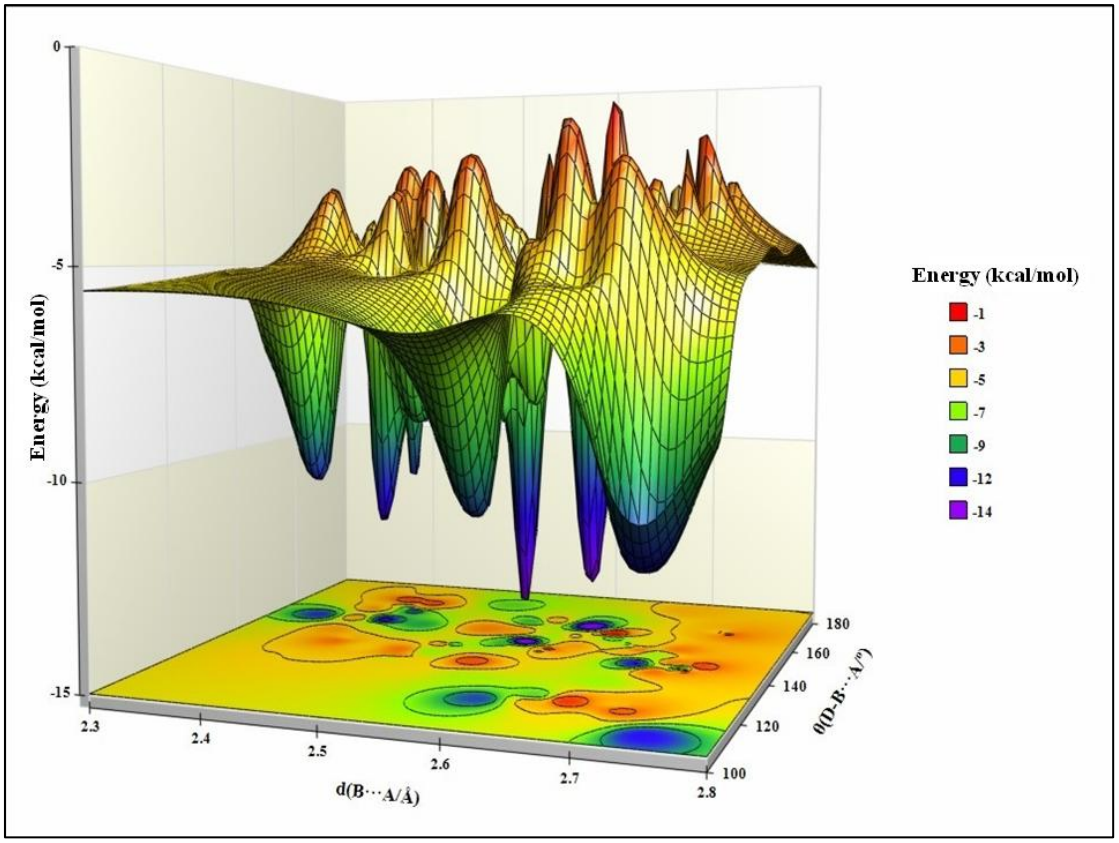

Figure 3.4.3: 3D graph representing the energies of various C–H···O interactions at their intermolecular distance and the angle

The 3D plot for C–H···O interactions was also plotted (Figure 3.4.3) and this shows all these interactions to be stabilising in nature. Here, only a few interactions have stabilization energy in Blue/Purple region (high stabilization) as compared to the C–H···F–C interactions and most of the C–H···O interactions have moderate stabilization energy.

Several interactions studied in this chapter displayed different types of intermolecular C–F···F–C contacts (namely Type I, Type II and quasi Type-I/Type-II). It has always been debated that the C–F···F–C contacts are generally symmetry driven (mostly across an inversion centre). But in our study, we have observed that the C–F···F–C interactions were responsible for forming molecular dimer through bifurcated

C–F···F–C contacts in 4a-17 (Figure 3.4.4a). It is noteworthy that the F3···F1A contact is between an ordered and disordered fluorophenyl ring. The stabilization energy for this dimer is calculated to be -4.7 kcal mol^{-1}. Both the C–F···F–C interaction in this molecule are of Quasi Type I/Type II type. Also, in the molecule, 4a-22, two bifurcated C–F···F–C interactions are observed (Figure 3.4.4b) where one interaction is between F2 and F4 and is a Type II kind of interaction whereas the other interaction is in between F4 and F4 which is a Type I kind of interaction. This dimer has a stabilization energy of -4.3 kcal mol^{-1}. The C–F···F–C interactions observed in all the molecules are given below (Table 3.4.4). The compound 4a-12 displays a unique C–F···F–C interaction between two molecules in the asymmetric unit, needless to mention that these molecules do not have any symmetry relation between them and they have different molecular conformation as well (Figure 3.4.4c). The stabilization energy of this time (4a-12) is also significant (-7.8 kcal/mol)

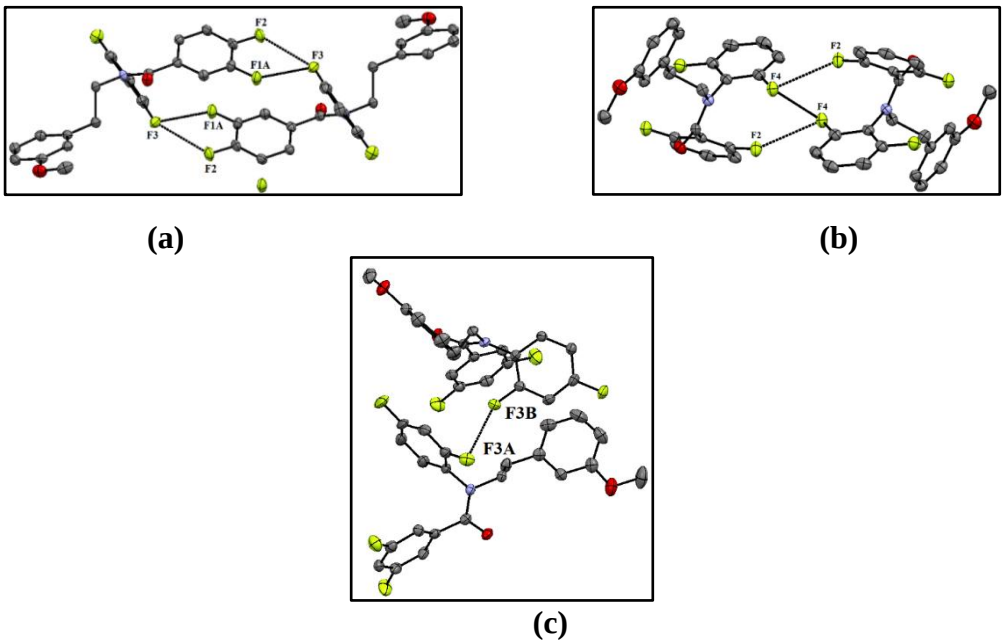

(a) **(b)**

(c)

Figure 3.4.4: (a) Bifurcated C–F···F–C interaction in 4a-17; (b): bifurcated C–F···F–C interaction in 4a-22; (c) C–F···F–C interaction in 4a-12 between two independent molecules in the asymmetric unit.

Table 3.4.4: Geometric parameters of the C–F···F–C intermolecular interactions involved in crystal structures

D–B···A	**d(D···A) (Å)**	**d(B···A) (Å)**	**∠D-B···A (°)**	**ΔE (kcal mol^{-1})**	**Symmetry**
4a-4					
C11–F3···F4'–C12' and C11–F3···F3'–C11'	3.640 (1) and 3.170 (1)	2.839(6) and 2.897(11)	116.05/90.49 and 90.49/90.49	-4.0	-x+2, -y+2, -z+1
4a-7					
C19A–F2A···F4B'–C13B'	3.881(5)	2.945(4)	142.41/124.91	-2.2	-x,-y+1,-z+1
4a-10					
C11B–F3A···F4'–C13B'	3.508(12)	2.934(10)	151.53/103.44	-1.1	-x,+y-½,-z+½
4a-11					
C19–F1···F3'–C11'	3.551(3)	3.167(3)	109.73/88.41	-2.7	x,+y+1,+z
4a-12					
C11A–F3A···F3B'–C11B'	2.976	2.769	85.29/148.67	-7.8	x, ½-y, ½+z
4a-16					
C22–F3···F3'–C22'	3.965(14)	2.988(10)	142.67/142.67	-3.7	-x+1,-y+1,-z+2
C11–F1···F2'–C14'	3.394(13)	2.946(10)	98.48/97.05	-9.2	x-1,+y,+z
4a-17					
C20A–F2···F2'–C20B'	3.621(3)	2.981(2)	108.14/108.14	-2.0	-x-1,-y+1,-z+1
C20A–F2···F3'–C11' and C19B–F1A···F3'–C11'	3.739(3) and 3.760(2)	2.828(2) and 2.884(1)	123.57/148.12 and 120.95/92.22	-4.7	-x,-y+1,-z+1
4a-18					
C19–F1···F3'–C11'	3.1225(7)	2.819(7)	116.76/89.83	-5.5	-x+2,-y+1,-z+1
C21–F2···F3'–C11'	4.256	2.949(1)	164.69/162.26	-8.9	x+1,+y,+z
4a-22					
C22–F2···F4'–C11' and C11–F4···F4'–C11'	2.991(5) and 2.804(5)	3.673(6) and 3.197(7)	143.65/109.80 and 94.10/94.10	-4.3	-x+1,-y+2,-z+1
4a-25					
C13B–F4···F1A'–C18A'	3.421(10)	2.963(9)	124.12/99.41	-2.8	-x,+y-1/2,-z+1/2
C18A–F1A···F3A'–C12A'	3.692(11)	2.632(9)	137.64/152.05	-0.2	x,+y+1,+z
4a-35					
C12–F4···F4'–C12'	4.193	2.997(15)	144.30/144.30	-0.3	-x+2,-y+1,-z
C12–F4···F1'–C19'	3.361(13)	2.743(16)	108.32/105.32	-1.0	x-1,+y,+z
4a-36					
C19–F2···F2'–C19'	3.245(3)	2.937(3)	90.45/90.45	-1.9	-x+1,-y+1,-z

Table 3.4.5: C–F···F–C intermolecular interactions found in the molecules

4a-4 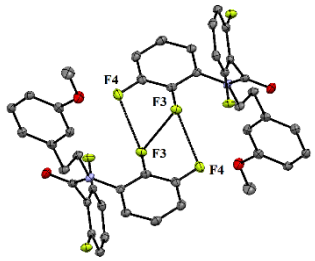	**4a-7** 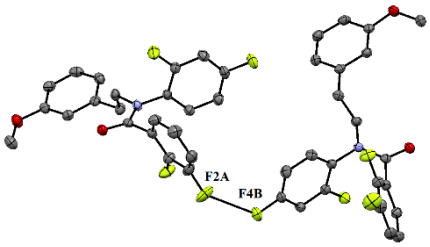
4a-10 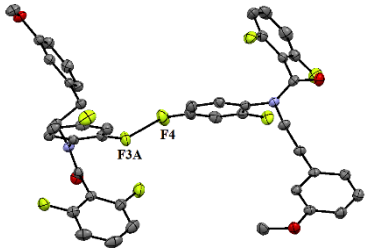	**4a-11** 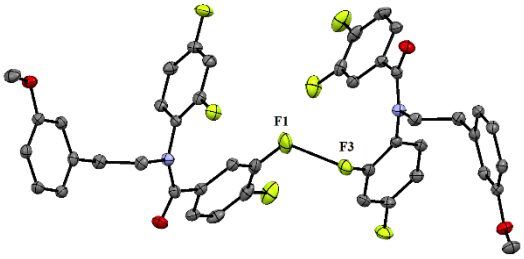
4a-16 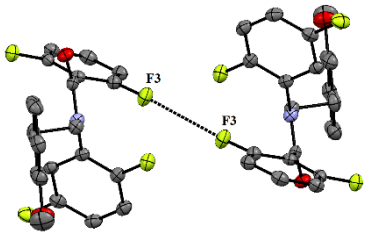	**4a-16** 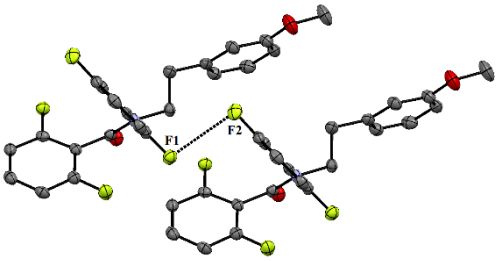
4a-17 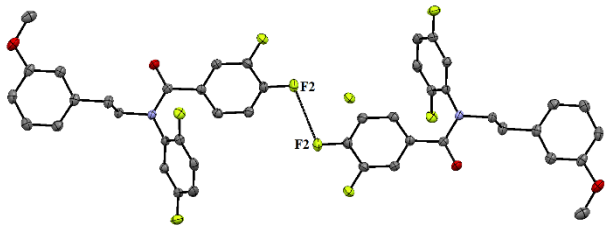	**4a-18** 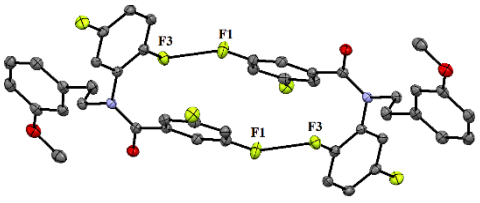

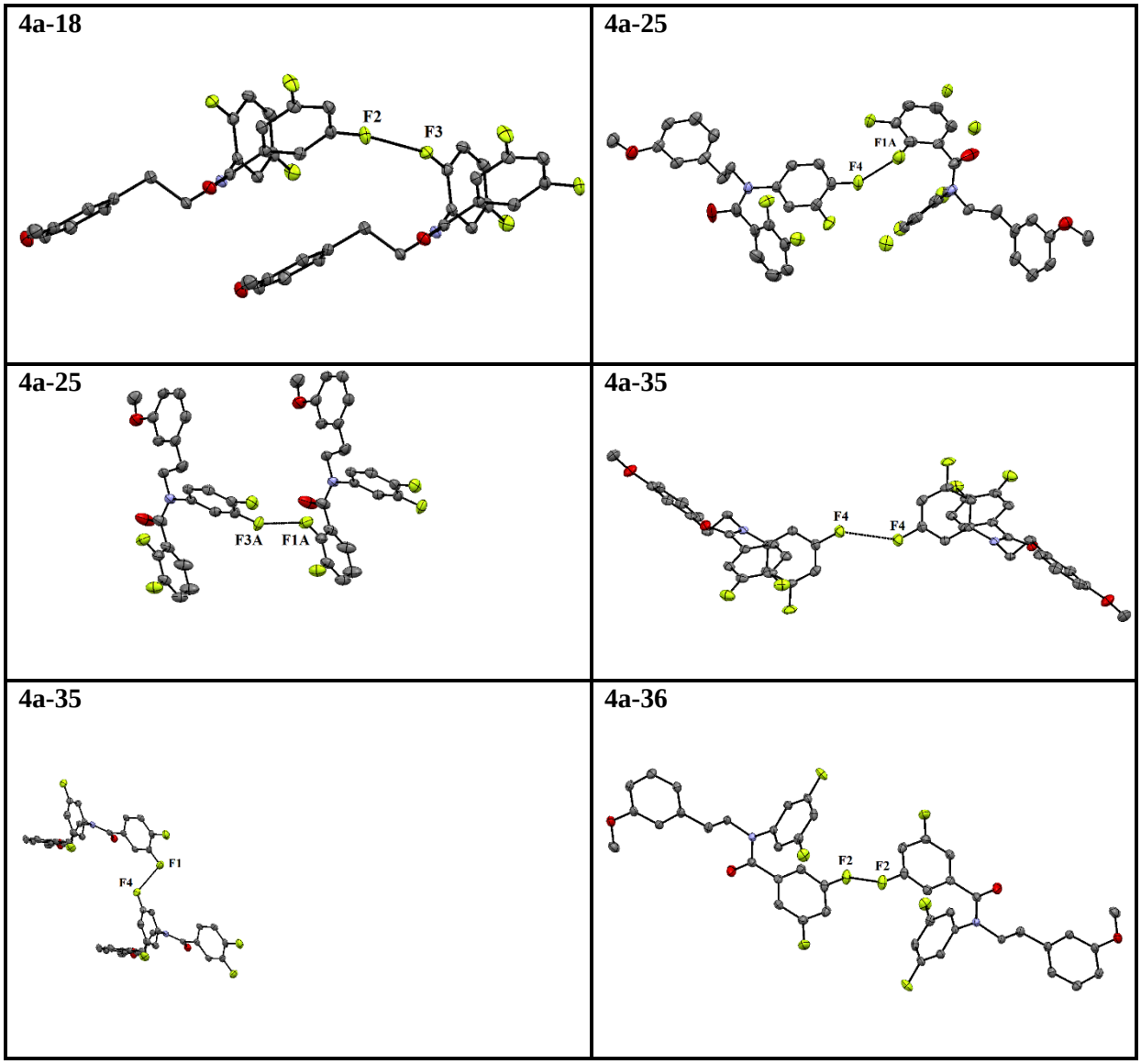

3.5 Conclusion

We have analysed the crystal structures of a library of small organic molecules containing four aromatic C–F bonds along with a carbonyl group in all the compounds. From the above analyses, it is evident that the molecules, though isomeric, adopt a wide range of crystal structures having a variety of space groups. The in-depth analysis indicates that all the fluorinated compounds reported herein are generally packed by several weak C–H···F–C, C–H···O–C, and C–H···O=C hydrogen bonds. Needless to mention that the structures of the fluorinated derivatives are significantly different from the non-fluorinated analogue (4a-37). We have observed 13 different synthons that help in

the formation of C–H···F–C hydrogen bonded dimers and these synthons were found in many structures reported herein. This indicates that the fluorine mediated interactions are important in fine tuning the crystal structures of small organic molecules in the presence of other weak hydrogen bonds. The appearance of C–F···F–C hydrogen bonds between the molecules is an indication that these interactions play an important role in providing stability to the structure. The energy calculations also show that these interactions are stabilizing in nature and help in the formation of dimer. In addition to the stabilization offered by C–H···F–C, C–H···O–C, and C–H···O=C hydrogen bonds, a variety of C–F···F–C interactions have also been found to provide stability to these structures. The presence of C–F···F–C between two molecules in the asymmetric unit (not related by any symmetry) emphasise the significance of such interactions in the crystal lattice. A careful experimental charge density analysis will reveal the importance of such interactions in crystal engineering, which is discussed in Chapter 5.

Chapter 4

Evaluation of fluorine mediated intermolecular interactions in tetra-fluorinated tetra-hydro isoquinoline derivatives: Computational and Topological Studies

Chapter 4

4.1 Introduction

In the previous chapter, we discussed the nature of organic fluorine mediated interactions in the tetra substituted secondary amides. From the computational analysis, we inferred that the interactions offered by the organic fluorine group are mostly strong in nature. It was also pointed out that the linear geometry is not common for these interactions. A comparison between the C–H···O=C, C–H···O–C, and C–H···F–C interactions is made to understand its nature. In the current chapter, a similar study is performed on the isoquinoline derivatives where the possibility of C–H···O=C interactions is absent. Isoquinoline, the linkage isomer of quinoline is a heterocyclic aromatic compound (Scheme 4.1.1).

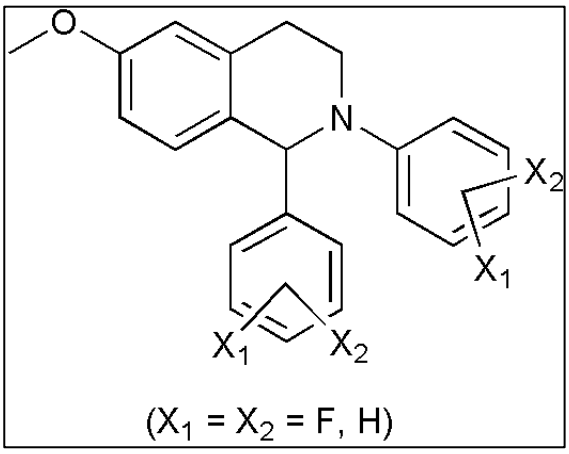

Scheme 4.1.1

We aim at the analysis of fluorine mediated interactions in a series of conformationally flexible fluorinated tetrahydroisoquinoline molecules containing four fluorine atoms in each. An earlier report on mono-halogenated (F, Cl and Br) diphenyl-tetrahydroisoquinoline derivatives reported anti-implantation activity displayed by the fluoro analogue while the chloro, bromo and non-halogenated analogues were inactive.[133] Subsequently, Choudhury *et al.*[37], reported the structural analysis of some of the compounds synthesized by Nagarajan *et al.*[133] Choudhury *et al.*[37] indicated that the fluorine mediated weak intermolecular interactions were responsible for their crystal packing and they emphasized that the interaction involving fluorine might be responsible for the biological activity of the fluorinated diphenyl tetrahydroisoquinoline. Further, Choudhury and Guru Row reported structural analysis of few more novel molecules belonging to the same molecular skeleton with two fluorine substitutions on two different phenyl rings and showed that the incorporation of second fluorine atom in the molecule resulted into a wider range of structural variations and several fluorine mediated supramolecular synthons were evident.[38,40] In another report, the structural analysis of the corresponding chloro and bromo analogues were discussed[39] and their structural differences with their fluorinated analogues were emphasized. It was shown that the fluorinated molecules represented unique features, which were not observed in their chloro or bromo analogues. Following these indications, a library of tetrafluorinated diphenyl-tetrahydroisoquinoline derivatives was synthesised (Scheme 4.1.2) earlier by Dr. Hare Ram Yadav for structural studies. Herein, in this chapter, computational and topological data are analysed to understand the role of "organic fluorine" in packing of flexible organic molecules in the absence of other stronger hydrogen bonds.

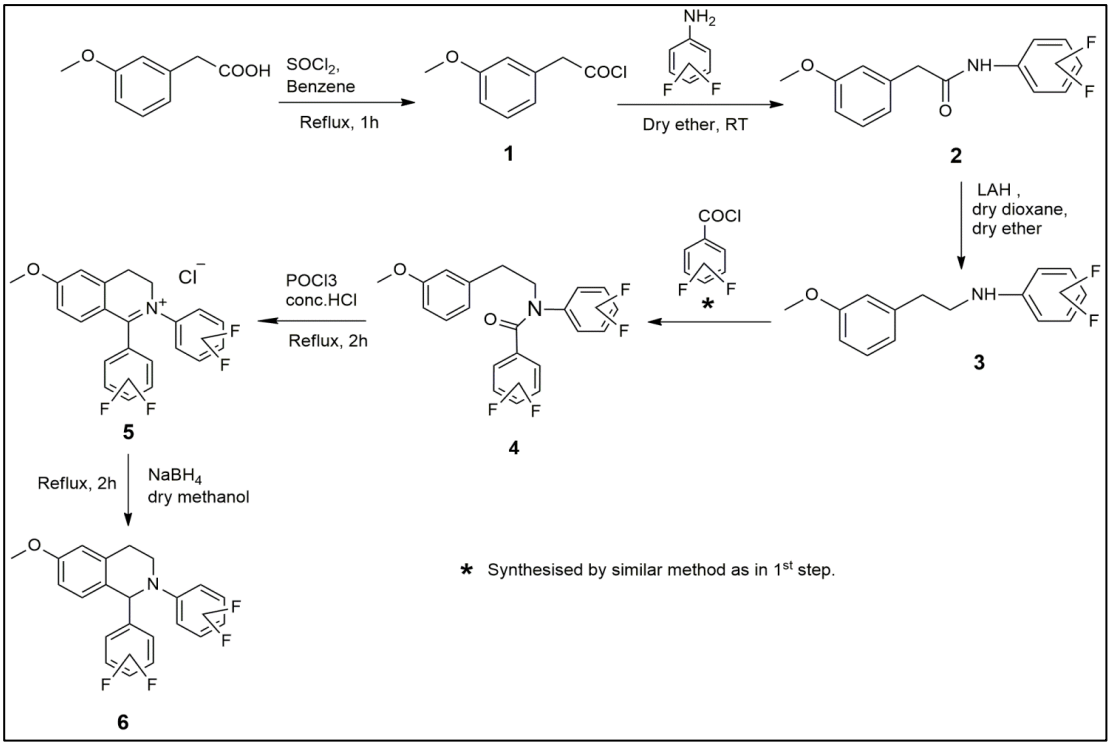

Scheme 4.1.2: Synthetic scheme for making the target molecules (Reproduced from the Ph. D. thesis of Dr. Hare Ram Yadav)

4.2 Experimental

4.2.1. Synthesis and Characterization

All the molecules reported herein were synthesized following the chemical scheme 4.1.2, as per the reported procedure[133] by Dr. Yadav in 2013-16 and the structural details of the compounds were elaborated in his thesis,[132] and later published with the computational analysis by us.[135] All the synthesized compounds were characterized by ^{1}H, ^{13}C and ^{19}F NMR and FTIR spectroscopy.[132] 36 tetrafluorinated isoquinoline derivatives (Scheme 4.2.1) and 1 unsubstituted analogue were synthesized. Among these 37 compounds, we could crystallize 20 compounds (rest were gummy liquids at RT) and the unit cell details for the crystals (collected at 100K) for these compounds are included in this chapter (Table 4.2.1-4.2.3).

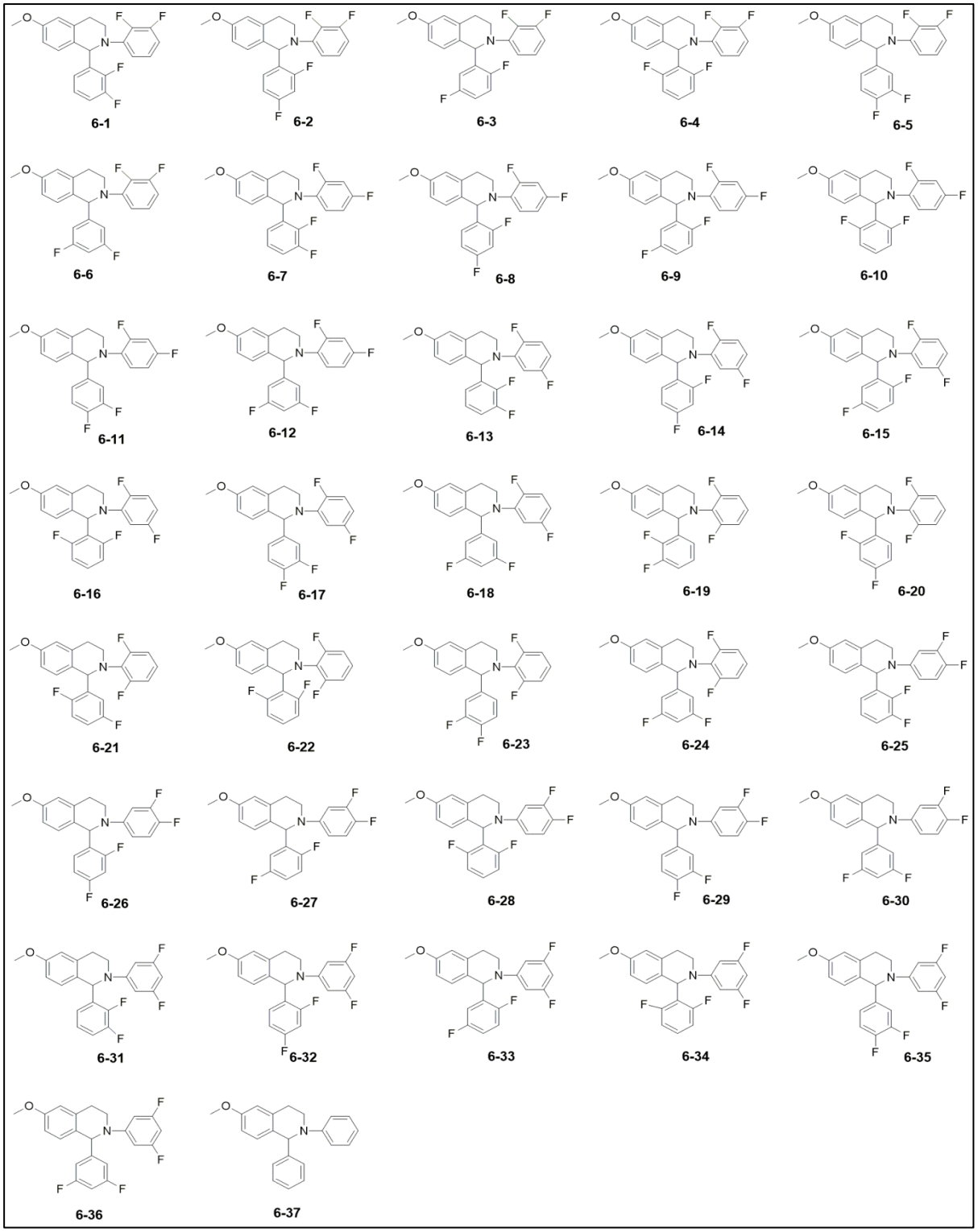

Scheme 4.2.1: Numbering scheme of the molecules reported in this chapter. (Reproduced from the Ph. D. thesis of Dr. Hare Ram Yadav)

Table 4.2.1: Single crystal X-ray diffraction data of 6-1 to 6-6. (Reproduced from the Ph. D. thesis of Dr. Hare Ram Yadav)

Identification code	**6-1**	**6-2**	**6-3**	**6-4**	**6-5**	**6-6**
CCDC No	1540717	1540721	1540725	1540731	1540732	1540733
Formula	$C_{22}H_{17}F_4NO$	$C_{22}H_{17}F_4NO$	$C_{22}H_{17}F_4NO$	$C_{22}H_{17}F_4NO$	$C_{22}H_{17}F_4NO$	$C_{22}H_{17}F_4NO$
Formula weight	387.37	387.37	387.37	387.37	387.37	387.37
Temperature (K)	100.0(2)	100.0(2)	100.0(2)	100.0(2)	100.0(2)	100.0(2)
Crystal system	Monoclinic	Monoclinic	Monoclinic	Monoclinic	Monoclinic	Monoclinic
Space group	$P2_1$	$P2_1/c$	$P2_1/c$	$P2_1$	$P2_1/c$	$C2/c$
***a* (Å)**	8.210(4)	9.705(3)	9.642(2)	8.317(3)	13.3660(13)	22.323(8)
***b* (Å)**	6.330(2)	13.476(3)	13.292(2)	6.0774(19)	11.6008(10)	13.499(5)
***c* (Å)**	17.277(9)	13.843(4)	13.931(3)	17.513(6)	30.052(3)	11.828(5)
***α* (°)**	90	90	90	90	90	90
***β* (°)**	102.410(19)	101.162(11)	99.890(9)	103.095(13)	130.787(3)	98.459(17)
***γ* (°)**	90	90	90	90	90	90
***V* (Å^3)**	876.9(7)	1776.3(8)	1758.9(6)	862.2(5)	3528.1(6)	3526(2)

Table 4.2.2: Single crystal X-ray diffraction data of 6-7 to 6-21. (Reproduced from the Ph. D. thesis of Dr. Hare Ram Yadav)

Identification code	**6-7**	**6-8**	**6-9**	**6-13**	**6-16**	**6-19**	**6-21**
CCDC No	1540734	1540735	1540736	1540718	1540719	1540720	1540722
Formula	$C_{22}H_{17}F_4NO$	$C_{22}H_{17}F_4NO$	$C_{22}H_{17}F_4NO$	$C_{22}H_{17}F_4NO$	$C_{22}H_{17}F_4NO$	$C_{22}H_{17}F_4NO$	$C_{22}H_{17}F_4NO$
Formula weight	387.37	387.37	387.37	387.37	387.37	387.37	387.37
Temperature (K)	100.0(2)	100.0(2)	100.0(2)	100.0(2)	100.0(2)	100.0(2)	100.0(2)
Crystal system	Monoclinic	Orthorhombic	Monoclinic	Monoclinic	Monoclinic	Monoclinic	Monoclinic
Space group	$C2/c$	$Pca2_1$	$P2_1/c$	$C2/c$	Pc	$P2_1/c$	Pn
***a* (Å)**	36.448(11)	16.559(2)	9.445(6)	36.079(4)	17.468(3)	18.194(6)	7.6714(11)
***b* (Å)**	6.1171(18)	17.595(2)	21.293(11)	6.2372(6)	6.2025(10)	6.147(2)	7.1287(9)
***c* (Å)**	16.087(4)	6.1048(9)	9.590(6)	16.051(2)	16.338(3)	16.182(5)	16.428(2)
***α* (°)**	90	90	90	90	90	90	90
***β* (°)**	102.193(7)	90	112.96(2)	104.627(6)	92.208(9)	104.903(11)	100.298(6)
***γ* (°)**	90	90	90	90	90	90	90
***V* (Å^3)**	3505.8(17)	1778.7(4)	1775.9(18)	3495.0(7)	1768.9(5)	1749.0(10)	883.9(2)

T**able 4.2.3:** Single crystal X-ray diffraction data of **6-23** to **6-37.** (Reproduced from the Ph. D. thesis of Dr. Hare Ram Yadav)

Identification code	**6-23**	**6-25**	**6-30**	**6-31**	**6-33**	**6-34**	**6-37**
CCDC No	1540723	1540724	1540726	1540727	1540728	1540729	1540730
Formula	$C_{22}H_{17}F_4NO$	$C_{22}H_{17}F_4NO$	$C_{22}H_{17}F_4NO$	$C_{22}H_{17}F_4NO$	$C_{22}H_{17}F_4NO$	$C_{22}H_{17}F_4NO$	$C_{22}H_{21}NO$
Formula weight	387.37	387.37	387.36	387.38	387.38	387.38	315.40
Temperature (K)	100.0(2)	100.0(2)	100.0(2)	100.0(2)	100.0(2)	100.0(2)	100.0(2)
Crystal system	Orthorhombic	Monoclinic	Monoclinic	Triclinic	Triclinic	Monoclinic	Monoclinic
Space group	*Pbca*	$P2_1/c$	$P2_1/c$	$P\bar{1}$	$P\bar{1}$	$P2_1$/c	*Pbca*
***a* (Å)**	16.643(3)	12.287(2)	12.947(3)	11.13700(10)	10.6975(7)	11.322(2)	10.3744(14)
***b* (Å)**	6.1042(10)	11.3169(16)	10.4113(18)	11.8983(2)	13.2186(4)	12.437(2)	16.379(2)
***c* (Å)**	35.217(7)	22.191(4)	22.590(5)	15.127	13.6339(2)	20.012(3)	19.851(3)
***α* (°)**	90	90	90	73.675(12)	68.667(14)	90	90
***β* (°)**	90	145.954(6)	145.306(10)	71.730(13)	80.428(18)	140.922(8)	90
***γ* (°)**	90	90	90	72.936(11)	81.09(2)	90	90
***V* (Å^3)**	3577.8(11)	1727.5(5)	1733.2(7)	1779.8(2)	1761.4(2)	1776.3(5)	3373.2(8)

4.2.2 Computational Analysis

The fluorinated molecules were found to crystallize through various fluorine and oxygen mediated interactions (C–H···F–C, C–F···F–C and C–H···O) forming different types of dimers. Of all the interactions observed in the crystal systems, our primary interest was to look at the role played by C–H···F–C hydrogen bonds in crystal packing. The stabilization energies of these dimers (involving C–H···F–C only) were calculated through Gaussian09[129] using MP2/6-31+G(d) level of theory. Gauss view[130] was used as a graphical interface for Gaussian09. Experimental CIFs were used for the primary coordinates of the molecules under study. C–H···F–C mediated monomers were first identified and the energy of each individual molecule was calculated ($E_{monomer}$). Similarly the energy of the dimer involving C–H···F–C interaction was calculated (E_{dimer}). The energy of the dimers was corrected for basis set superposition error (BSSE) using the counterpoise method. All these stabilization energy calculations are gas-phase

calculations. The stabilization energy ΔE^{F}_{dimer} of the dimeric motifs were then calculated using the following equations.

$$\Delta E^{F}_{dimer} = E_{dimer} - 2 \times E_{monomer} \quad \ldots\ldots\ldots\ldots\ldots\ldots 1$$

Equation 1 provides the stabilization energy of the dimer involving C–H···F–C hydrogen bond. The data for stabilization energies is given in table 4.3.1.

4.2.3 Topological Analysis

Bader's Quantum Theory of Atoms In Molecules[99] (QTAIM) calculations were performed to find the topological parameters (like electron density (ρ_c) and Laplacian ($\nabla^2 \rho_c$) at the bond critical points (BCP)) using AIM2000[134] package for the observed interaction after generating the suitable input wave-function files using Gaussian09 using the command (output=wfn) in the input file for the single point energy calculation. During the calculations, all the default options were used in the package. BCPs and Bond Path (BP) were computed between the interacting atoms.

4.3 Results and Discussions

As none of these compounds have any N–H group, there is no possibility of formation of strong hydrogen bonds in the crystal lattice. Only weak hydrogen bonds like C–H···F, C–H···O, C–F···F–C and C–H···π interactions are possible in crystal packing of these molecules.

The intermolecular interactions were analysed using PARST[127] and the energy calculations were done using Gaussian09 and are listed below. For understanding the topological properties, AIM calculations were also performed. Table 4.3.1 includes the

data of electron density and Laplacian of electron density obtained from AIM calculations.

The structures of the tetrafluorinated isoquinoline derivatives reported in this chapter display a library of supramolecular assemblies involving mostly the C–F group, which were historically refuted in stabilizing the crystal structures. Fluorine mediated interactions are responsible for building different crystalline architecture in these molecules. The structures of these compounds revealed that the aromatic C–F acceptor groups not only form hydrogen bonds with aromatic C–H donors, but also form hydrogen bonds with $–CH_2–$ groups and the $–CH_3$ group present in the molecule.

Table 4.3.1: Geometric parameters of all the intermolecular interactions involved in 20 crystal structures

D–B···A	**d(D···A) (Å)**	**d(B···A) (Å)**	**∠D-B···A (°)**	**ΔE (kcal mol^{-1})**	**ρ (×10^{-2}) (eÅ^{-3})**	**$\nabla^2\rho$ (×10^{-3}) (eÅ^{-5})**	**Symmetry**
6-1							
C2–H2B···F1	3.005(1)	2.27	129	-5.6	0.369	1.225	x, y-1, z
C7–H7···O1	3.456(1)	2.65	142	-6.1	0.669	1.658	2-x, +y, 1-z
6-2							
C6–H6···F1	3.500(2)	2.61	156	-1.5	0.321	0.875	-x, 2-y, 1-z
C15–H15···F1	3.257(2)	2.56	130	-2.0	0.615	1.874	x, -y+½+1, +z-½
C3–H3A···F2	3.337(2)	2.67	125	-6.2	0.975	0.676	x-1, y, z
C2–H2A···F3	3.279(2)	2.36	154	-2.2	0.419	1.289	-x, y-½, ½-z
C21–H21···F4	3.450(2)	2.53	163	-9.1	0.510	1.589	-x-1, 2-y, -z
C14–H14···O1	3.393(2)	2.67	133	-1.7	0.631	1.599	x+1, 3/2-y, z-½
6-3							
C3–H3B···F2	3.360(2)	2.69	125	-2.2	0.0920	0.379	x-1, y, z
C2–H2B···F3	3.233(2)	2.45	136	-6.8	0.830	2.416	1-x, y+½, ½-z
C10–H10B···F4	3.456(2)	2.69	136	-7.9	0.301	0.835	-x, -y, -z+1
C15–H15···F1	3.285(2)	2.55	134	-4.2	0.487	1.547	x, -y+½, +z-½
C14–H14···O1	3.333(2)	2.63	128	-1.7	0.695	1.745	x+1, ½-y, z-½
6-4							
C2–H2A···F1	3.001(1)	2.21	136	-6.9	1.274	3.575	x, y+1, z
6-5							
C36–H36···F3	3.312(2)	2.57	130	-2.5	0.503	1.609	1-x, 1-y, 1-z
C18–H18···F3	3.440(2)	2.64	142	-5.6	0.602	1.869	1-x, -y, 1-z
C22–H22···F5	3.415(2)	2.52	158	-2.5	0.287	0.972	-x, y-½, ½-z
6-6							
C3–H3B···F1	3.571(1)	2.63	159	-8.3	0.440	1.404	x, 1-y, z+½
C15–H15···F2	3.496(1)	2.59	158	-1.2	0.477	1.520	x, -y, z+½
C1–H1···F3	3.378(1)	2.51	144	-8.3	0.440	1.404	3/2-x, ½-y, 1-z

C18–H18···F3	3.335(1)	2.55	140	-4.2	0.566	1.785	3/2-x, y+½, 3/2-z
C14–H14···O1	3.502(1)	2.68	144	-2.2	0.552	1.447	x, y-1, z
6-7							
C2–H2A···F1	3.519(2)	2.59	157	-1.2	0.327	1.153	x, y-1, z
C16–H16···F3	3.269(2)	2.37	157	-6.8	0.523	1.604	x, y-1, z
C13–H13···F4	3.344(1)	2.61	134	-10.2	0.557	1.743	-x+1, -y+2, -z+1
C22–H22···O1	3.332(2)	2.68	126	-5.8	0.465	1.208	3/2-x, y-½, 3/2-z
6-8							
C2–H2B···F1	3.188(1)	2.27	153	-6.3	0.666	2.103	x, +y, z+1
C19–H19···F2	3.321(1)	2.56	137	-3.3	0.472	1.462	1-x, -y, z-½
C16–H16···F3	3.533(1)	2.58	175	-1.2	0.783	2.451	x, y, z+1
C21–H21···O1	3.347(1)	2.68	127	-6.5	0.386	1.008	1-x, 1-y, z+½
6-9							
C6–H6···F1	3.332(1)	2.63	132	-2.8	0.500	1.601	x, y, z-1
C13–H13···F3	3.279(1)	2.38	158	-0.9	0.215	0.761	x, y, z+1
C4–H4···F4	3.393(1)	2.48	161	-5.6	0.139	0.450	-x, 1-y, 1-z
C15–H15···F4	3.597(2)	2.67	167	-2.8	0.903	2.596	x+1, 3/2-y, z+½
6-13							
C2–H2A···F1	3.408(1)	2.51	151	-6.9	0.761	2.368	x, y-1, z
C16–H16···F3	3.289(2)	2.36	164	-10.0	0.523	1.642	x, y-1, z
C13–H13···F4	3.146(2)	2.48	127	-6.9	0.416	1.307	1-x, 2-y, 1-z
C21–H21···O1	3.345(2)	2.74	122	-6.2	0.015	0.040	½-x, y-½, ½-z
C15–F2···F4–C19	4.104(1)	2.90	130/88	-2.8	0.596	1.959	-x, -y, -z
6-16							
C4–H4···F8	3.389(1)	2.66	134	-7.8	0.405	1.289	x, y, z
C16–H16···F4	3.233(1)	2.34	157	-1.9	0.776	2.417	x, y-1, z
C29–H29···F8	3.570(1)	2.69	154	-6.0	0.845	2.569	x, y-1, z
C38–H38···F7	3.250(1)	2.37	154	-6.0	0.395	1.265	x, y+1, z
C7–H7···F3	3.590(1)	2.69	157	-6.0	0.405	1.289	x, y+1, z
C32–H32B···F1	3.383(1)	2.69	128	-2.1	0.099	0.389	x, +y-1, +z
C41–H41···F2	3.081(1)	2.48	121	-7.8	0.092	0.379	x+1, +y, +z
C25–H25···O1	3.542(1)	2.71	141	-2.1	0.564	1.498	x, 1-y, z+½

6-19							
C2–H2B···F2	3.270(1)	2.40	148	-10.1	0.620	1.962	x, y-1, z
C13–H13···F4	3.260(1)	2.49	140	-5.6	0.517	1.340	x, 3/2-y, z-½
C15–H15···F3	3.333(1)	2.68	127	-5.6	0.219	0.765	-x+2, y-½, -z+3/2
C21–H21···O1	3.376(1)	2.72	128	-5.7	0.623	1.563	1-x, y-½, 3/2-z
6-21							
C3–H3A···F3	3.437(1)	2.69	133	-5.1	0.134	0.422	x, y-1, z
C3–H3A···F1	3.236(1)	2.57	125	-5.1	0.120	0.378	x, y-1, z
C4–H4···F4	3.536(1)	2.69	147	-1.9	0.291	0.956	x-½, -y, z-½
C19–H19···O1	3.294(1)	2.65	126	-4.3	0.706	1.795	x-½, 1-y, z+½
6-23							
C2–H2B···F1	3.297(1)	2.36	158	-6.6	0.101	0.403	x, y-1, z
C18A–H18B···F2	3.323(1)	2.40	164	-6.6	0.283	1.113	x, y+1, z
6-25							
C16–H16···F2	3.156(1)	2.34	144	-4.8	0.499	1.562	-x, y+½, 3/2-z
C20–H20···F2	3.226(2)	2.58	126	-3.8	0.675	2.065	1-x, 1-y, 2-z
C13–F1···F4–C19	5.049(2)	2.88	136/126	0.4	0.527	1.746	x, 1+y, z
6-30							
C22–H22···F3	3.415(1)	2.53	159	-3.5	0.025	0.063	x-1, 3/2-y, z-½
C16–H16···F2	3.154(1)	2.52	126	-1.5	0.423	1.430	-x, y+½, ½-z
C20–H20···F2	3.351(2)	2.57	142	-4.1	0.207	0.650	1-x, 1-y, 1-z
C20–H20···F4	3.389(2)	2.65	137	-3.0	0.387	1.351	1-x, 2-y, 1-z
C13–F1···F4–C21	4.198(2)	2.87	109/93	-1.6	0.550	0.707	x, y -1, z
6-31							
C38–H38···F5	3.304(1)	2.50	144	-1.1	0.641	1.983	1 - x, 2 - y, - z
C23–H23···F5	3.464(1)	2.67	138	-1.5	0.387	1.215	1 - x, 2 - y, - z
C16–H16···F2	3.336(1)	2.59	141	-4.9	0.968	2.940	- x, - y, 1 - z
C14–H14···F1	3.476(1)	2.57	164	-13.9	0.439	1.351	1 - x, - y, 1 - z
C43–H43···F2	3.292(1)	2.63	128	-5.7	0.675	2.065	x, -y+1, +z
C42–H42···F2	3.538(1)	2.65	159	-5.7	0.675	2.065	-x, -y+1, -z+1
C25–H25A···F4	3.467(1)	2.61	148	-4.1	0.552	1.768	x + 1, y, z

C13–F1···F4–C19	5.185(2)	2.92	140/131	-4.1	0.420	1.537	1 - x, 1 - y, 1 - z
C15–F2···F3–C18	4.277(2)	2.95	127/85	0.3	0.251	1.058	- x, 2 - y, 1 - z
C37–F5···F7–C40	3.977(2)	2.80	120/90	-5.7	0.857	2.655	1 - x, 2 - y, - z
6-33							
C2–H2B···F1	3.204(1)	2.56	121	1.8	0.439	1.357	-x+1, -y+1, -z
C36–H36···F2	3.202(2)	2.43	135	-3.1	0.225	0.700	1 - x, - y, 1 - z
C14–H14···F6	3.314(2)	2.54	139	-1.0	0.600	1.794	x - 1, y + 1, z - 1
C41–H41···F2	3.195(2)	2.49	130	-6.1	0.361	1.170	x + 1, y, z
C29–H29···F4	3.235(1)	2.50	132	2.5	0.353	1.135	x, y, z
C10–H10B···F8	3.282(1)	2.63	123	-10.6	0.639	1.916	-x+2, -y, -z+1
C10–H10A···F6	3.331(1)	2.57	135	-1.0	0.600	1.794	x, +y, +z-1
C19–H19···F5	3.261(1)	2.64	121	-1.8	0.605	1.870	x-1, +y, +z
C32–H32C···F4	3.281(1)	2.47	140	-1.1	0.616	1.810	x+1, -y+1, -z+1
C32–H32B···F1	3.207(1)	2.54	125	3.2	0.652	1.958	x, +y, +z+1
C21–F4···F8–C43	3.527(2)	2.84	106/96	-1.1	0.760	2.284	- x, 1 - y, 1 - z
6-34							
C21–H21···F2	3.239(1)	2.51	134	-3.7	0.234	0.720	1 - x, 1 - y, 1 - z
C14–H14···O1	3.377(1)	2.73	125	-3.2	0.620	1.578	x, ½ - y, z + ½
6-37							
C15–H15···O1	3.270(2)	2.51	138	-3.8	0.915	2.288	½ - x, y - ½, z
C19–H19···O1	3.508(2)	2.60	162	-1.4	0.712	1.732	3/2 - x, y - ½, z

Out of these 20 crystals, 15 are centrosymmetric, 5 are non-centrosymmetric; including 2 (6-1 and 6-4) crystallizing in chiral space group $P2_1$. Aromatic fluorine (Fluorine bonded to aromatic ring) is seen to form dimers through 13 different synthons (Figure 4.3.1), which generated 71 intermolecular interactions in the structures reported herein. Among these, some of the synthons involve fluorine or hydrogen in bifurcated interactions.

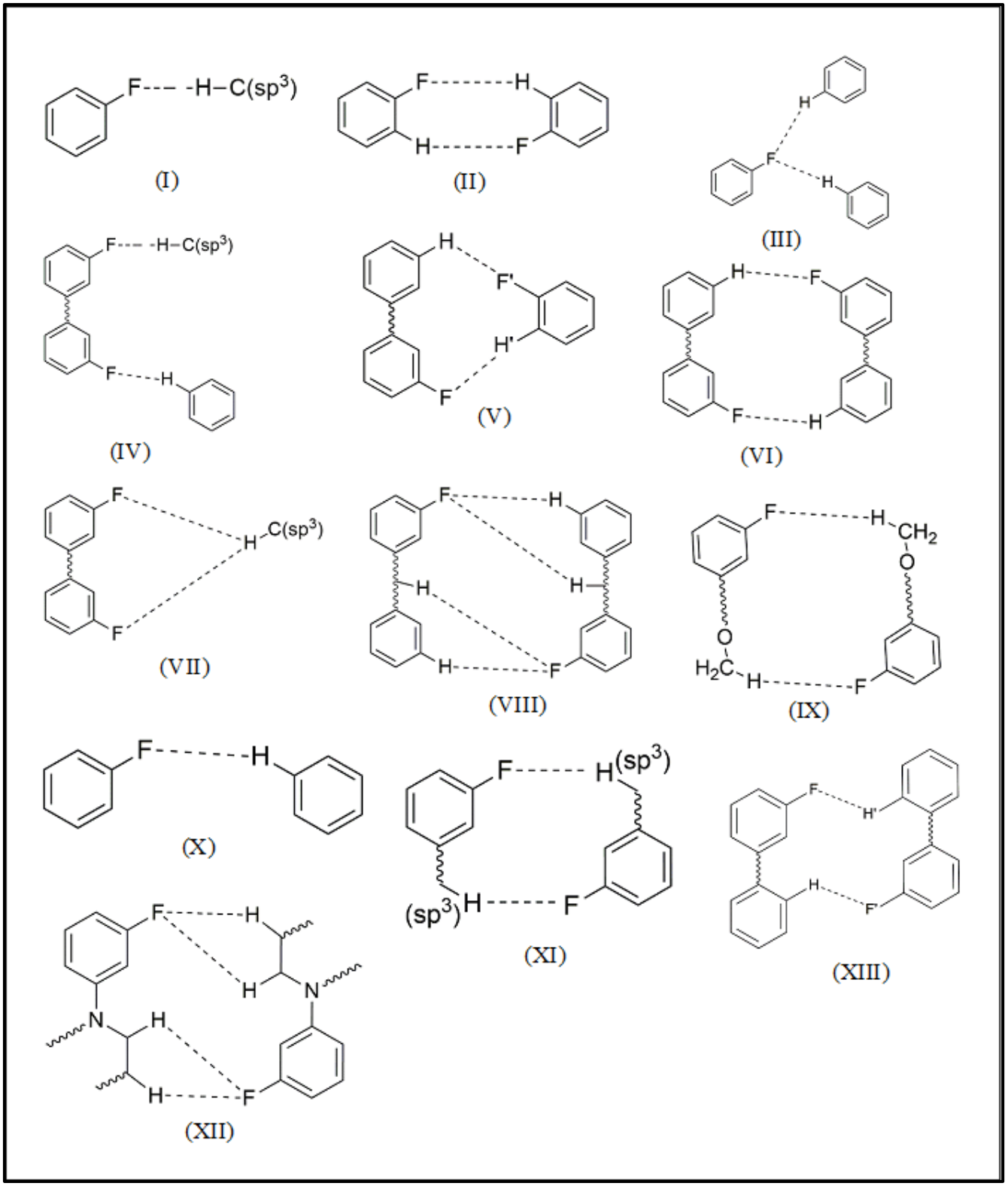

Figure 4.3.1: Supramolecular dimer synthons involving C–F groups

Synthon	Representative structure
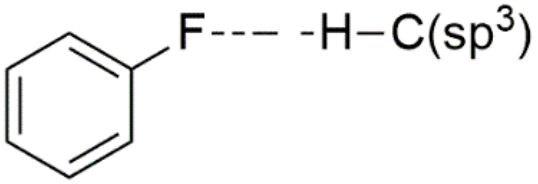	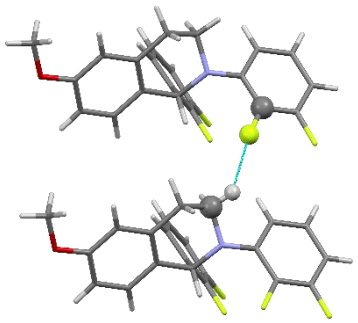 **6-1**
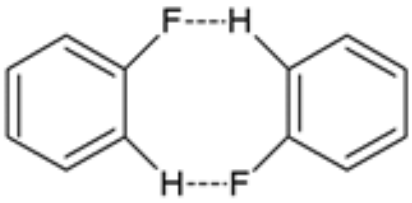	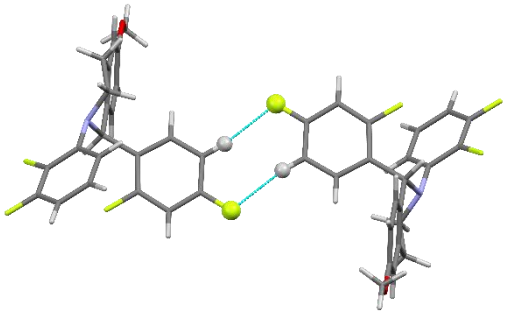 **6-2**
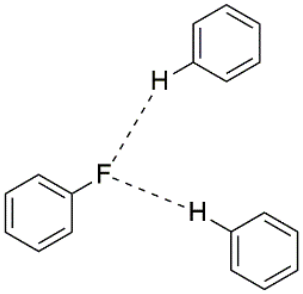	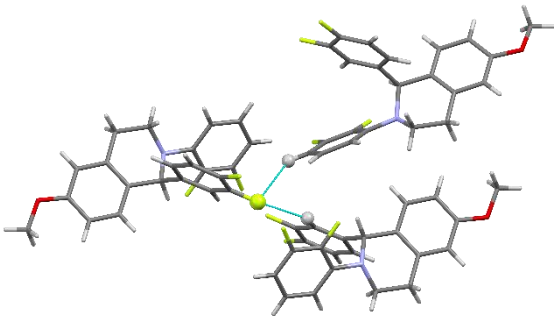 **6-5**
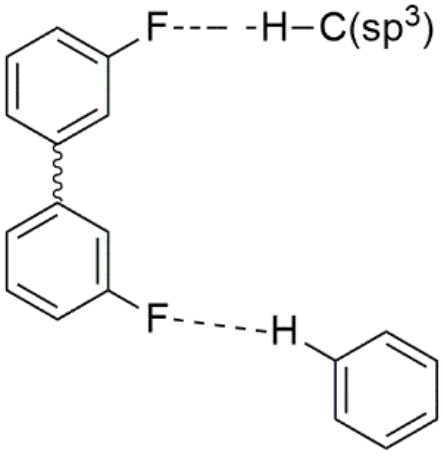	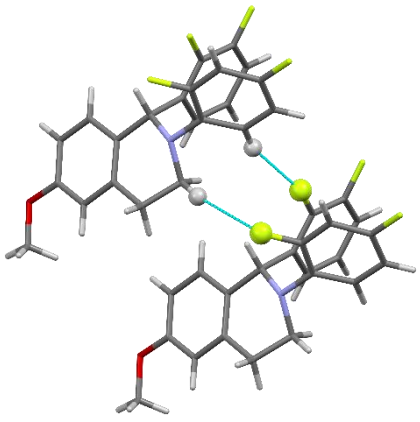 **6-7**

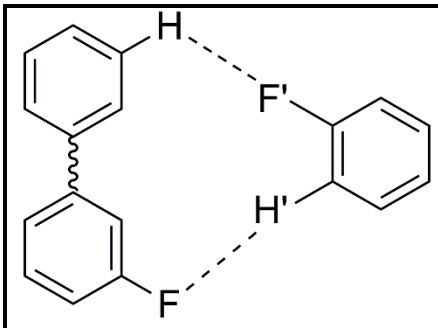	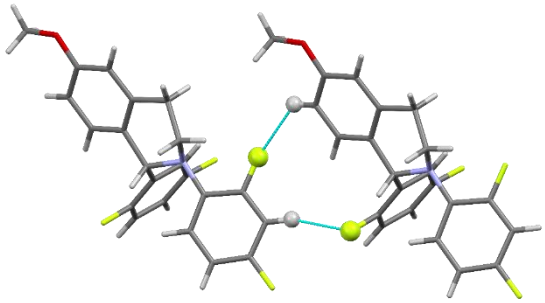 **6-9**
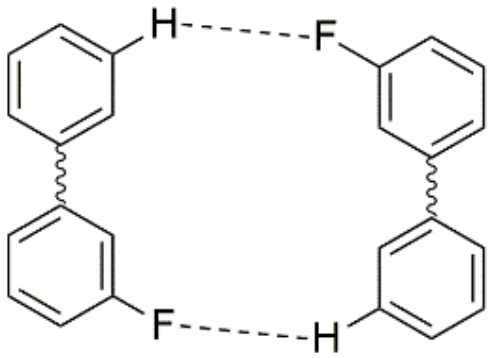	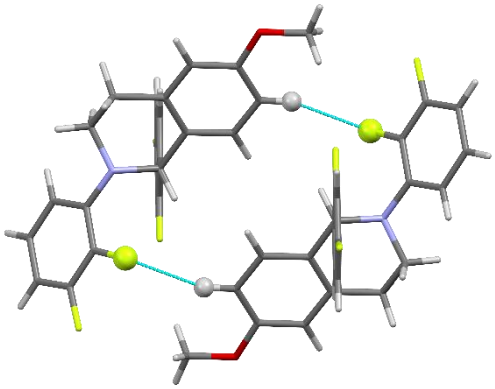 **6-2**
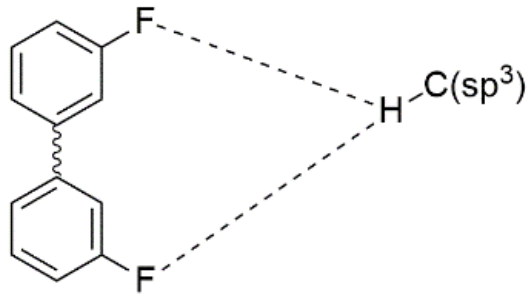	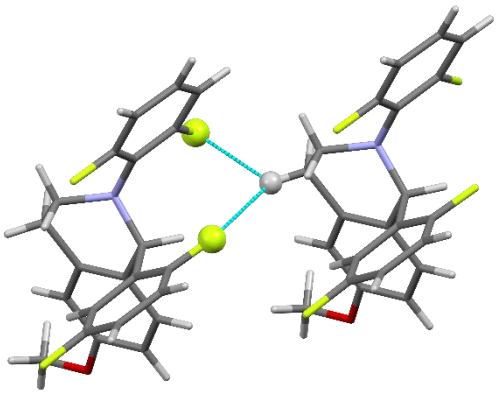 **6-21**

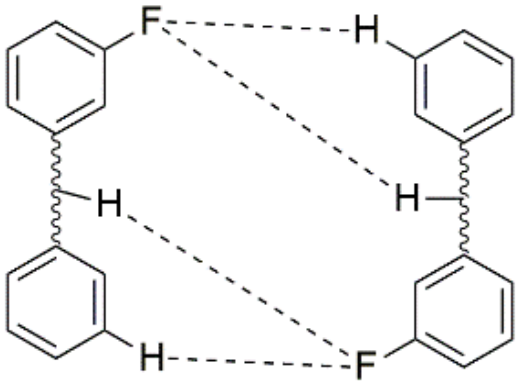 F H H H H F	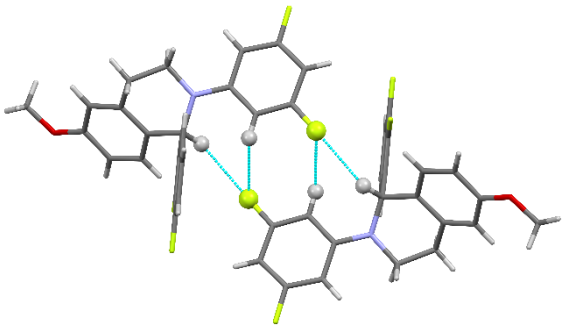 **6-31**
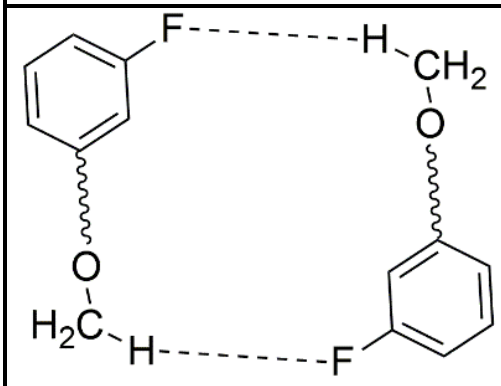 F H CH2 O O H2C H F	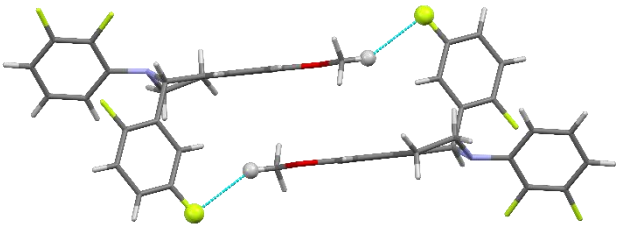 **6-3**
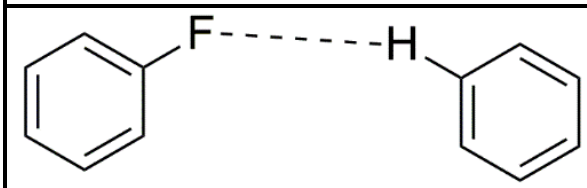 F H	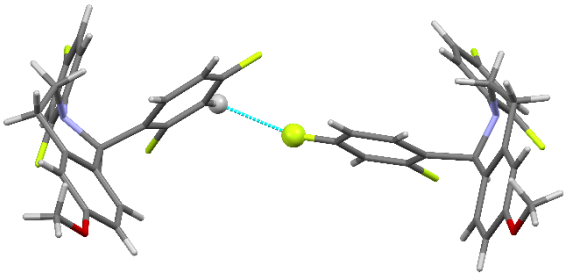 **6-8**
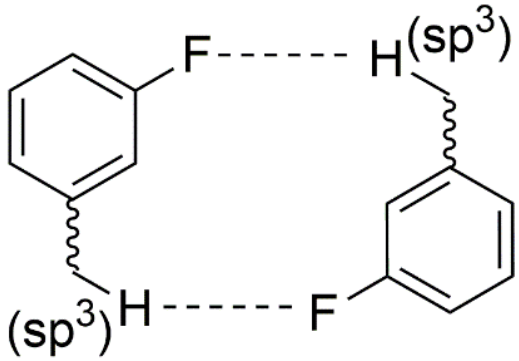 F H(sp3) (sp3)H F	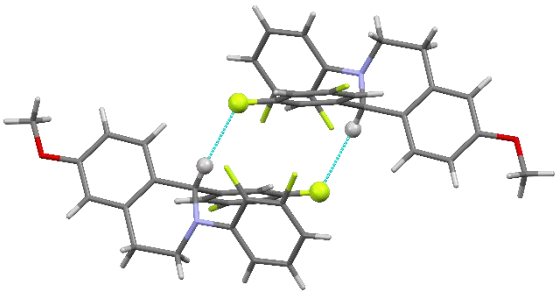 **6-6**

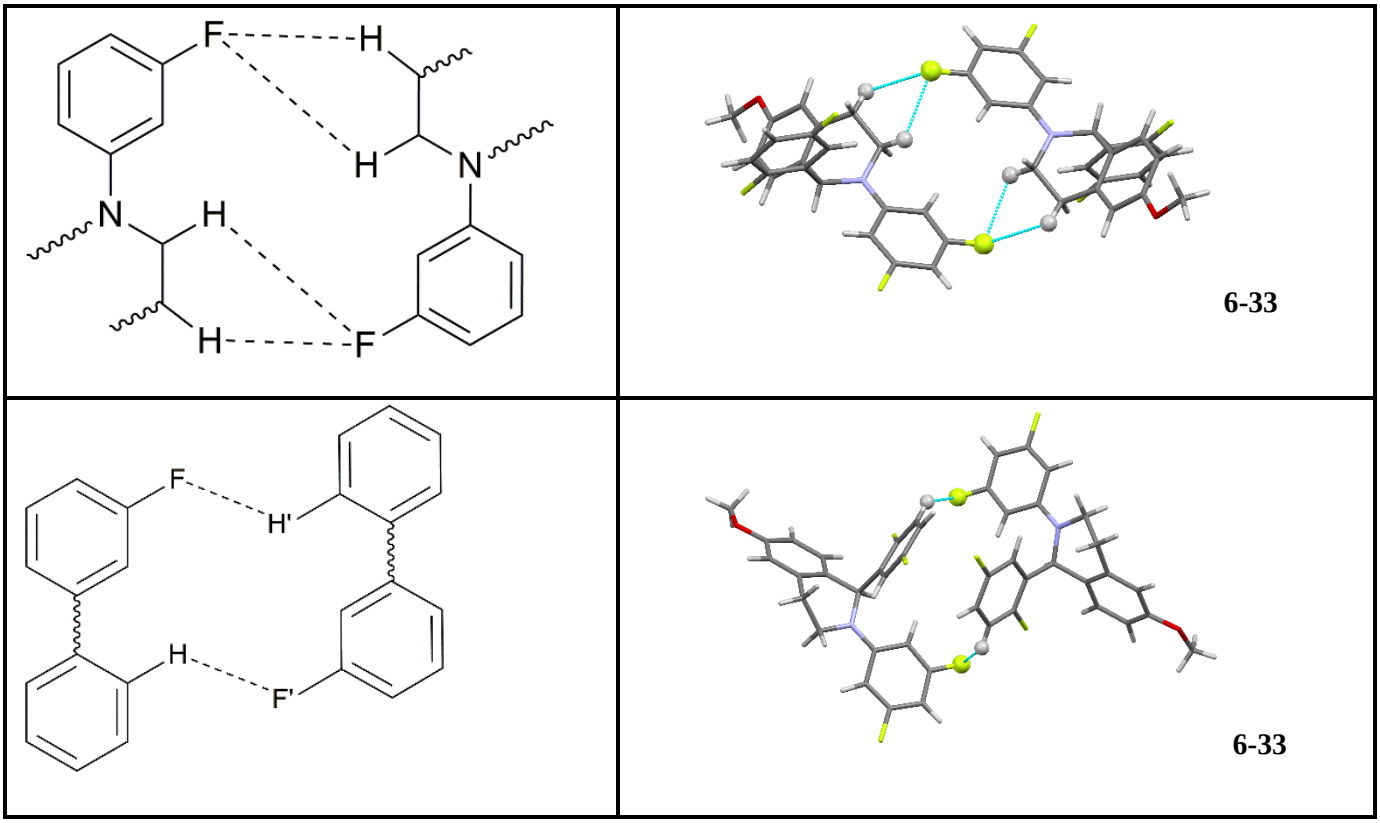

Figure 4.3.2: Supramolecular dimer synthons with examples involving C–F groups

The position of C–F group in an aromatic ring does not have any particular preference for the formation of a particular synthon but the change in the position of the C–F group from *ortho*- to *meta*- or from *meta*- to *para*- maintains the same supramolecular synthon as is seen in many cases. In addition to the formation of weak C–H···F hydrogen bond, the molecules have been seen to offer different C–F···F–C interactions in the structure of many molecules. A careful investigation of these C–F···F–C interactions indicate that these interactions can also be classified as one of Type I, Type II or quasi Type I/Type II, just like the same was considered for other C–X···X–C (X = Cl, Br and I) interactions by Tothadi *et al.*[74] It is also noted that the C–F···F–C interactions can also be bifurcated in nature, with the intermolecular distance being 2.80Å and 2.88Å (as seen in the molecule 6-31, Figure 4.3.3) and hence this observation indirectly indicates that the electron density distribution around the F atom in a C–F bond is non-uniformly

distributed; hence there are electron rich and electron deficient regions, which can either donate or accept electrons simultaneously from another similar C–F group. This can only be established by an accurate experimental charge density analysis of these molecules, which is beyond the scope of the current chapter.

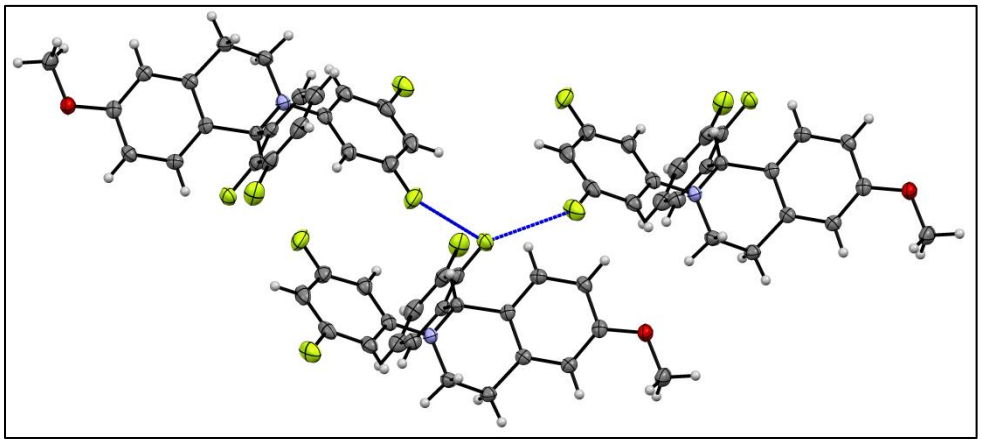

Figure 4.3.3: Bifurcated C–F···F–C interaction in 6-31

The angles and the distances at which the bond formation is taking place were also analysed. Table 4.3.1 lists a statistical summary of weak hydrogen bonds observed in this series of compounds. This table indicates that the most stable (with highest stabilization energy) interactions were found in the angle range from 160° to 170° and the distance was between 2.5Å and 2.6Å. But, most of the C–H···F–C interactions preferred the angle between 130° and 140° and the distance where most of the bonds are formed is between 2.5Å and 2.7Å. It is noteworthy that only one interaction was found with the angle range 170-180° and the stabilization energy for that was found to be -1.2 kcal/mol, which happens to be a weak interaction. Therefore, it can be concluded that this is not a favourable angle range for C–H···F–C interactions.

It is also evident from this table that the frequency of fluorine mediated interaction is more than those involving the methoxy group.

Table 4.3.1: Statistical Summary of C–H···F and C–H···O hydrogen bonds

H···F Distance Range (Å)	**Number of C–H···F hydrogen bonds**	**Angle Range ∠C–H···F (°)**	**Number of C–H···F hydrogen bonds**
2.2≥d>2.0	0	130≥θ>120.0	15
2.3≥d>2.2	2	140≥θ>130.0	21
2.4≥d>2.3	8	150≥θ>140.0	11
2.5≥d>2.4	11	160≥θ>150.0	16
2.6≥d>2.5	25	170≥θ>160.0	7
2.7≥d>2.6	25	180≥θ>170.0	1
H···O Distance Range (Å)	**Number of C–H···O hydrogen bonds**	**Angle Range ∠C–H···O (°)**	**Number of C–H···O hydrogen bonds**
2.3≥d>2.2	0	130≥θ>120.0	7
2.4≥d>2.3	0	140≥θ>130.0	2
2.5≥d>2.4	0	150≥θ>140.0	3
2.6≥d>2.5	1	160≥θ>150.0	0
2.7≥d>2.6	8	170≥θ>160.0	1
2.8≥d>2.7	4	180≥θ>170.0	0

In these 20 compounds (19 tetrafluorinated isoquinolines and 1 unsubstituted isoquinoline), we have observed 71 C–H···F–C interactions, 13 C–H···O–C and 7 C–F···F–C interactions. Among the 7 C–F···F–C interactions, 3 were found to be Type I, 3 were Type II and 1 interaction was quasi Type I/ Type II kind of interaction. After calculating the stabilisation energy for these interactions using Gaussian09, we have plotted the same in a 3D graph (Figure 4.3.4) against the angle and the distances at which the interactions are taking place. It can be seen from the graph as well as the values mentioned above (Table 4.3.1) that C–H···F interactions offer stability to the dimer with large value of stabilisation energy. The stabilisation energy provided by C–H···F hydrogen bond is considerably more than that of C–H···O hydrogen bonds.

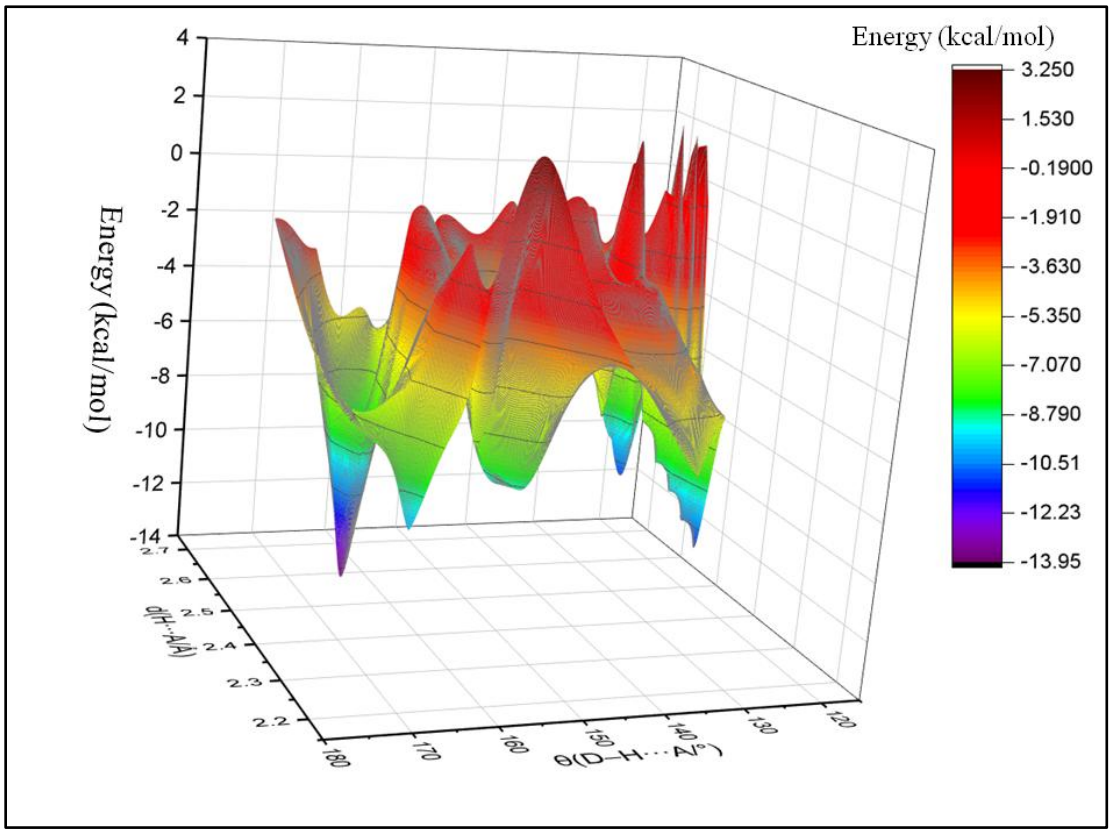

Figure 4.3.4: 3D graph representing the energies of various C–H···F–C interactions at their intermolecular distance and the angle.

G. R. Desiraju and Thomas Steiner,[6] have classified the hydrogen bond as very strong, strong and weak. As per the classification, the bond energy between -15 and -40 kcal/mol represent very strong hydrogen bonds, bond energies between -4 and -15 kcal/mol represent strong hydrogen bonds and if the bond energy is less than -4 kcal/mol, the interaction is said to be a weak hydrogen bond interaction. For C–H···F–C interactions; out of 71 total interactions, 39 lie in the region of strong hydrogen bonds, accounting for 54.92% and the rest, 45.07% interactions i.e. 32 out of 71 represent weak hydrogen bonds. From this observation, it should be concluded that the C–H···F–C interactions are significant in building supramolecular architecture, especially in the absence of other stronger interactions like strong hydrogen bonds and hence they should not be refuted or ignored.

To understand the topological properties of the C–H···F–C interactions, we did the AIM (Atoms in molecules) calculations. These enabled us to find the Bond Critical Points (BCPs) and also to analyse the values of electron density (ρ_c)) and the Laplacian of electron density ($\nabla^2 \rho_c$) at BCPs. The electron densities at BCPs are positive quantities which indicate that there is electron density present between both the atoms which indicate an interaction. Also, the positive value of Laplacian infers that the interaction is a closed interaction, typically ionic or van der Waals as stated by Bader.[99]

4.4 Conclusion

The computational and topological analyses of the fluorinated isoquinoline derivatives have been carried out using the crystal information file (CIF) obtained from the crystal solution from the single crystal X-ray diffraction data collected at low temperature (100K). Among the molecules, for which we could obtain the crystals, we studied their intermolecular interactions and have found that among 19 fluorinated derivatives we had 71 intermolecular interactions which were originated by 13 different types of supramolecular synthons. The intermolecular interaction energies for these C–H···F–C interactions were studied along with C–H···O and C–F···F–C using Gaussian09 and GaussView was used as the visualisation software. The topology of the interactions was also studied using AIM2000 and it was observed that the interactions play a very important role in stabilization of the compounds. The Bond Critical Points were calculated for all the studied interactions and the value of electron density and Laplacian calculated at the Bond Critical Point were found to be positive quantities. The presence of C–F···F–C interactions in the molecules indicate that these interactions too are important in crystal engineering and play a significant role in the stabilisation of the crystal structure. The symmetry of the interaction i.e. how the interactions are oriented,

play a vital role in deciding the conformation of the molecule. Also, we have found that 54.92% of the interactions studied fall in the region of strong hydrogen bonds as stated by Desiraju and Steiner. Therefore, from these analyses, we conclude that the C–H···F–C interactions play significant role in crystal packing and these are directional in nature. Hence, the interactions cannot be taken as mere a van der Waals interaction and its importance cannot be refuted.

Chapter 5

Understanding of C–F···F–C interactions using experimental charge density analysis

Chapter 5

5.1 Introduction

The influence of organic fluorine mediated interactions in the presence and absence of other strong/weak hydrogen bonds has been established in the previous chapters. The interactions involving the organic fluorine (C–H···F–C and C–F···F–C) were identified and analysed using the computational and the topological methods. The gas phase calculations (Gaussian09, MP2 level, 6+31G* basis set with counterpoise correction) enabled us to understand the strength of these intermolecular interactions by calculating the stabilization energies for the interacting dimers. Further, the topological analysis of the tetra fluorinated isoquinolines enabled us to understand the nature of these interactions in the absence of any other weak hydrogen bonds. But, all these analyses were based on the structural information generated using the independent atom model using spherical atom approximation. The spherical atom approximation assumes the electron density to be spherical, which is a good approximation for the heavier elements but not for the lighter atoms where the effect of bonding is more pronounced. A detailed drawback of the spherical atom approximation is discussed in the Chapter 1 of this thesis.

Therefore, to gain a comprehensive understanding of these interactions, one needs to utilize the charge density analysis, which is based on the aspherical modelling of the electron density of the system under investigation. This method takes into account the

bonding and lone pair electron densities of the atoms within the molecule and thus provides a convincing tool for the understanding of these interactions beyond mere geometric proximity. Several reviews have elucidated the chemical application of the charge density studies.[100,136-140] Detail investigation of several weak interactions (C–H···X; X = F, Cl, Br, O, π) have also been reported using experimental charge density analysis to establish the nature of these interactions like hydrogen bond type, van der Waals interaction, *etc*.[141-149] An earlier report by Chopra *et al.*, highlighted the significance of type I C−F···F−C contact in the case of a monofluorinated isoquinoline derivative.[150] This is the first study to understand C–F···F–C contacts, involving CF_3 groups, wherein the 3D deformation density maps clearly establish the presence of σ holes (Charge Deficient (CD) region) along every C–F bond and which interact with the charge-concentrated (CC) region of the fluorine atoms, hence establishing the electrostatic nature of these contacts. After the multipole modelling of the molecule, various properties of the molecules like net charge, dipole or quadrupole moments, interaction energies, *etc*. can be evaluated with substantial accuracy. On the basis of these accurate analyses, the nature of interactions can be identified.

In the earlier studies on fluorinated molecules by some of us, we encountered a number of molecules which were found to crystallize using weak C−F···F−C, C−H···F−C interactions. Based on our earlier studies, a few molecules were selected as model compounds for the details understanding of C−F···F−C interactions. In the current chapter, we are reporting the charge density analyses of weak interactions mediated by organic fluorine in N-(2,5-difluorophenyl)-3,5-difluoro-N-(3-methoxyphenethyl)benzamide (code: S-AD-25-35), the structural analysis of which was discussed by us earlier.[151] The halogen-halogen interactions offered by organic fluorine is classified in three categories (Type I, Type II and Quasi Type I/ Type II) by Tothadi et

al.[74] In our molecule, S-AD-25-35 (Scheme 5.1), among the halogen-halogen interaction, we have observed Type I and Quasi Type I/ Type II of interactions between the molecules. The interaction C2−F1···F4−C9 is a type I interaction with θ_1 and θ_2 being 162.26˚ and 164.69˚ respectively with an angle difference of 2.43˚ and the intermolecular distance is 2.949Å (Figure 5.1(a)). Quasi type I/ type II interaction is offered by C2−F1···F3−C11 with θ_1 and θ_2 being 116.76˚ and 89.83˚ respectively and difference in angles being 26.93˚ with the intermolecular distance being 2.819Å (Figure 5.1(b)). We have given the qualitative analysis of these interactions based on the gas phase calculation but the quantitative nature of these intermolecular interactions has not been discussed. Therefore, we decided to study these interactions using the experimental charge density analysis for better understanding of these interactions. To get an insight about the C−F···F−C interactions, we carried out a CSD search and the details for this are discussed herein.

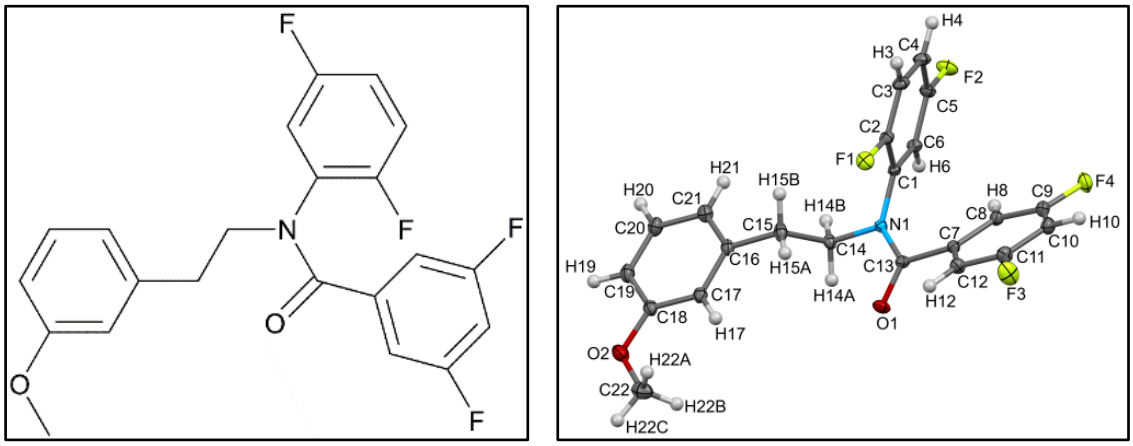

(a) **(b)**

Scheme 5.1: (a) Molecular structure of S-AD-25-35, (b) ORTEP of the compound S-AD-25-35 at 50% ellipsoid probability

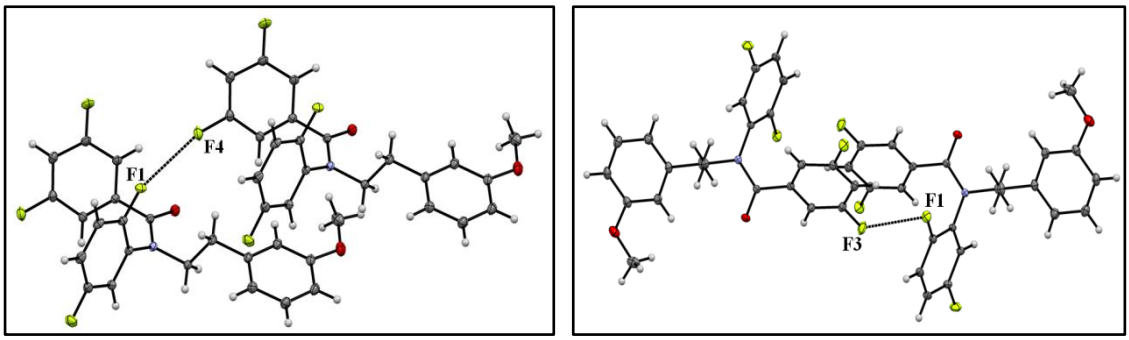

(a) **(b)**

Figure 5.1: (a) Type I C2−F1···F4−C9 interaction, **(b)** Quasi type I/ type II C2−F1···F3−C11 interaction

5.2 Experimental

5.2.1 Synthesis and Crystal growth

The compound S-AD-25-35 was synthesized as per the procedure reported by us earlier.[151] The compound after purification through column chromatography was recrystallized using various organic samples. The best quality single crystals for charge density data collection were grown from DCM/Hexane solvent.

5.2.2 Data Collection and Structure Refinement

The colourless block shaped, good quality crystals were chosen for the high-resolution X-ray diffraction data collection. The data was collected using Rigaku XtaLAB AFC12 (RCD3) four circle diffractometer equipped with a Mo rotating anode X-ray tube and hybrid pixel array detector at 100 K. The crystal to detector distance was kept at 40 mm. The data were collected up to the resolution of 0.45Å (2θ = 104.31˚), requiring a total of 44 hrs for data collection. The frame width was set to 0.5˚.Omega scans were used for the data collection. The data reduction was performed using CrysAlisPro.[122] The structure solution and structure refinement were performed using SHELXT[125] and SHELXL[152] program in OLEX2 suite.[123] All the non-hydrogen atoms were refined for

anisotropic refinement and hydrogens were fixed. The structural description of the molecule is mentioned in the SI (Table S1). The reflection file was merged using SORTAV[153] in WINGX.[154]

5.2.3 Multipole refinement

The final parameters from the independent atom model (IAM) were imported to XD using the module XDINI. The multipole refinement based on the least square refinement method was performed using the module XDLSM. Initially, the scaling was performed for all reflection in order to check the accuracy of data. Next, the non-H atomic position and anistropic thermal parameter (U_{ij}) were refined using high-order diffraction data ($Sin\ \theta/\lambda \geq 0.8$ Å^{-1}). During this refinement, the position of the H atoms in the model were kept at neutron bond distance values (C(Aliphatic)-H = 1.066 Å, C(Aromatic)-H = 1.083 Å). The isotropic thermal parameters for H-atom were then refined using lower angle diffraction data ($Sin\ \theta/\lambda \leq 0.8$ Å^{-1}). In the multipoles model refinement, the C atoms were treated up to octapole level ($l = 3$), but F, O, N atoms were up to hexadecapole level ($l = 4$) and the H-atoms were up to dipole level ($l = 1$). A total of 19 different sets of k and k' parameters were assigned for a chemically different types of non-H atoms and the k and k' values of H-atoms were fixed at 1.2. Finally, a refinement was performed including all these parameters and using all reflections. The anisotropic displacement parameters (U_{ij}) of H atoms were obtained from *SHADE2.1*.[155] The refinement steps as carried out above were then repeated with U_{ij} values of H-atoms set to the estimated values. Subsequently, the anharmonic thermal motion of only the F-atom and N-atom were modeled by refining the Gram-Charlier expansion[156] up to the fourth-order. Then the refinement steps as carried out above were repeated.

The crystal data along with the refinement parameters based on both IAM and multipole model are listed in Table 5.2.1

Table 5.2.1: Crystal data at 100K and refinement parameters

Parameters		
Chemical Formula	$C_{22}H_{17}F_4NO_2$	
Formula weight	403.36	
Space group	$P2_1/n$	
***a*(Å)**	7.7131(7)	
***b*(Å)**	14.5985(15)	
***c*(Å)**	16.6719(14)	
***β*(°)**	100.4704(8)	
Volume (Å^3), *Z*	1846.00(3), 4	
Resolution (d_{min}) (Å)	0.4500	
2θ range	3.73˚ to 104.31˚	
(hkl) range	-17,17; -31,32; -37,37	
Density (g cm^{-3})	1.451	
***F*(000)**	832.0	
μ (mm^{-1})	0.120	
T_{min}, T_{max}	0.9582,0.9758	
R_{int}, R_{merge}	0.0677, 0.0432	
Measured reflections	210051	
Unique reflections	21197	
Completeness (%)	100.0	
Redundancy	9.8	
After Refinement		
Parameters	**IAM**	**Multipole**
Reflections used [I>3σ(I)]	21196	15838
R(F^2), R_w(F^2)	0.0232/0.1278	0.0217/0.0254
***Goodness of fit* (S)**	1.104	1.1172
$\Delta\rho_{max}$, $\Delta\rho_{min}$/ eÅ^3	0.70, -0.30	0.214/-0.166

The ratio for number of variables and the number of parameters after the multipole refinement was **17.8**.

5.3 Observation & Results

5.3.1 Accuracy of multipole model and diffraction data

The final multipole model was assessed for its accuracy based on the plots of Gaussian distribution of residual electron densities vs the pixel population densities (Figure 5.3.1.1). The narrow parabolic nature of the fractal dimension curves (Figure 5.3.1.2) clearly indicates the high accuracy of the multipole model and the data quality.

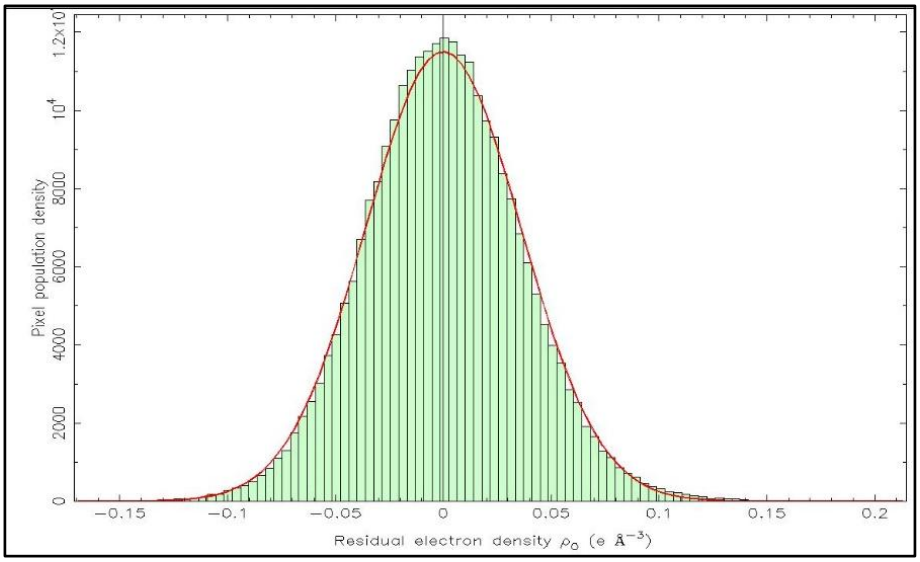

Figure 5.3.1.1: Residual electron density distribution plot

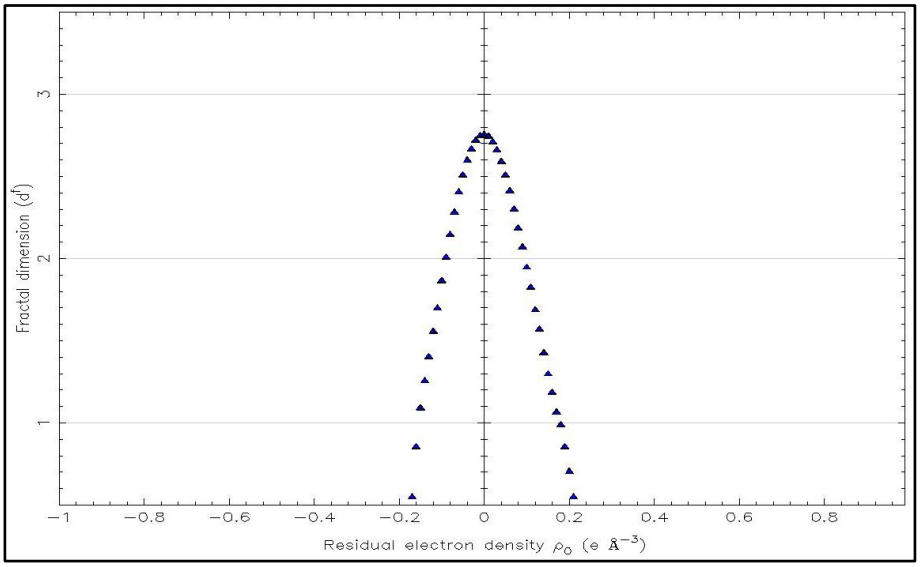

Figure 5.3.1.2: Fractal electron density distribution plot.

Further, investigation of the model and data quality was carried out based on the DRK-plots.[157,158] There is a small deviation of the scale factor value from unity with respect to the resolutions of the diffraction data and the good agreement between the experimental and the expected residuals ascertain the good quality of both the diffraction data and the multipole model. (Figure 5.3.1.3 and Figure 5.3.1.4).

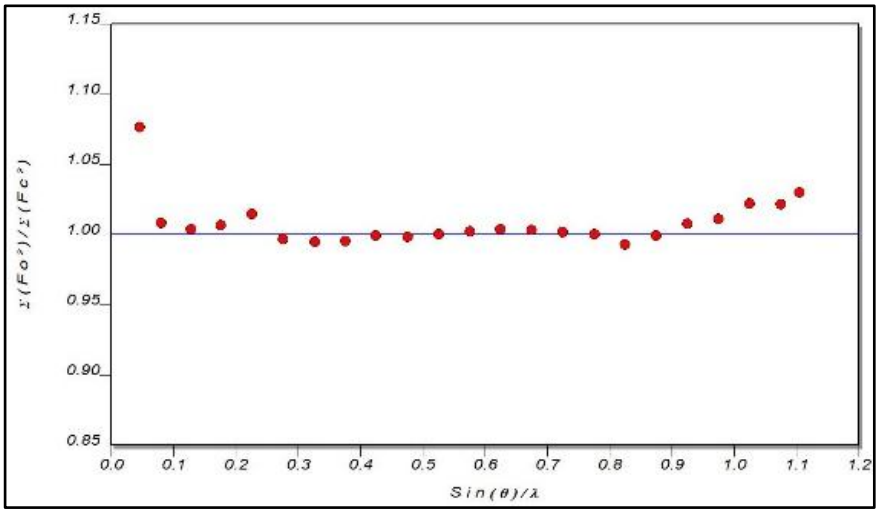

Figure 5.3.1.3: Variation of Scale factor with respect to the resolution of the diffracted data

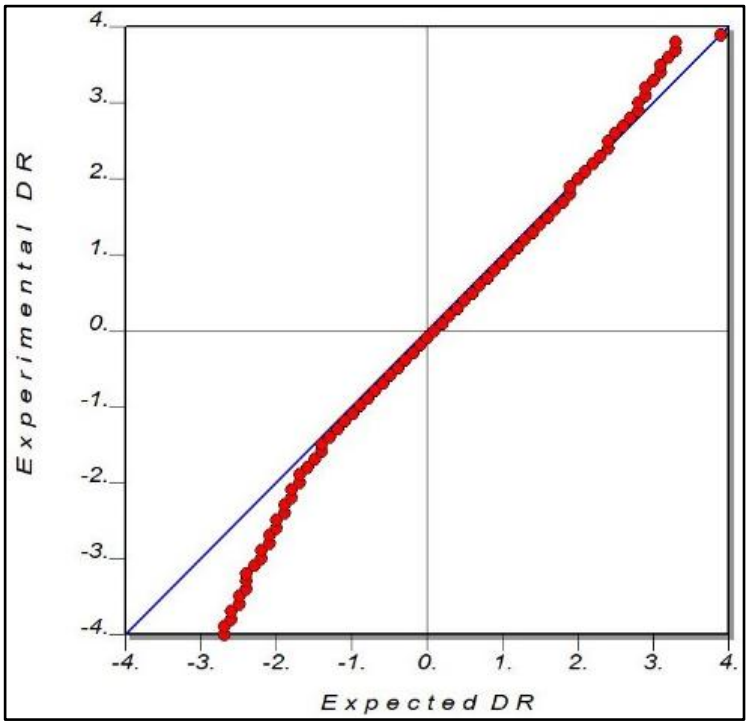

Figure 5.3.1.4: The normal probability distribution plot

Further, the featureless residual electron density plots (Figure 5.3.1.5) clearly support the accuracy of the multipole model.

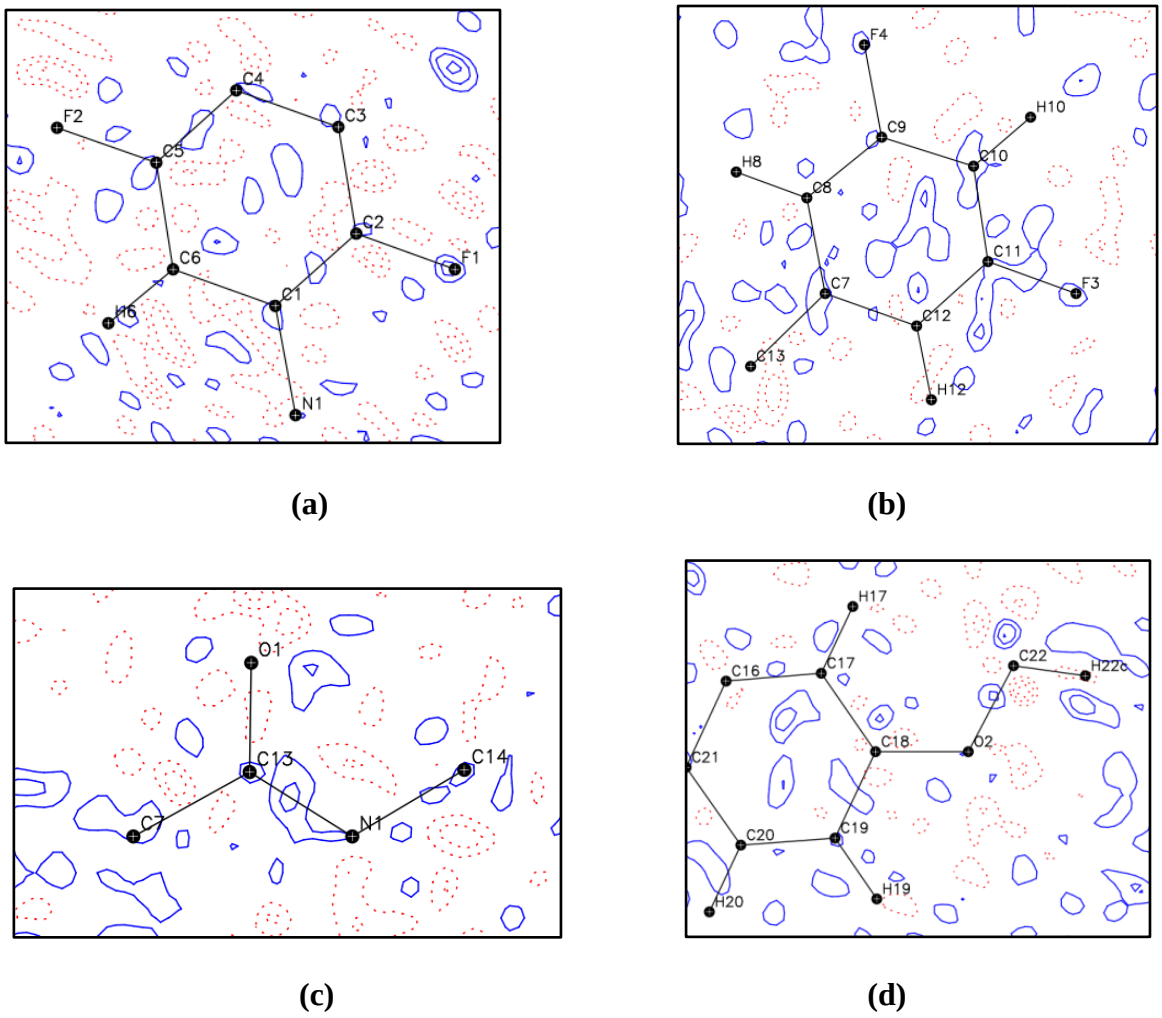

Figure 5.3.1.5: Residual density maps, drawn in the molecular plane containing C1F1F2 (a), C7F3F4 (b), C7N1O1 (c) and C18O2C22 (d) atoms using positive (blue, solid line) and negative (red, dotted line) with contour intervals at ± 0.05 e $Å^{-3}$.

5.3.2 Deformation Density analysis

Deformation density maps highlights the accurate features of chemical bonding densities as well as the location and orientations of the lone-pair of electrons *via* qualitative analysis of the valence densities. The 2D deformation density maps show the accurate features of the bond densities for the interactions observed in the molecule. The

lone pairs of electrons of the O, N and F atoms are clearly visible in the deformation electron density maps. The deformation electron density maps associated with the benzene ring of the molecule were also shown to have accurate bonding features (Figure 5.3.2.1).

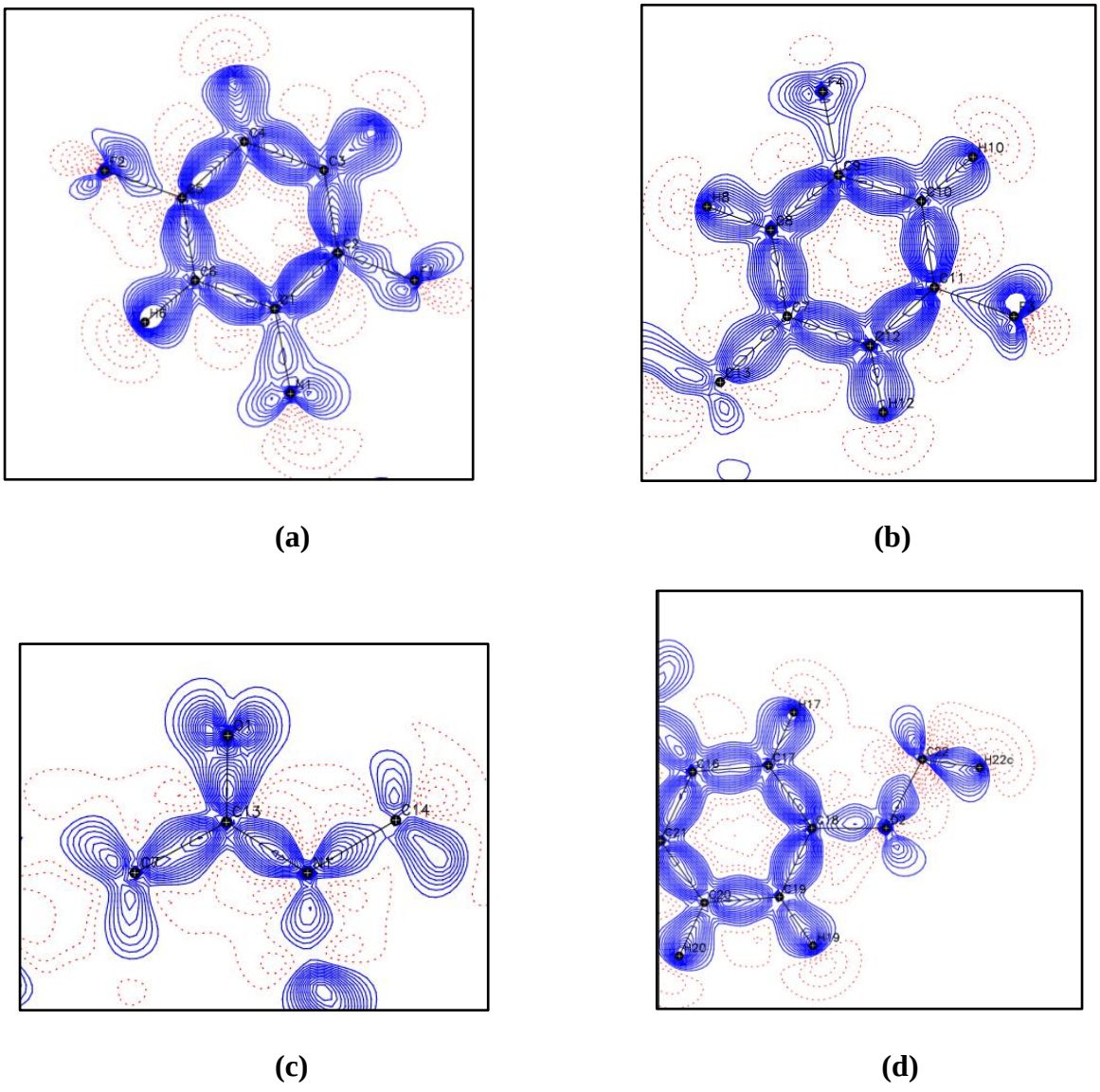

(a) **(b)**

(c) **(d)**

Figure 5.3.2.1: The 2D static deformation density maps, drawn in the molecular plane containing C1F1F2 (a), C7F3F4 (b), C7N1O1 (c) and C18O2C22 (d) atoms using positive (blue, solid line) and negative (red, dotted line) with contour intervals at ± 0.05 e $Å^{-3}$.

The accumulation and depletion of electron densities in the molecule is represented in terms of the 3D deformation density map as shown in Figure 5.3.2.2.

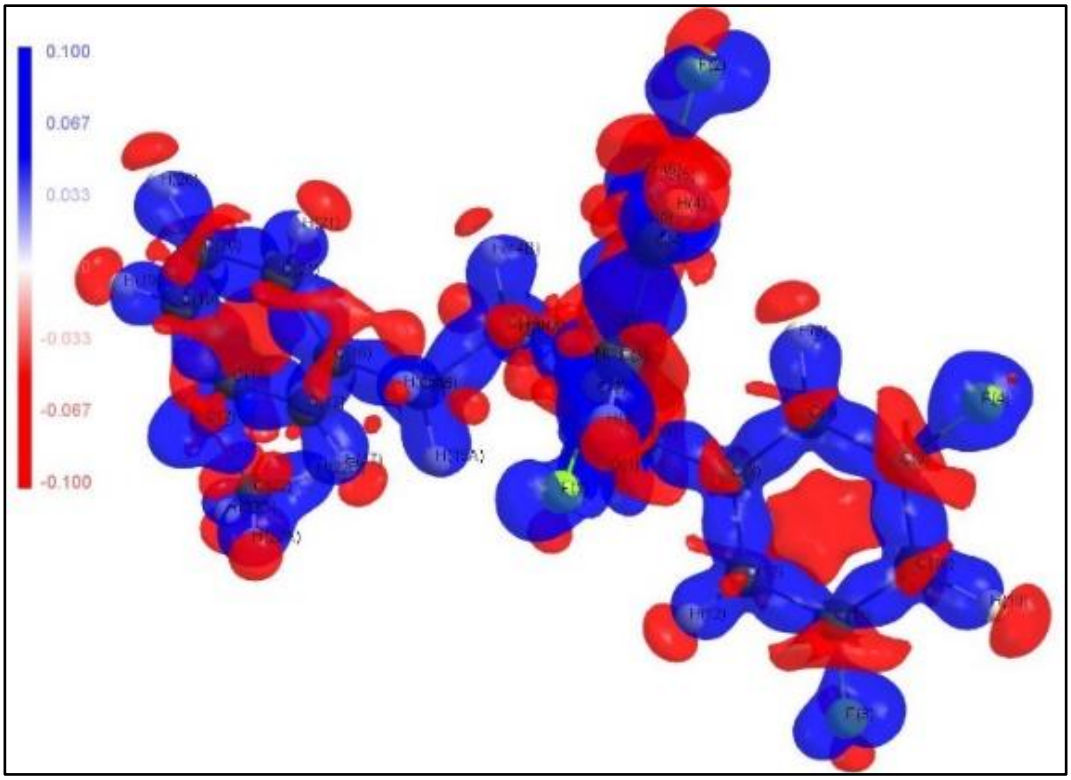

Figure 5.3.2.2: The 3D static deformation density maps with positive (blue surface) and negative (red surface) contours starting at ±0.05 e $Å^{-3}$ with an interval of ±0.1 e $Å^{-3}$.

5.3.3 Laplacian Maps and Bond Critical Points

The charge concentration is uniform throughout the sphere in an atom, but as a molecule is formed from atoms, the charge concentration becomes non-uniform leading to the formation of local minima and local maxima in the valence shell. Laplacian of electron density helps revealing the local minima and local maxima in the valence shell. In the Laplacian maps (Figure 5.3.3.1), the regions of charge concentration and depletion are revealed to understand the distribution of charge density and bonding features of atoms.

The topological properties of the electron densities and the interactions were carried out based on Bader's quantum theory of Atoms in Molecule (QTAIM)[98] approach using the module XDPROP in XD package.[153] The bond critical points (BCP) between the intermolecular interactions were calculated and studied. The BCPs are of type (3, -1) which indicate the pair of nuclei is linked by a chemical bond. The BCPs and the Ring critical points for the molecule are shown in the Figure 5.3.3.2.

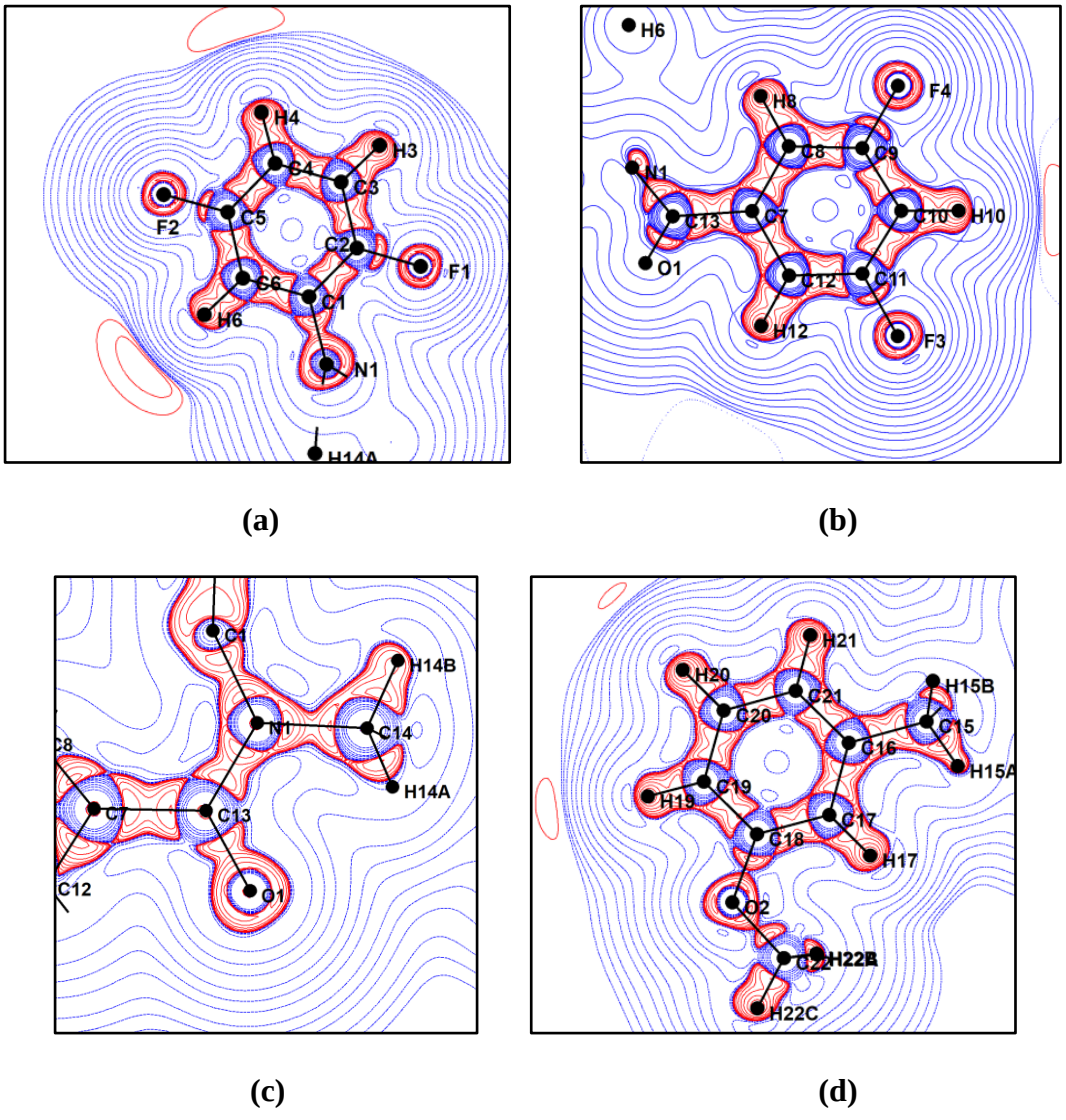

Figure 5.3.3.1: The 2D Laplacian maps, drawn in the molecular plane containing C1F1F2 (a), C7F3F4 (b), C7N1O1 (c) and C18O2C22 (d) atoms using positive (blue, solid line) and negative (red, dotted line) with contour intervals at ± 0.05 e $Å^{-3}$.

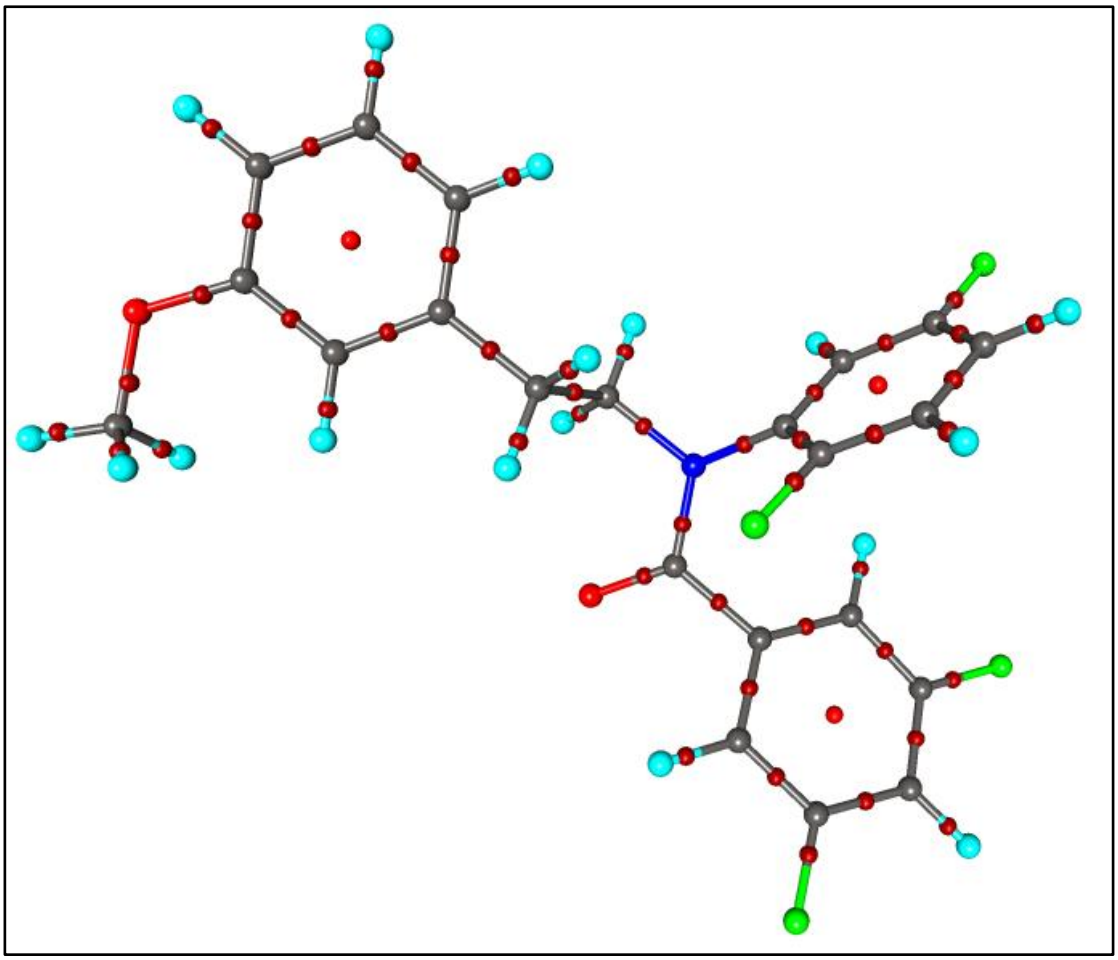

Figure 5.3.3.2: The molgraph view of the bond critical points (red dots) and ring critical points (yellow dots) for the molecule.

5.3.4 Topological analysis of intermolecular interactions

A detailed analysis of interactions involving organic fluorine (C−F···F−C and C−H···F−C) were carried out to elucidate the nature and the strength of these interactions. The analysis of topological properties of electron densities were carried out using the program MoPro.[159] Among the studied interactions, Type I C−F···F−C interaction was observed for C2−F1···F4−C9 halogen-halogen interaction. The interaction C2−F1···F3−C11 is a Quasi Type I/ Type II kind of interaction observed in the molecule. The interactions with the bond critical points (red dots) and the Laplacian plot showing

the three atoms F1, F3 and F4 are shown in the Figure 5.3.4.1. The bond paths for both these interactions are shown in the red line (Figure 5.3.4.1a).

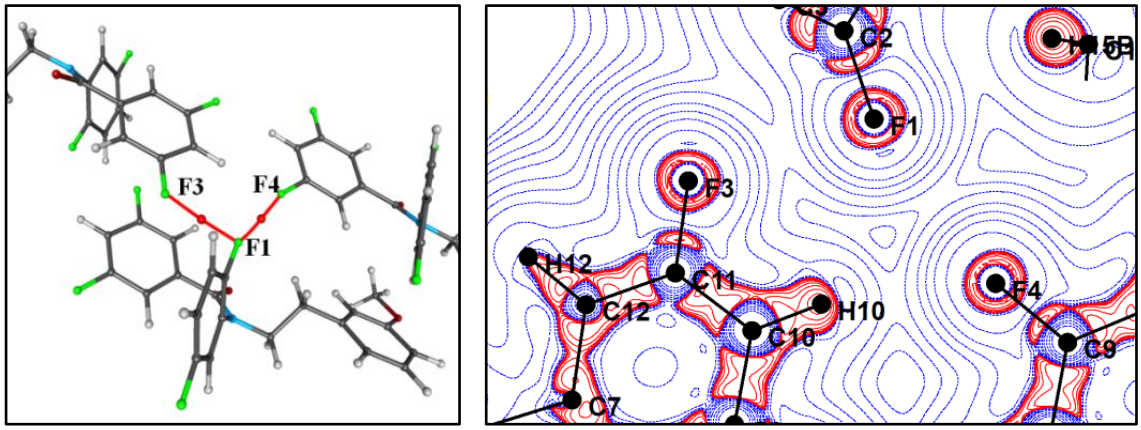

(a) **(b)**

Figure 5.3.4.1: (a) The BCP and bond path for the interaction C2−F1···F4−C9 and interaction C2−F1···F3−C11. (b) Laplacian maps for the interaction C2−F1···F4−C9 and C2−F1···F3−C11 drawn at the logarithmic interval of $-\nabla^2\rho_b$ e Å^{-5}

In addition to these C−F···F−C interactions, a weak C10−H10···F4−C9 hydrogen bond dimer was also observed. The BCP and the Laplacian plot for this interaction were also calculated and are shown in the Figure 5.3.4.2. The bond path for this dimer formation is represented by the red line (Figure 5.3.4.2a) and these are not straight lines. Bond paths are the lines of maximum electron density and need not necessarily be straight lines as shown in this intermolecular interaction.

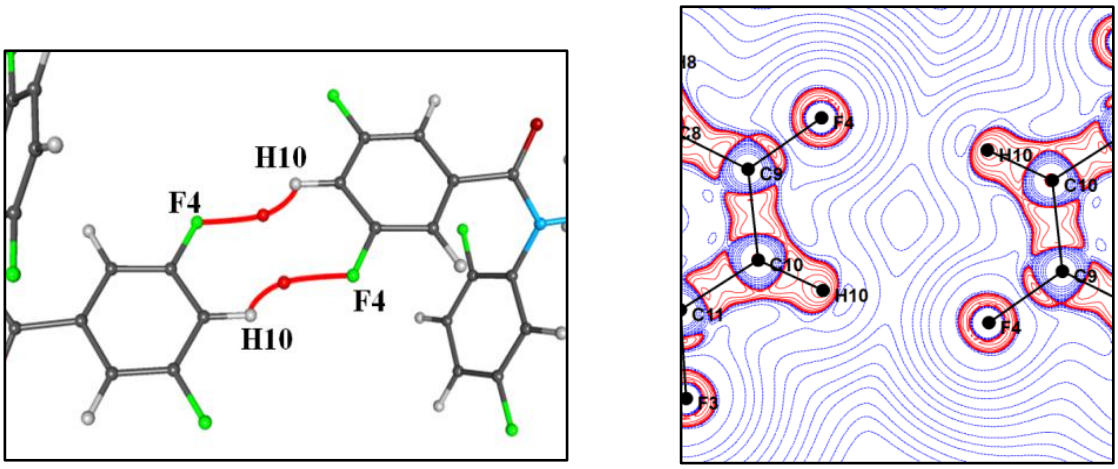

(a) **(b)**

Figure 5.3.4.2: (a) The BCP and the bond path for the interaction C10−H10···F4. (b) Laplacian maps for the dimer C10−H10···F4 drawn at the logarithmic interval of $-\nabla^2\rho_b$ e Å^{-5}

Table 5.3.4.1 includes the topological parameters for the mentioned interactions in the molecule under study. It includes the electron density (ρ), Laplacian of electron density ($\nabla^2\rho$), Rij value, d1, d2 values, the eigen values generated by Hessian matrix ($\lambda_1, \lambda_2, \lambda_3$), ellipticity, the local potential energy and kinetic energy at the BCPs.

For the interaction with (3,-1) type of critical points (CPs), all these properties provide the utmost important information. The strength of the bond is defined by the electron density present at the BCP which is given by the quantity ρ, and its second derivative, Laplacian represents the chemical feature of the bond. If Laplacian is less than zero, it represents the density is locally concentrated and the interactions are shared interactions whereas a value of Laplacian greater than zero represents closed-shell interactions. The eigenvalues (λ_1, λ_2, λ_3 with $\lambda_1 \leq \lambda_2 \leq \lambda_3$) determine the profile of electron density. For the cylindrical bonds, λ_1 is equal to λ_2 which defines the curvature of the cylindrical bond but the bond path (BP) deviates from its cylindrical nature when the charged is accumulated preferentially

in a particular plane along the BP and in that case these two values are not same and it defines the elliptical nature of the bond. The quantitative measure of the ellipticity is defined by (ε) which is given by $\varepsilon = \lambda_1/\lambda_2 - 1$. The Charge density at the BCP is another important parameter in defining the nature of the bond. This parameter E_{HB} (Hydrogen Bond energy)[160] can be evaluated by using the local potential energy density V_{cp} using the equation

$$E_{cp} = 1/2(V_{cp})$$

Table 5.3.4.1: Topological parameters of the interactions

Interactions	ρ(eÅ^{-3})	$\nabla^2\rho$(eÅ^{-5})	R_{ij} (Å)	d_1 (Å)	d_2 (Å)	λ_1	λ_2	λ_3	Ellipticity (ε)	G_{cp} **kJ/mol/Å^3**	V_{cp} **kJ/mol/Å^3**
C2−F1···F4−C9	0.02 (2)	0.50 (8)	2.9532	1.4900	1.4658	-0.065	-0.018	0.583	2.5812	9.48	-5.33
C2−F1···F3−C11	0.05 (3)	0.94 (9)	2.8224	1.4227	1.4012	-0.187	-0.124	1.254	0.5061	19.16	-12.63
C10−H10···F4	0.01 (2)	0.43 (6)	2.5310	1.5091	1.0611	-0.060	-0.040	0.529	0.4814	8.01	-4.32

The topological parameters for all the covalent interactions are given in the Table 5.3.4.2.

5.3.5 3D deformation density plots for the intermolecular interactions

3D static deformation density plots have been plotted in C2−F1···F4−C9, C2−F1···F3−C11 and C10−H10···F4−C9 intermolecular regions (Figure 5.3.5.1). As the C−F···F−C interactions are of different type, the directionality of the plots also differ.

Table 5.3.4.2: Topological parameters for the covalent interactions

Interactions		ρ(eÅ^{-3})	$\nabla^2\rho$(eÅ^{-5})	R_{ij} (Å)	d_1 (Å)	d_2 (Å)	λ_1	λ_2	λ_3	Ellipticity (ε)	G_{cp} kJ/mol/Å^3	V_{cp} kJ/mol/Å^3
Atom 1	Atom 2											
F1	C2	2.03	-12.46	1.35	0.79	0.56	-17.33	-16.21	21.08	0.069	792.22	-1923.90
F2	C5	1.86	-13.45	1.35	0.83	0.52	-15.18	-14.29	16.02	0.063	634.73	-1635.70
F4	C9	1.93	-12.38	1.35	0.82	0.54	-16.14	-14.76	18.53	0.093	712.34	-1761.74
F3	C11	1.89	-14.32	1.35	0.83	0.52	-16.15	-14.59	16.42	0.107	643.02	-1676.18
O1	C13	2.79	-27.97	1.23	0.79	0.44	-27.41	-23.40	22.85	0.172	1223.67	-3209.13
O2	C18	1.98	-16.02	1.36	0.83	0.53	-15.66	-14.28	13.93	0.096	683.47	-1803.17
O2	C22	1.78	-14.84	1.42	0.88	0.55	-15.48	-11.02	11.65	0.405	545.34	-1494.91
N1	C1	1.85	-10.72	1.42	0.80	0.62	-13.83	-12.68	15.80	0.090	677.57	-1646.97
N1	C13	2.21	-20.42	1.37	0.79	0.57	-19.49	-14.88	13.96	0.310	805.12	-2166.30
N1	C14	1.67	-8.11	1.47	0.85	0.63	-12.03	-10.82	14.74	0.112	588.49	-1397.77
C1	C2	2.21	-19.14	1.39	0.69	0.71	-18.93	-13.97	13.76	0.355	822.84	-2167.09
C1	C6	2.13	-17.33	1.40	0.71	0.69	-16.98	-13.40	13.05	0.267	789.92	-2051.77
C2	C3	2.09	-17.06	1.39	0.73	0.65	-16.83	-12.96	12.73	0.299	756.67	-1977.92
C6	C5	2.09	-16.87	1.38	0.66	0.72	-16.74	-13.03	12.90	0.284	763.09	-1985.73
C6	H6	1.99	-18.46	1.08	0.66	0.42	-18.20	-16.75	16.49	0.087	647.22	-1797.37
C7	C8	2.11	-15.65	1.40	0.70	0.70	-16.69	-13.72	14.77	0.216	799.73	-2025.69
C7	C13	1.74	-10.69	1.50	0.73	0.77	-13.17	-11.56	14.04	0.139	595.38	-1481.98
C7	C12	2.11	-15.93	1.40	0.69	0.71	-16.78	-13.60	14.45	0.234	797.51	-2028.79
C17	C18	2.15	-17.50	1.40	0.67	0.73	-17.06	-13.32	12.88	0.280	800.10	-2076.90
C17	C16	2.04	-15.25	1.40	0.70	0.70	-15.49	-12.69	12.93	0.220	748.90	-1913.25
C17	H17	1.79	-15.37	1.08	0.70	0.38	-16.97	-15.96	17.56	0.063	549.73	-1518.07
C8	C9	2.18	-18.58	1.39	0.67	0.72	-17.62	-14.28	13.32	0.233	809.96	-2126.06
C8	H8	1.80	-16.65	1.08	0.71	0.37	-17.53	-16.45	17.33	0.065	531.28	-1516.15
C5	C4	2.24	-20.03	1.39	0.73	0.66	-18.82	-14.59	13.37	0.290	834.43	-2214.41
C18	C19	2.14	-18.00	1.40	0.73	0.67	-17.24	-13.35	12.59	0.292	783.25	-2056.85
C16	C21	2.13	-17.34	1.39	0.70	0.70	-17.02	-13.22	12.90	0.288	784.35	-2041.02
C16	C15	1.71	-10.56	1.51	0.76	0.74	-11.93	-11.14	12.51	0.071	570.12	-1427.76
C14	C15	1.71	-9.65	1.53	0.77	0.76	-11.93	-10.88	13.16	0.097	590.08	-1443.02
C14	H14A	1.87	-16.45	1.07	0.68	0.39	-17.41	-16.49	17.45	0.055	585.47	-1618.98
C14	H14B	1.82	-14.99	1.07	0.67	0.40	-16.65	-15.62	17.28	0.066	582.55	-1573.49
C9	C10	2.19	-18.31	1.39	0.70	0.68	-18.00	-13.98	13.68	0.288	821.18	-2140.97
C10	C11	2.22	-18.96	1.39	0.67	0.72	-18.49	-14.26	13.79	0.297	838.63	-2193.72
C10	H10	1.79	-16.96	1.08	0.71	0.37	-17.23	-16.30	16.57	0.057	516.00	-1493.84
C12	C11	2.26	-20.73	1.38	0.68	0.71	-18.89	-15.122	13.28	0.249	842.22	-2249.01
C12	H12	1.81	-17.94	1.08	0.74	0.34	-18.52	-17.56	18.14	0.055	518.61	-1525.92
C3	C4	2.15	-18.14	1.40	0.67	0.72	-17.16	-13.81	12.83	0.242	793.32	-2080.71
C3	H3	1.87	-16.25	1.08	0.69	0.39	-17.51	-16.67	17.92	0.050	594.41	-1631.43
C4	H4	1.84	-17.03	1.08	0.68	0.40	-17.15	-15.91	16.03	0.078	557.89	-1579.64
C20	C19	2.10	-17.46	1.39	0.71	0.67	-16.53	-13.38	12.45	0.236	758.99	-1993.63
C20	C21	2.12	-17.45	1.40	0.69	0.71	-16.99	-13.40	12.93	0.268	779.77	-2034.92
C20	H20	1.80	-16.00	1.08	0.69	0.39	-17.24	-15.77	17.01	0.093	544.32	-1524.57
C19	H19	1.79	-16.42	1.08	0.71	0.37	-17.35	-16.30	17.22	0.065	525.72	-1498.67
C21	H21	1.76	-16.00	1.08	0.72	0.36	-17.35	-16.44	17.79	0.056	511.05	-1457.91
C15	H15A	1.77	-14.35	1.07	0.71	0.35	-16.81	-15.83	18.29	0.061	550.49	-1491.78
C15	H15B	1.69	-13.15	1.07	0.69	0.37	-15.24	-14.68	16.77	0.038	513.98	-1386.04
C22	H22A	1.90	-15.71	1.07	0.65	0.42	-17.74	-15.06	17.10	0.178	627.04	-1682.01
C22	H22B	1.82	-13.32	1.07	0.73	0.33	-18.83	-17.92	23.43	0.051	610.49	-1583.82
C22	H22C	1.72	-16.37	1.07	0.72	0.35	-18.35	-16.30	18.28	0.125	479.39	-1404.72

The interaction C2−F1···F3−C11 is expected to be less attractive than C2−F1···F4−C9 as per the observation by one of our earlier studies where we carried out the gas phase calculations for the same molecule using Gaussian09 and the stabilization energies for these two interactions were calculated to be -5.5 kcal/mol and -8.9 kcal/mol respectively.[149] In Figure 5.3.5.1(a), the valence shell charge concentration (VSCC) region of F4 is facing the charge depletion region (σ hole) of F1 and in figure 5.3.5.1(b), the VSCC region of F1 is facing the σ hole of F3 atom. The Laplacian plot in figure 5.3.4.1(b) shows a little signature of the polar flattering effect for the fluorine atoms.[161] The C10−H10···F4−C9 hydrogen bond forms a dimer, which can clearly be seen in the 3D deformation plot and it is seen that the electron deficient region over H points towards the electron rich region over F which signifies the attractive nature of the interaction (Figure 5.3.5.1(c)).

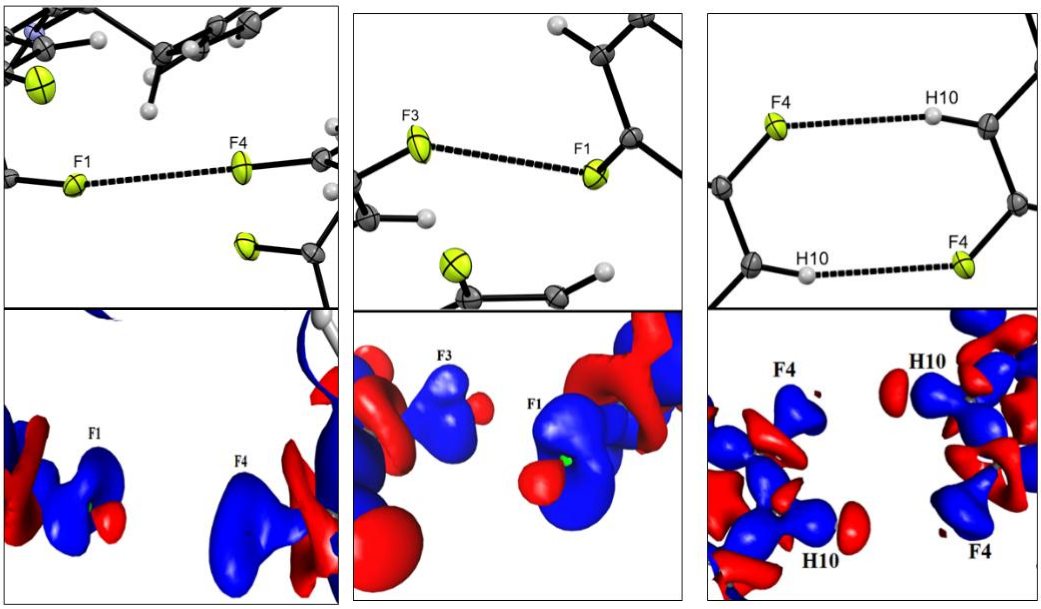

(a) **(b)** **(c)**

Figure 5.3.5.1: 3D deformation density plots in the intermolecular region for the interactions (a) C2−F1···F4−C9, (b) C2−F1···F3−C11 and (c) C10−H10···F4

5.3.6. Electrostatic potential

The electrostatic potential for the molecule is calculated from the experimental electron density distribution. This is a very sensitive physical property that reflects even the minor changes in the crystalline environment. It provides information about the electron rich and the electron deficient sites in the molecule and helps in understanding the interactions. Here (Figure 5.3.6.1) we have mapped the ESP plot for the molecule. The electronegative atoms (oxygen, fluorine and nitrogen) have negative electrostatic region whereas the hydrogen and the carbon atoms has electropositive and neutral potential respectively. The electrostatic map for the benzene rings with fluorine substitutions is yellowish (negative potential) which is the result of the polar nature of C−F group.[162] However, the benzene ring with the methoxy group has a greenish (neutral potential) electrostatic map. The electron density on F1 is more negative as compared to the other two interacting fluorine atoms i.e. F3 and F4. This difference on isosurface can be either because both the halogen halogen interactions involve F1 atom hence resulting into higher electron density or because of the substitution effect as F1 is in close proximity to the nitrogen atom which is making its surface more electronegative.[161] The electrostatic maps for the intermolecular interactions are shown in figure 5.3.6.2.

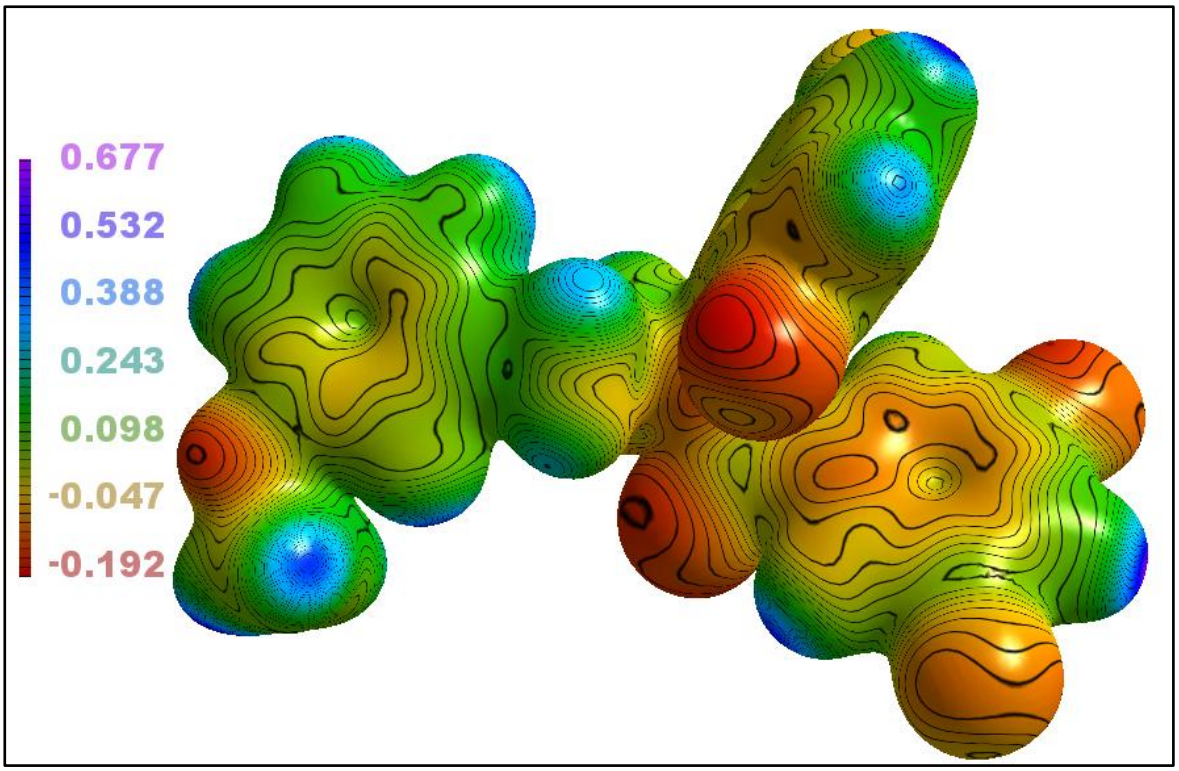

Figure 5.3.6.1: ESP map of the molecule drawn at the interval of ±0.1 eÅ^{-3}.

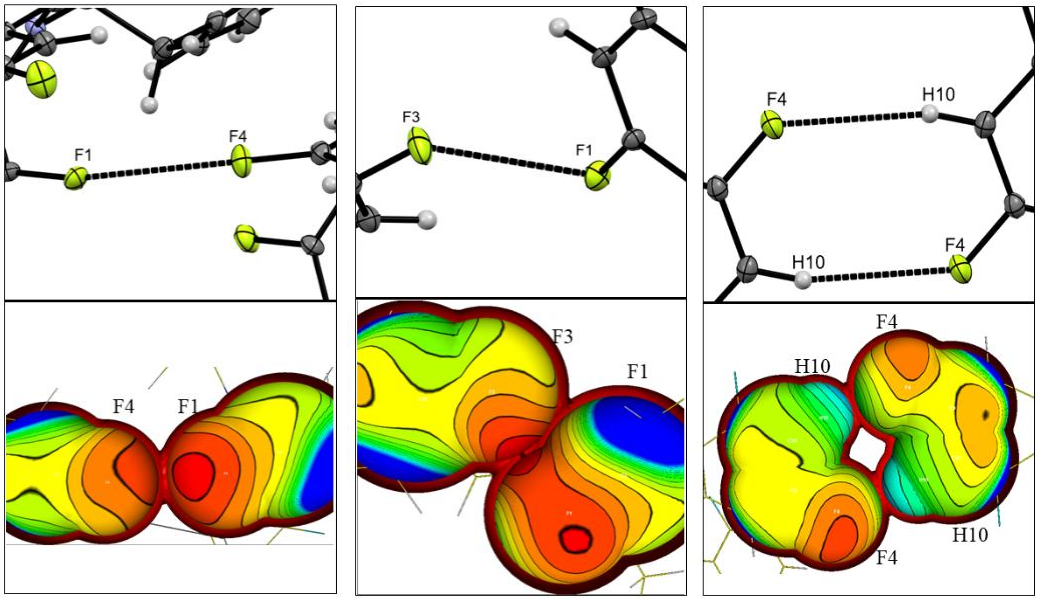

(a) **(b)** **(c)**

Figure 5.3.6.2: 3D electrostatic potential maps in the intermolecular region for the interactions (a) C2−F1···F4−C9, (b) C2−F1···F3−C11 and (c) C10−H10···F4

5.3.7. Atomic Charges

The atomic charges for all the elements after the final refinement is mentioned in Table 5.3.7.1. It is to be noted that the same elements have different charges depending upon how they are participating in the inter- and intra-molecular interactions.

Table 5.3.7: Atomic charges for all elements after final refinement

Atom	Atomic charge *(e)*	Atom	Atomic charge *(e)*
F(1)	-0.216(23)	C(18)	-0.056(64)
F(2)	-0.270(25)	C(16)	-0.058(36)
F(4)	-0.289(27)	C(14)	+0.125(33)
F(3)	-0.251(27)	C(9)	+0.149(41)
O(1)	-0.315(32)	C(10)	-0.077(38)
O(2)	-0.433(34)	C(12)	-0.230(36)
N(1)	-0.274(39)	C(11)	+0.165(41)
C(1)	+0.005(54)	C(3)	+0.052(33)
C(2)	+0.044(43)	C(4)	-0.045(34)
C(6)	+0.005(38)	C(20)	-0.012(34)
C(7)	+0.130(58)	C(19)	+0.035(44)
C(17)	-0.082(51)	C(21)	-0.100(39)
C(8)	-0.140(36)	C(15)	-0.211(36)
C(13)	+0.073(34)	C(22)	+0.073(40)
C(5)	+0.115(40)		

5.4 CSD analysis of C−F···F−C interactions

We searched the Cambridge Structure Database (CSD) for C−F···F−C interactions where fluorine is bonded to aromatic carbon. The distance range was selected between 2.00 Å and 2.96Å with θ_1 and θ_2 ranging from 0˚ to 180˚. We did not add any other restriction for R-factor, organic compounds, 3D coordinates, disordered, polymeric or ions. From our search we got a total of 10350 entries. Among these the Type I C−F···F−C interactions were 4524 entries and 1819 of these have $\theta_1 = \theta_2$. 2009 interactions have $|\theta_1-\theta_2|$ less than 10˚ and 696 interactions have $|\theta_1-\theta_2|$ between 10˚ and 15˚. 3804 C−F···F−C interactions were found to be falling in Type II interactions. Quasi Type I/Type II kind of interaction accounted for 2022 entries among which 97 entries

have $|\theta_1-\theta_2|$ ranging between 85˚ and 95˚. The histograms for the searches are added below (Figure 5.4.1).

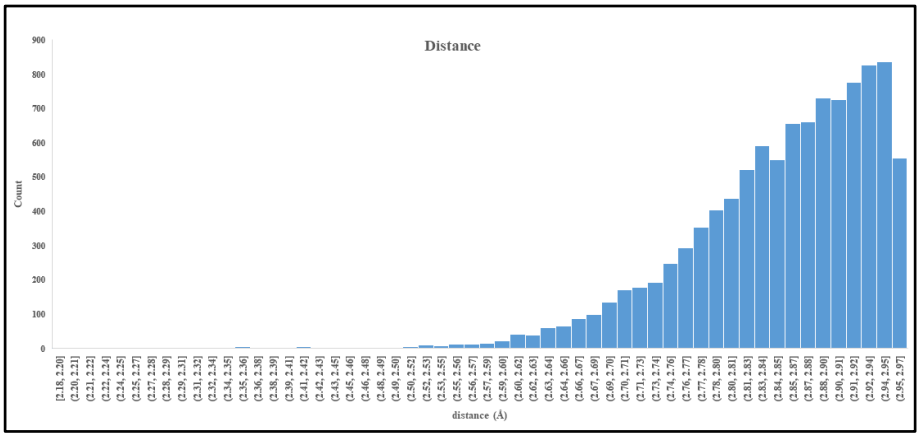

(a)

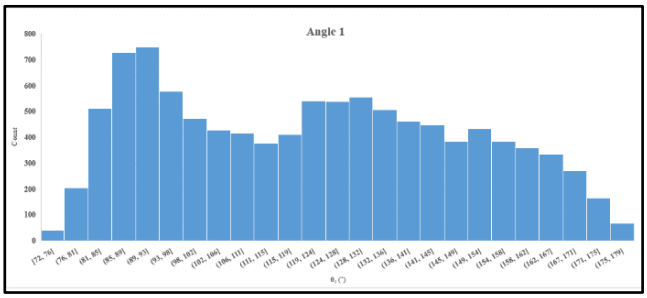

(b)

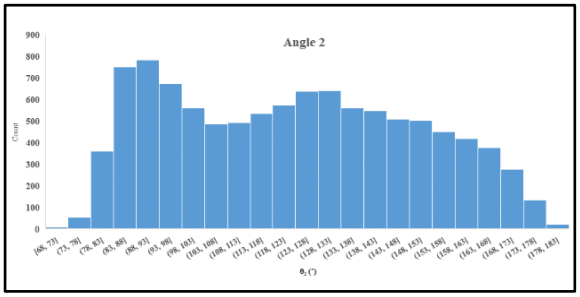

(c)

Figure 5.4.1: (a) Distance histogram for the interactions searched on CSD. **(b)** Histogram for Angle 1 for the C−F···F−C interactions. **(c)** Histogram for angle 2 for the C−F···F−C interactions.

5.5 Comparison of topological properties of electron densities for F···F interactions

Further, the topological properties of electron densities for the F···F interactions are compared with those reported based on experimental charge density studies.[146,159,160] The topological properties of the F···F interactions reported here compare well with those reported in the literature (Table 5.5.1). The topological properties of the electron densities of Cl···Cl intermolecular interactions reported for various halogenated molecules are also

listed in Table 3.[142] The results suggest that the F···F interactions are stronger than the Cl···Cl interactions.

Table 5.5.1: Comparison of electron density topology of F···F and Cl···Cl halogen interactions.

Interactions	$\rho_{CP}(\mathbf{r})$ **(eÅ^{-3})**	$\nabla^2\rho_{CP}(\mathbf{r})$ **(eÅ^{-5})**	R_{ij} **(Å)**	$G_{CP}(\mathbf{r})$ **kJ/mol/Å^3**	$V_{CP}(\mathbf{r})$ **kJ/mol/Å^3**
F···F[146]	0.07	0.93	2.6589	36.9	-27.9
F···F[146]	0.05	1.03	2.8091	37.8	-24.5
F···F (type I)[160]	0.04	0.82	2.8187	16.0	-9.6
F1···F3[160] quasi-type I/II	0.05	0.94	2.8224	19.2	-12.6
F6A···F4A[159]	0.04	0.70	2.899	*	*
F1···F4[160] (type I)	0.02	0.50	2.9532	9.5	-5.3
Cl···Cl[142]	0.02	0.31	3.7212	6.1	-3.6
Cl···Cl[142]	0.03	0.41	3.7655	8.0	-4.7

* Not reported

5.6 Discussion & Conclusion

We have analysed Type I and Quasi Type I/ Type II of C−F···F−C interactions, along with one weak C−H···F−C hydrogen bond. The charge density distribution on these interactions were analysed in detail using the topological properties via QTAIM. We have performed multipole modelling refinement on the high resolution data and the accuracy of the model was checked by DRK plots. All the fast Fourier transformation residual density maps, 2D deformation density maps and Laplacian maps were plotted to check the accuracy of the model. Bond critical points (BCPs) were calculated for the intra- and inter-molecular interactions observed in the molecule. The presence of BCPs indicated the presence of intermolecular interactions. The value of electron density and Laplacian

of electron density were calculated at the BCPs. Further, the VSCC and σ hole on the fluorine atoms in the 3D deformation density plots revealed the chemical bond density features of these interactions. The distribution of electron densities on the atoms within the molecule was studied using the 3D electrostatic potential maps which signified the polar nature of the C–F group.

From our analysis, we conclude that charge density gives us a fairly accurate and reliable representation of the nature of interactions in terms of electron properties and the 3D deformation densities. From the topological analysis, we elucidate that the organic fluorine mediated interactions discussed in the manuscript are closed-shell type of interactions and not mere van der Waals interaction resulting from some force of attraction. The hydrogen bond energy calculated using the local potential energy shows that the studied interactions are stabilizing in nature. The precise value of atomic charges is calculated using charge density analysis and we unravel that all the fluorine atoms behave differently in the crystal structure of the molecule under study.

Concluding Remarks

Hydrogen bonds play a vital role in our daily life activities. Be it the water molecules bonded by the hydrogen bonds or the DNA strands coming together with the help of hydrogen bonds. The first definition of hydrogen bonds was given by L. Pauling in 1939 and since then several groups across the globe have carried out various experimental and computational approaches to understand these bonds. While studying the hydrogen bonds, one interesting interactions were observed which were between two halogens. These were named the halogen-halogen interactions. Among these both type of interactions, the hydrogen bonds and the halogen-halogen bonds, the interactions formed by organic fluorine ("C–F" group) has always been a discussion. Given the small size and high eletronegativity of fluorine, the nature and the geometry of the interactions offered by organic fluorine group has never found a conclusion.

We, in our study have evaluated the organic fluorine mediated interactions for different systems under different environments. Our first study involves fluorine substituted "bridge-flipped" isomers. These molecules have the possibility of C–H···F–C interactions and C–F···F–C interactions in the presence of strong N–H···O=C hydrogen bonds. We studied these molecules for their structural analysis and calculated the stabilization of all kind of interactions present with the help of computational tools like Gaussian09. We observed that the presence of organic fluorine mediated interactions influence the strong hydrogen bonds. The strong hydrogen bonds present in the molecules should decide the geometry and the orientation of the molecule and thus all the compounds should crystallize in the same space group. However, the presence of fluorine mediated interactions has caused the compounds to crystallize in different space groups (triclinic and monoclinic). From the computational calculations too, we have observed that the number and position of the fluorine substitution in the molecules effect the

stabilization energy of the strong N–H···O=C hydrogen bonds. Also, the geometric parameters for N–H···O=C hydrogen bonds also vary with the fluorine substitution.

Our second study involves the tetra-fluoro substituted secondary amides that do not have the possibility of N–H···O=C hydrogen bonds but they have C–H···O=C hydrogen bonds along with the C–H···F–C interactions, C–F···F–C interactions and C–H···O–C interactions. All of these interactions were studied computationally using Gaussian09 and the geometric parameters for the interactions were analysed to understand the most probable distance and angle for these interactions. From the computational calculations, we conclude that these interaction are stabilizing in nature with more than 50% of the interactions falling in strong hydrogen bond region as per the classification by Desiraju and Steiner. The geometric parameter suggest that the linear geometry is not very probable for C–H···F–C and C–F···F–C interactions. The most probable distance and angle for the C–H···F–C interactions and C–F···F–C interactions is between 2.5 Å and 2.6 Å and between 150° and 160° respectively. Further, in our third study, we chose tetra-fluoro substituted isoquinoline derivatives for our computational and topological studies where the only possibility is for C–H···F–C interactions and C–F···F–C interactions along with some C–H···O–C interactions which are mediated from the methoxy group present in the molecule. The analysis of the computational calculations suggest the interactions to be stabilizing in nature with more than 50% interactions falling in strong hydrogen bond region. QTAIM (Quantum Theory of Atoms In Molecules) analysis enabled us to calculate the electron density and the Laplacian of electron density which inferred that the fluorine mediated interactions are the closed-shell interaction.

Thereafter, we carried out an experimental charge density analysis to understand the C–F···F–C interactions both quantitatively and qualitatively. We collected a high resolution single crystal X-ray diffraction data on one of the secondary amides studied

earlier and refined it using the kappa formalism and Hansen-Coppens multipole formalism using XD package. It differs from the routine structure refinement as it does not consider atoms to be spherical in nature and takes in account the polarizability factor. The topological analysis was followed after the multipole refinement using QTAIM. From the topological analysis, we calculated the bond critical points, electron density and the Laplacian of electron density from the BCPs and also the local potential and local kinetic energies were calculated for the interactions involved in the molecule. From our analysis, using the 3D deformation density and the 3D electrostatic potential plot, we deduce that the organic fluorine mediated interactions are stabilizing. The local potential energy values for these interactions backs this conclusion. Also, the different values of atomic charges on all the fluorine atoms give information about the difference in behaviour of same elements in a molecules.

Therefore, to conclude, through our thorough investigation on different systems involving fluorine, it may be said that the interactions offered by organic fluorine group play an important role in crystal engineering. They can alter, control and direct the crystal packing of the molecule through various supramolecular synthons. They also can influence the strong hydrogen bonds in a molecule. So, the organic fluorine mediated interactions cannot be treated as mere a van der Waals interactions.

Appendix

Statistical insight on weak hydrogen bonds involving C=O and C–F groups as hydrogen bond acceptor: A comprehensive database analysis

Appendix

A.1 Introduction

In the previous chapters, we have evaluated the organic fluorine mediated interactions using various tools like structural analysis, computational study, topological analysis and experimental charge density studies. From these studies, we have inferred that the interactions offered by the "C–F" group are stabilizing in nature, they are directional and are closed-shell type of interactions typically ionic in nature. Different research groups across the globe have carried out a systematic analysis of the crystal structures which are available in the Cambridge Structure Database (CSD). The nature of the C–F group and the acceptance power of the organic fluorine group has been debated over the CSD analysis too.[14,33,163,164]

Shimoni and Glusker from their CSD analysis, claimed that C–H···F–C hydrogen bonds contributes in crystal packing;[33] Howard *et al.,* refuted the importance of such interaction in crystal packing and classified them to have little significance and considered them as Van der waals interaction.[14] Dunitz and Taylor too concluded that organic fluorine does not accept any hydrogen bonds.[34] But the C–H group has been found to be a moderate hydrogen bond donor and the influence of weak C–H···O=C, C–H···N, C–H···Cl etc were found to be useful in crystal engineering as hydrogen bonds.[165-168] This has triggered the

systematic studies (experimental, computational and database) on the existence and nature of C–H···F–C interaction.[11] Research group of Guru Row through their extensive experimental evidences showed that "organic fluorine" is capable of altering the packing mode of various (mono/di/multi) fluorinated small organic molecules and also established that the weak interactions like C–F···F–C, C–H···F–C, and C–F···π offer stability to the crystal lattice in the absence of other strong hydrogen bonds.[29,47] Thakur *et al.*, indicated C–H···F–C to be very weak interactions but directional in nature.[169] Dalvit *et al.*, concluded from their experimental evidences and computational studies that organic fluorine can accept hydrogen bonds.[170] They showed that RCH_2F moiety accepts hydrogen bond superior to that of $RCHF_2$ and RCF_3 but the hydrogen bond energy was less favourable than acetophenone.

In 2016, Gavezzotti and Lo Presti (G & LP) re-analysed the structures containing C, H and O; C, H and F; C, H and Cl and C, H and N reported in CSD (with variable R factors (≤5% or ≤7.5% for different groups of element batches and having total number of atoms in a molecule less than 30 and 35 for molecules containing C, H, O; C, H, N elements and C, H, F; and C, H, Cl respectively) and concluded that the C–H···F–C contacts are very rare and are weak like Van der Waals interactions.[171] Subsequently, Taylor's CSD analysis (with R factor ≤5% and same datasets as of G & LP but included one additional dataset having C, H, F and O elements) concluded that C–H···F–C interactions are more frequent than C–H···O=C interactions and the former have a significant influence on crystal packing.[172] Another recent (2018) database analysis by Saha and co-workers[173] showed C–H···F–C to be definitely more favourable than C–H···π and C–F···F–C, but not more than C–H···O=C. In their study, they have carried out a CSD analysis on molecules containing C, H, F and O elements only and were restricted to structures with R factor ≤5%. They analysed the accessible surface areas (using Crystal Explorer[174]) of atoms and

from their observed/random contacts ratio, they showed C–H···O=C to be more favourable than C–H···F–C. They also conducted a population analysis and showed that the C–H···F–C are more favoured at higher angles (170° to 180°). It is noteworthy that the reports by G & LP[171] and Saha and co-workers[173] are based on high restrictions in terms of combination of elements selected, the maximum number of atoms in a molecule (in case of G & LP) and they have used R factors ≤5% or ≤7.5% in some cases. We believe that their studies were conducted using an extremely narrow pool of sample but they made general conclusions. From our earlier experimental experiences, we envisaged that the sampling from the database (CSD) should be done with a broader pool of molecules. We have earlier examined several molecules containing C, H, O, F and N, through structural analysis and observed that the frequency of occurrence of C–H···F–C was much higher than the occurrence of C–H···O=C hydrogen bonds even in the presence of other stronger hydrogen bonds.[110] Furthermore, for various reasons (like room temperature data, weakly diffracting crystals with poor I/σ(I) statistics etc), the R factor of a structure can be higher than 5% but the structure may be free from errors or major A or B level alerts and are publishable/published in the literature. Therefore, we decided to re-examine the CSD with a wider pool of structures, being segregated based on the elements they contained (Set 1: CHOF, Set 2: CHOFN, Set 3: CHONS and Set 4: CHONFS) and based on the interactions they possessed (Subset A: Both C–H···F–C and C–H···O=C present, Subset B: Only C–H···F–C present and Subset C: Only C–H···O=C present). We included the structures with R factor up to 10%, without any errors, no powder structures were taken and were restricted to organic molecules only. No restriction was applied on the hybridization of C bonded to F or H in case of C–H···F–C and C–H···O=C hydrogen bonds. A systematic analysis has been conducted among the compounds appeared in the CSD search based on the types of interactions they possessed (molecules having both

C–H···F–C and C–H···O=C hydrogen bonds and molecules with only C–H···F–C or C–H···O=C hydrogen bonds). Herein, we report our observation on the propensity of a C–F group over a C=O group for the formation of weak C–H···X (X = F–C or O=C) hydrogen bond.

A.2 Methodology

A.2.1 Cambridge Structural Database search

CSD was searched (version 5.39, November 2017 and Conquest Version 1.21 of CSD 2018) for the structures having elements only C, H, F, O, N and S; F and O present only as terminal groups and O–H, N–H, C–H···N–C, C–H···O–C interactions being absent, no other elements allowed, 3D coordinates determined, only non-disordered, no polymeric and no ions. The H···F and H···O distances were considered between 1.80 Å and 2.67 Å and the H···O distances were considered between 1.80 Å and 2.72 Å (Sum of their Van der Waals radii). The angles ∠C–H···F, ∠C–F···H, ∠C–H···O and ∠C=O···H were ranging from 80° to 180°. Table A.2.1 summarizes the number of hits found in various sub-groups of searches.

Table A.2.1: Summary of the number of hits found in different CSD searches

Serial no	**Elements**	**Interactions**	**Number of Hits(structures)/ molecules**	**Number of interactions**
1	CHFO	Both C–H···F–C and C–H···O=C present	172	798
2		Only C–H···F–C present	58	120
3		Only C–H···O=C present	36	69
4	CHFON	Both C–H···F–C and C–H···O=C present	71	267
5		Only C–H···F–C present	60	111
6		Only C–H···O=C present	45	71
7	CHFOS	Both C–H···F–C and C–H···O=C present	45	163
8		Only C–H···F–C present	82	139

9		Only C–H···O=C present	24	46
10	CHFONS	Both C–H···F–C and C–H···O=C present	14	52
11		Only C–H···F–C present	56	85
12		Only C–H···O=C present	7	10

From the CSD search carried out as listed in Table 1, we had a total of 112 (Sl. No. 3 + 6 + 9 + 12) molecules that contained C–H···O=C interactions only**,** 256 (Sl. No. 2 + 5+ 8 + 11) molecules containing C–H···F–C interactions only and 302 (Sl. No. 1 + 4 + 7 + 10) molecules had both the interactions present. Out of all these, all the molecules having C–H···O=C interactions were taken for Hirshfeld analysis, from these 112 molecules; we were able to generate the Hirshfeld surface areas for only 97 molecules. Therefore, same number of molecules were chosen at random (without any bias on H···F distance or ∠C–H···F and ∠C–F···H) from 256 molecules having C–H···F–C interactions only for Hirshfeld surface area analysis and 286 molecules out of 302 were selected at random from the ones that had both the interactions present. Hence, we had a pool of 480 molecules which we studied using the Hirshfeld surface area analysis.

A.2.2 Hirshfeld Surface Area Analysis

Total molecular surface area (S_M) and % contact areas between different atoms were calculated using the Hirshfeld surface area and fingerprint plot respectively using Crystal Explorer program.[174] The formulae used for the calculations were same as used by Saha et al.[173] and are listed below:

$$S_{X(i)} = \sum \frac{S_{All(e)\ldots X(i)}\%}{100} \times S_M \ldots. \qquad (1)$$

$$S_{x(e)} = \sum \frac{S_{X(e)\ldots All(i)}\%}{100} \times S_M \ldots. \qquad (2)$$

Where, $S_{x(i)}$ is the observed surface area for a particular type of atom X present within the concerned molecule and $S_{x(e)}$ is the observed surface area in the surrounding molecules. $S_{All(e)\ldots X(i)}$ % is the percentage surface area between all the atoms from surrounding and the atom X within the concerned molecule and $S_{X(e)\ldots All(i)}$ % is the percentage surface area between all the atoms within the molecule and the atom X from the surrounding molecules. The observed intermolecular contact surface area between two atoms Y and X was calculated as

$$OB_{Y\text{-}X} = \sum [(\frac{S_{Y(e)\ldots X(i)}\%}{100} + \frac{S_{X(e)\ldots Y(i)}\%}{100}) \times S_M] \ldots. \quad (3)$$

Where, $S_{Y(e)\ldots X(i)}$ % is the percentage contact surface area between Y atoms from surroundings (e) and X atoms from concerned molecule (i) and $S_{X(e)\ldots Y(i)}$ % is the percentage contact surface area between X atoms from surrounding (e) and Y atoms from the concerned molecule (i) involved in the intermolecular contact. The expected contact surface area between the atoms Y and X were calculated on the basis of random distribution as

$$RA_{Y\text{-}X} = \sum[(\frac{S_{X(e)\ldots All(i)}\%}{100} \times \frac{S_{All(e)\ldots Y(i)}\%}{100} + \frac{S_{Y(e)\ldots All(i)}\%}{100} \times \frac{S_{All(e)\ldots X(i)}\%}{100}) \times S_M] \ldots. \quad (4)$$

$\frac{OB_{Y-X}}{RA_{Y-X}}$ >1, signifies that the observed contacts are more than that is expected from a random distribution; which emphasized the stabilising nature of such interaction. The observed and random % surface area on X covered by the interacting atom Y was also calculated by

$$OB_{Y\text{-}X\%} = \frac{OB_{Y-X}}{S_{X(i)}+S_{X(e)}} \times 100 \ldots. \quad (5)$$

$$RA_{Y\text{-}X\%} = \frac{RA_{Y-X}}{S_{X(i)}+S_{X(e)}} \times 100 \ldots. \quad (6)$$

$$EX_{Y\text{-}X\%} = OB_{Y\text{-}X\%} - RA_{Y\text{-}X\%} \ldots. \quad (7)$$

A.3 Results And Discussion

We analysed 480 molecules having either C–H···F–C interaction or C–H···O=C interaction or both. We have analysed all these on the basis of Hirshfeld surface area by calculating the surface areas between various contacts and the surface area occupied by one atom over the other. Observed surface areas (the surface areas between the actually present interactions) and the random surface areas (the surface areas which would be there had the atoms in the molecules been randomly distributed) were calculated by using the formulae that are stated before.

Then, the ratio for observed and random surface areas was calculated as was done by Saha *et al.*, earlier.

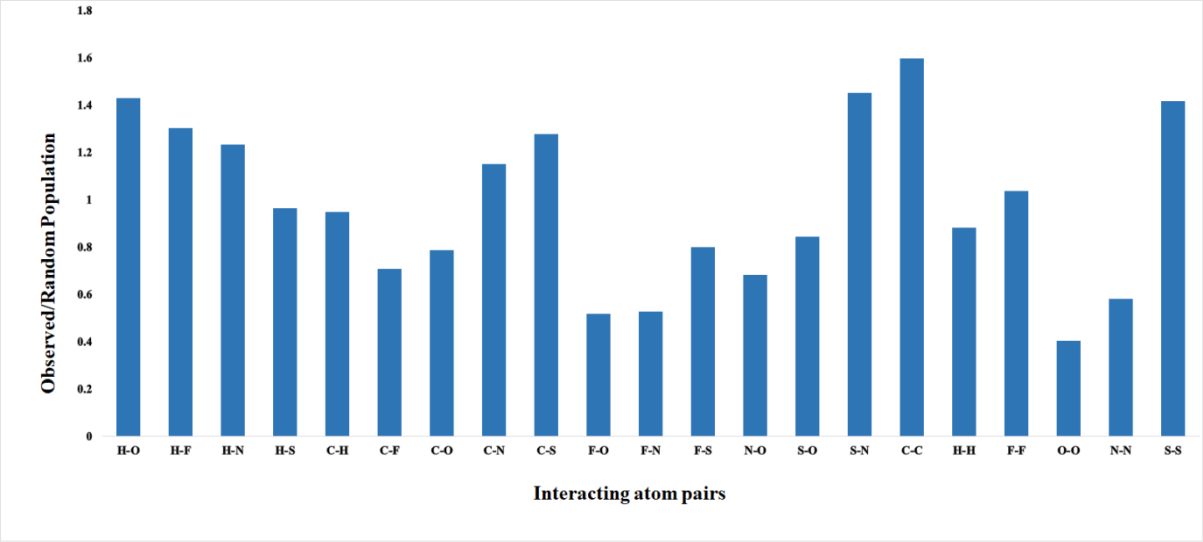

Figure A.3.1: Ratio of observed and random contact surface area for different interactions

It can be seen from Figure A.3.1 that F···O, F···N, N···O are the least stabilising among the hetero diatomic interactions and O···O, N···N, H···H occur slightly less than what would have been in a random distribution whereas the interactions involving C···C, S···S, F···F are observed more than the random distribution among the homoatomic interactions. We

also observed that the ratio for C–H···F–C interactions (1.303) is almost similar to that of C–H···O=C interactions (1.430), which therefore represents that both the interactions are stabilising in nature.

The percentage surface area occupied by one atom over the other was also calculated and the % excess surface area was also determined.

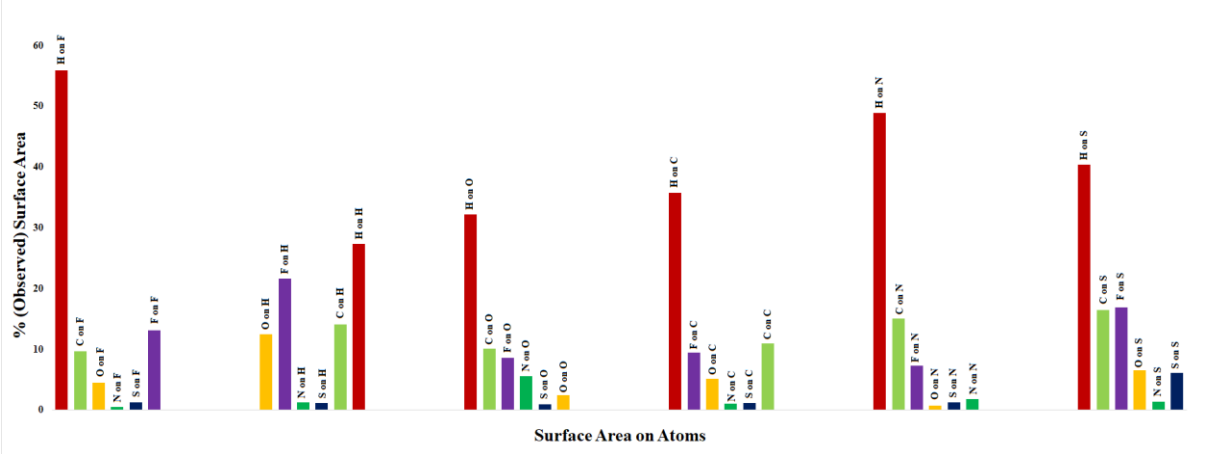

Figure A.3.2: Observed surface area on one atom occupied by the other atom.

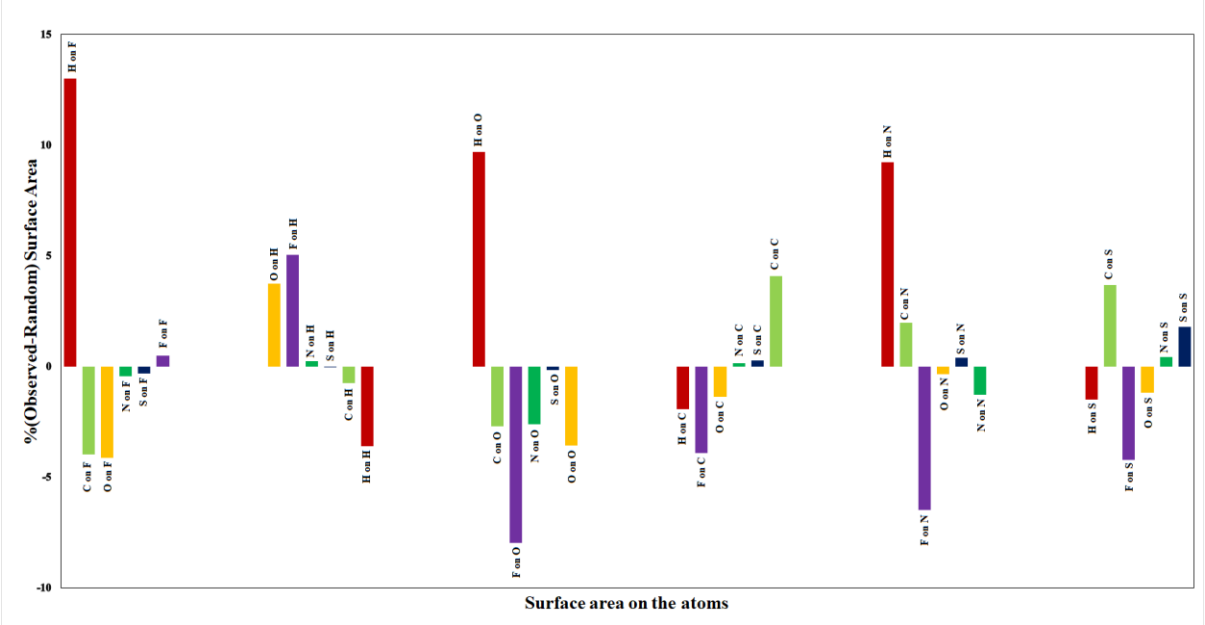

Figure A.3.3: Excess surface area on one atom occupied by the other atom.

From these plots (Figure A.3.2 and Figure A.3.3), it can be seen that the area occupied by H on F is more than that of H on O and also, the area occupied by F on H is higher than O on H. This means that H and F saturate one another's surface to a larger extent as compared to O and H. This represents that the interactions involving H and F are more prominent and more probable than the ones that involve H and O.

Further, we also analysed the angle and the distance distribution of all the interactions, which were found from the CSD searches to understand the most probable/suitable angle and the distance ranges for various interactions and also investigated whether any one particular interaction indirectly influences or alters the other type of interaction or not.

Table A.3.1: Most probable angle and distance for different interactions

Elements	**Type of Interaction**	**Number of interactions**	**Most Probable Angle (°) CHF/CHO**	**Most Probable Angle (°) CFH/COH**	**Most Probable Distance(Å)**
CHFO	Only C–H···F–C	120	130-140, 150-160	140-150	2.60-2.65
	Only C–H···O=C	69	120-130	140-150	2.50-2.60
	C–H···F–C when C–H···O=C are also present	380	130-150	120-130	2.60-2.65
	C–H···O=C when C–H···F–C are also present	418	150-160	130-140	2.65-2.70
CHFONS	Only C–H···F–C	85	130-140	130-150	2.60-2.65
	Only C–H···O=C	10	160-170	120-130	2.60-2.65
	C–H···F–C when C–H···O=C are also present	27	150-160	130-140	2.60-2.65
	C–H···O=C when C–H···F–C are also present	25	140-150	120-130	2.60-2.65
CHFOS	Only C–H···F–C	139	130-140	140-150	2.60-2.65
	Only C–H···O=C	46	130-140	130-140	2.50-2.60, 2.70-2.72
	C–H···F–C when C–H···O=C are also present	77	130-140	130-140	2.60-2.65
	C–H···O=C when C–H···F–C are also present	86	140-150	130-140	2.60-2.70

CHFON	Only C–H···F–C	111	130-140	130-140	2.60-2.65
	Only C–H···O=C	71	160-170	130-140	2.65-2.70
	C–H···F–C when C–H···O=C are also present	117	130-140	130-140	2.60-2.65
	C–H···O=C when C–H···F–C are also present	150	150-160	120-130	2.60-2.65

From Table A.3.1, it can be seen clearly that the number of interactions for C–H···O=C is always less than C–H···F–C interaction when these are present individually, whereas, in all the four set of compounds viz CHFO, CHFONS, CHFOS and CHFON, the number of interactions for C–H···O=C is more than C–H···F–C, just in CHFONS, the number of interactions are almost similar. This can be indicated that the C–H···F–C interactions may be helping to bring the O and H atoms in a close proximity which is further helping the atoms to form a weak bond.

Also, from Table A.3.1, it is evident that in the case of compounds with CHFO, CHFOS and CHFON elements, when "only" C–H···O=C interactions are present, the preference for ∠C–H···O is between 120°-130°, 130°-140° and 160°-170° respectively. Interestingly, in the presence of C–H···F–C interactions among the same group of molecules, the most probable angle range for ∠C–H···O shifts to 150°-160°, 140°-150° and 150°-160° respectively. The same is not observed for the C–H···F–C interactions in presence of C–H···O=C interactions. The most probable H···X (X = O or F) distance range for the C–H···O=C interactions also shifts by 0.05Å in presence of C–H···F–C interactions. Therefore, it may be inferred that the C–H···O=C interactions are more influenced by the presence of C–H···F–C interactions than the reverse.

The most probable angle for C–H···F–C interactions is about 130°-140° followed by 150°-160° in some cases, and is not linear as concluded by Saha *et al*. and also, the most

probable distance at which the C–H···F–C interactions occur is 2.60Å-2.65Å which is higher than the sum of their Van der Waals radii (1.10 Å for H and 1.46 Å for F; as taken by G&LP). G & LP in 2016, stated that the interactions involving C–H···F–C disappear at a threshold of 95% of the sum of their Van der Waals radii, But we differ for the earlier reports and would like to emphasise that the most probable and the most occurring bond length for this particular interaction is higher than the sum of the Van der Waals radii of the individual atoms involved therein. This indicates that the C–H···F–C interaction is stable even at a distance higher than the sum of Van der Waals radii and therefore cannot be mere a result of Van der Waals attractions.

It is noteworthy that in our earlier computational analysis of weak C–H···F–C hydrogen bonds using simple molecular pairs like fluoroethene and ethene, difluoroethene and ethane, fluoroethene and fluoroethene etc, we have demonstrated that the stabilization energy offered by C–H···F–C hydrogen bonds can be as high as 6.6 kcal/mol, which is highly significant in stabilising crystal structures.[30] We have also carried out the computational calculations for complex molecules like tetrafluorinated tetrahydroisoquinoline derivatives and have seen that the C–H···F–C interactions can be as stabilizing as 13.9 kcal/mol.[133] In the past, Guru Row and co-workers have demonstrated experimentally that fluorine offers various types of weak interactions in crystal packing, both in the presence and in the absence of other stronger interactions. A large number of compounds containing C, N, O, F, and H have been structurally analysed and the propensity for the formation of C–H···F–C hydrogen bond has been shown to be significant compared to the C–H···O–C/ C–H···O=C hydrogen bonds. Through the current database analysis, we have demonstrated that F is equally good acceptor as O in an organic environment. Therefore, we believe that both C–H···F–C and C–H···O=C

interactions are stabilising in nature and both qualify as weak hydrogen bonds and the former seems to be more prominent and more probable than the later.

A.4 Conclusion

We believe that the long-lasting debate that organic fluorine does/doesn't participate in the formation of hydrogen bond needs a final conclusion. Over the years, a large number of research groups have demonstrated experimentally, theoretically and through database analysis that the C–F bond is never silent in any organic environment and produced amazing intermolecular architectures using various weak interactions and hydrogen bonds both in the presence and in the absence of other intermolecular interactions (stronger or weaker). Through our current database analysis, we have demonstrated that the small organic molecules containing C, H, F, O, N, S elements (a various combinations of these elements) display significant number and variety of C–H···F–C hydrogen bonds and have significant contribution for the formation of crystal lattices. The database analysis on these molecules has indicated that C–H···F–C hydrogen bonds occur more frequently than C–H···O=C hydrogen bonds and from the Hirshfeld analysis followed by the calculations, we have demonstrated that the propensity for C–H···F–C hydrogen bonds is nearly same to that of C–H···O=C hydrogen bonds representing the stabilising nature of both the interactions. C–H···F–C interactions in crystals are also energetically significant and offers appreciable stabilization of the lattice through a large number of C–H···F–C hydrogen bonds than expected. The role of both of these interactions is vital in crystal packing and cannot be ignored at all in any case and the influence that C–H···F–C hydrogen bonds have is more prominent than C–H···O=C hydrogen bonds. Therefore, we conclude with the statement that organic fluorine is a poor hydrogen bond acceptor is a myth not a fact.

References:

1. Armstrong, H. E., *Proc. Roy. Soc. London, A*, **1923**, *03*, 610.
2. Pauling, L. *The nature of chemical Bond*, Cornell University Press, Ithaca, New York, **1939.**
3. Pimentel, G.C. and McClellan, A.L., *The hydrogen Bond*, W.H. Freeman, San Francisco, **1960**.
4. Steiner, T. and Saenger, W. **1993**, *J. Am. Chem. Soc.*, 115, 4540-4547.
5. Arunan, E.; Desiraju, G. R.; Klein, R. A.; Sadlej, J.; Scheiner, S.; Alkorta, I.; Clary, D. C.; Crabtree, R. H.; Dannenberg, J. J.; Hobza, P.; Kjaergaard, H. G.; Legon, A. C.; Mennucci, B.; Nesbitt, D. J., *Definition of the hydrogen bond*, **2011**, *Pure Appl. Chem*., 83 (*8*), 1637-1641.
6. Desiraju, G. R.; Steiner, T. *The weak hydrogen bond in structural chemistry and biology*, oxford University Press: Oxford, **1999**.
7. Gu, Y.; Kar, T.; Scheiner, S. *J. mol. struct.*, **2000**, *552 (3)*, 17-31.
8. Mazik, M.; Blaster, D.; Boese, R. *Tetrahedron*, **2001**, *57(27)*, 5791-5797.
9. Brandl, M.; Meyer, M.; Suhnel, J. *J. Biomol. struct. dynamics*, **2001**, *18(4)*, 545-555.
10. Dunitz, J. D.; Taylor, R. *Chem-A Eur. jour.*, **1997**, *3(1)*, 89-98.
11. Thalladi, V. R.; Wiess, H. C.; Bläser, D.; Boese, R.; Nangia, A.; Desiraju, G. R.; *J. Am. Chem. Soc.*, **1998**, *120*, 8702-8710.
12. Murray-Rust, P.; Stallings, W. C.; Monti, C. T.; Preston, R. K.; Glusker, J. P. *J. Am. Chem. Soc.* **1983**, *105*, 3206-3214.
13. Heinz, D. W.; Baase, W. A.; Dahlquist, F. W.; Matthews, B. W. *Nature*, **1993**, *361*, 561-564.
14. Howard, J. A. K.; Hoy, V. J.; O'Hagan, D.; Smith, G. T. *Tetrahedron*, **1996**, *52*, 12613-12622.
15. Dunitz, J. D.; Taylor, R. *Chem. Eur. J.* **1997**, 3, 89-98.
16. Moran, S.; Ren, R. X. -F.; Rumney S. IV.; Kool, E. T. *J. Am. Chem. Soc.* **1997**, *119*, 2056-2057.
17. Evans, T. A.; Seddon, K. R. *Chem. Commun.* **1997**, *21*, 2023-2024.
18. Kim, H. W.; Rossi, P.; Shoemaker, R. K.; Dimangno, S. G. *J. Am. Chem. Soc.*, **1998**, *120*, 9082-9083.
19. Prasanna, M. D.; Guru Row, T. N. *Cryst. Eng.* **2000**, *2*, 134-140.

20. Prasanna, M. D.; Guru Row, T. N. *J. Mol. Struct.* **2001**, *559*, 255-261.
21. Prasanna, M. D.; Guru Row, T. N. *J. Mol. Struct.* **2001**, *562*, 55-61.
22. Allen, F. H. *Acta Cryst.* **2002**, *58*, 380-388.
23. Bruno, I. J.; Cole, J. C.; Edgington, P. R.; Kessler, M.; Macrae, C. F.; McCabe, P.; Pearson, J.; Taylor, R. *Acta Cryst.* **2002**, *58*, 389-397.
24. Saraogi, I; Vijay, V. G.; Das, S.; Sekar, K.; Guru Row, T. N. *Cryst. Eng.* **2003**, *6*, 69-77.
25. Dunitz, J. D. *ChemBioChem*, **2004**, *5*, 614-621.
26. Maienfisch, P.; Hall, R. G. *CHIMIA International journal of chemistry*, **2004**, *58*, 93-99.
27. Reichenbacher, K.; Suss, H. I.; Hulliger, J. *Chem. Soc. Rev*, **2005**, *34*, 22-30.
28. Charles, M.; Veesler, S.; Bonnete, F. *Acta Cryst.* **2006**, *62*, 1311-1318.
29. Chopra, D.; Guru Row, T. N.; *CrystEngComm*, **2011**, *13*, 2175-2186.
30. Dev, S.; Maheswari, S.; Choudhury, A. R. *RSC Adv.* **2015**, *5*, 26932-26940.
31. Kaur, G.; Choudhury, A. R. *CrystEngComm*, **2015**, 17, 2949-2963.
32. Rust, P. M.; Stalling, W. C.; Monti, C. T.; Preston, R. K.; Glusker, J. P. *J. Am. Chem. Soc.*, **1983**, *105*, 3206-3214.
33. Shimoni, L.; Glusker, J. P. *Struct. Chem.* **1994**, *5*, 383-397.
34. Dunitz, J. D.; Taylor, R. *Chem. Eur. J.* **1997,** 3, 89–98.
35. Boese, R. *Z. Kristallogr.* **2014**, *229(9)*, 595-601.
36. Choudhury, A. R.; Nagarajan, K.; Guru Row, T. N. *Acta Crystallogr. Sect. C* **2004**, 60, o219−o222.
37. Choudhury, A. R.; Urs, U. K.; Guru Row, T. N.; Nagarajan, K. *J. Mol. Struct.* **2002**, 605, 71–77.
38. Choudhury, A. R.; Guru Row, T. N. *Cryst. Growth Des.* **2004**, 4, 47–52.
39. Choudhury, A. R.; Nagarajan, K.; Guru Row, T. N. *Cryst. Eng.* **2003**, 6, 145-152.
40. Choudhury, A. R.; Guru Row, T. N. *CrystEngComm* **2006**, 8, 265–274.
41. Chopra, D.; Guru Row, T. N. *CrystEngComm* **2008**, 10, 54– 67.
42. Nayak, S. K.; Reddy, M. K.; Guru Row, T. N.; Chopra, D. *Cryst. Growth Des.* **2011**, 11, 1578–1596.
43. Nayak, S. K.; Reddy, M. K.; Guru Row, T. N.; Chopra, D. *CrystEngComm.* **2012**, 14, 200-210.
44. Panini, P.; Chopra, D. *CrystEngComm* **2012**, 14, 1972–1989.

45. Panini, P.; Chopra, D. *CrystEngComm*. **2013**, 15, 3711–3733.
46. Karanam, M.; Choudhury, A. R. *Cryst. Growth Des.* **2013**, 13, 4803– 4814.
47. Kaur, G.; Panini, P.; Chopra, D.; Choudhury, A. R. *Cryst. Groth Des*. **2012**, 12, 5096–5110.
48. Kaur, G.; Choudhury, A. R. *Cryst. Growth Des.* **2014**, 14, 1600–1616.
49. Kaur, G.; Choudhury, A. R. *CrystEngCom.* **2015**, 17, 2949–2963.
50. Kaur, G.; Singh, S.; Sreekumar, A.; Choudhury, A. R. *J. Mol. Struct*. **2016**, 1106, 154–169.
51. Nayak, S. K.; Kumar, V.; Murray, J. S.; Politzer, P.; Terraneo, G.; Pilati, T.; Metrangolo, P.; Resnati, G. *CrystEngComm*. **2017**, 19, 4955-4959.
52. Dunitz, J. D.; *ChemBioChem.* **2004**, *5*, 614-621.
53. Reichenbacher, K.; Suss, H. I.; Hulliger, J. *Chem. Soc. Rev.* **2005**, *34*, 22-30.
54. Murray, J. S.; Seybold, P. G.; Politzer, P. *J. Chem. Thermodyn.* **2021**, *156*, 106382-393.
55. Varadwaj, A.; Marques, H. M.; Varadwaj, P. R. *J. comput. chem.* **2019**, *40*, 1836-1860.
56. Cole, J. C.; Taylor, R. *Cryst. Growth Des.* **2022**, *22*, 1352-1364 and the references within.
57. O'Hagan, D.; Rzepa, H. S. *Chem. Commun.* **1997**, *7*, 645-652.
58. Smart, B. E. *J. Fluorine Chem.*, **2001**, *109*, 3-11.
59. Berger, R.; Resnati, G.; Metrangolo, P.; Weber, E.; Hullige, J. *Chem. Soc. Rev.* **2011**, *40*, 3496-3508 and references therein.
60. Desiraju, G. R. *Acc. Chem. Res*. **2002**, *35*, 565-573.
61. D'Oria, E.; Novoa, J. J. *CrystEngComm*. **2008**, *10*, 423-436.
62. Ramasubbu, N.; Parthasarathy, R.; Murray-Rust, P. *J. Am. Chem. Soc*. **1986**, *108*, 4308−4314.
63. Desiraju, G. R.; Partasarathy, R. *J. Am. Chem. Soc.* **1989**, 111, 8725−8726.
64. Hathwar, V. R.; Roopan, S. M.; Subashini, R.; Khan, F. N.; Guru Row, T. N. *J. Chem. Sci*. **2010**, 122, 677–685.
65. Schwarzer, A.; Seichter, W.; Weber, E.; Stoeckli-Evans, H.; Losada, M.; Hulliger, J. *CrystEngComm*, **2004**, 6, 567−572.
66. Schwarzer, A.; Weber, E. *Cryst. Growth Des*. **2008**, 8, 2862−2874.
67. Asensio, G.; Medio-Simon, M.; Alema´n, P.; Arellano, C. R. de. *Cryst. Growth Des*. **2006**, 6, 2769−2778.

68. Schwarzer, A.; Bombicz, P.; Weber, E. *J. Fluorine Chem*. **2010**, 131, 345−356.
69. Prasanna, M. D.; Guru Row, T. N. *Cryst. Eng*. **2000**, 3, 135−154.
70. Chopra, D.; Guru Row, T. N. *CrystEngComm.* **2011**, 13, 2175–2186.
71. Chopra, D. *Cryst. Growth Des.* **2012**, 12, 541–546.
72. Shukla, R.; Chopra, D. *CrystEngComm*. **2015**, 17, 3596–3609.
73. Koch, U.; Popelier, P. L. *J. Phys. Chem*. **1995**, 99, 9747-9754.
74. Thotadi, S.; Joseph, S.; Desiraju, G. R. *Cryst growth Des.* **2013**, 13, 3242-3254.
75. O'Hagan, D.; Rzepa, H. S. *Chem. Commun.* **1997**, *7*, 645-652.
76. Schlosser, M. *Angew. Chem. Int. Ed.*, **1998**, *110*, 1496-1513 and references therein.
77. https://www.ccdc.cam.ac.uk/solutions/csd-core/components/csd/
78. http://www.pdb.org/
79. http://ndbserver.rutgers.edu/
80. http://bmcd.ibbr.umd.edu/
81. http://www.crystallography.net/cod/
82. https://paulingfile.com/
83. https://www.icdd.com/
84. https://www.fiz-karlsruhe.de/en/produkte-und-dienstleistungen/inorganic-crystal-structure-database-icsd
85. Bruno, I. J.; Cole, J. C.; Edgington, P. R.; Kessler, M.; Maccrae, C. F.; McCabe, P.: Pearson, J.; Taylor, R. *Acta Cryst.* **2002**, *58*, 389-397.
86. Desiraju, G. R., *Angewandte Chemei*, **1995a**, *34*, 2311-2327.
87. Scheiner, S. *Hydrogen bonding: A theoretical perspective;* Oxford University press: Oxford, **1997**
88. Nobeli, I.; Price, S. L.; Lommerse, J. P. M.; Taylor, R., *J. Computational Chemistry*, **1997**, *18*, 2060-2074.
89. Schrödinger, E. *Phys. Rev.* **1926**, *28*, 1049-1070.
90. Rogers W. D., *Computational chemistry using pc*, John Wiley & Sons, Inc. : Canada, **2003**.
91. Funabashi, K.; Magee, J. L. *J. Chem. Phys.*, **1957**, *26*, 390-407.
92. Raghavachari, K.; Anderson, J. B. *J. Phys. Chem.* **1996**, *100*, 12960-12973.
93. Møller, C.; Plesset, M. S. *Phys. Rev.* **1934**, *46*, 618-622.

94. (a) Pople, J. A.; Binkley, J. S.; Seeger, R. *Int. J. Quantum Chem. Suppl. Y-10*, **1976**, 1-19. (b) Pople, J. A.; Seeger, R.; Krishnan, R.; *Int. J. Quantum Chem. Suppl. Y-11*, **1977**, 149-63.
95. Raghavachari, K.; Pople, J. J. *Int. J. Quantum Chem*. **1978**, *14*, 91-100.
96. Raghavachari, K.; Pople, J. J., Replogle, E. S., Gordon, M. H. *J. Phys. Chem.* **1990**, *94*, 5579-86.
97. Almlof, J.; Helgaker, T.; Taylor, P. R. *J. Phys. Chem.* **1988**, *92*, 3029-3033.
98. Bader, R. F. W. *Atoms in molecules: A Quantum Theory*; Clarendon Press: Oxford, 1990.
99. Bader, R. F. W. *Chem. Rev*. **1991**, *91*, 893-928.
100. Spackman, M. A.korti *Chem. Rev.* **1992**, *92*, 1769-1797.
101. Zhurov, V. V.; Zhurova, E. A.; Pinkerton, A. A. *J. Appl. Cryst.* **2008**, *41*, 340-349.
102. Pinkerton, A. A. *Acta Cryst.* **2021,** *A77*, 83-84.
103. Zuo, J. M.; Kim, M.; O'Keefee, M.; Spence, J. C. H. *Nature*, **1999**, *401*, 49-52.
104. Coppens, P. *X-ray charge densities and chemical bonding*,Oxford university press: Oxford, UK, **1997.**
105. Coppens, P.; Guru Row, T. N.; Leung, P.; Stevens, E. D.; Becker, P. J.; Yang, Y. W. *Acta Crystallogr.* **1979**, *A35*, 63-72.
106. Volkov, A.; Macchi, P.; Farrugia, L. J.; Gatti, C.; Mallinson, P.; Richter, T.; Koritsanszky, T. **2006**.
107. Hansen, N. K.; Coppens, P. *Acta Cryst.* **1978**, *A34*, 909-921.
108. Berski, S.; Lundell, J.; Latajka, Z.; Leszczynski, J. *J. Phys. Chem. A*, **1998**, *102(52)*, 10768-10776.
109. Pauling, L. *J. Am. Chem. Soc.* **1931**, *53* (4), 1367–1400.
110. Vasylyeva, V.; Shishkin, O. V.; Maleev, A. V.; Merz, K. *Cryst. Growth Des.* **2012**, *12* (2), 1032–1039.
111. Merz, K.; Evers, M. V.; Uhl, F.; Zubatyuk, R. I.; Shishkin, O. V. *Cryst. Growth Des.* **2014**, *14* (6), 3124–3130.
112. Yadav, H. R.; Choudhury, A. R. *J. Mol. Struct.* **2017**, *1150*, 469–480.
113. Choudhury, A. R.; Nagarajan, K.; Row, T. N. G. *Crystal engineering*, **2003**, *6*, 43-55.
114. Hassel, O.; Romming, C. *Quart. Rev. Chem. Soc*. **1962**, 16, 1−18.
115. Politzer, P.; Lane, P.; Concha, M. C.; Ma, Y.; Murray, J. S. *J. Mol. Model*. **2007**, *13*, 305–311.

116. Clark, T.; Hennemann, M.; Murray, J. S.; Politzer, P. *J. Mol. Model*. **2007**, 13, 291–296.

117. Herlitzke, B. J.; Ojala, W. H. Abstracts of Papers, *247th ACS National Meeting & Exposition*, Dallas, TX, United States, March 16−20, **2014**, CHED−1113.

118. Bertolotti, F.; Cavallo, G.; Metrangolo, P.; Nayak, S. K.; Resnati, G.; Terraneo, G. *Supramolecular chemistry*. **2013**, *25*, 718-727.

119. Cheng, N.; Yan, Q.; Liu, S.; Zhao, D. *CrystEngComm*, **2014**, *16(20)*, 4265-4273.

120. Boultif, A.; Louer, D. *J. Appl. Cryst.* **2004,** *37*, 724-731.

121. Macrae, C. F.; Bruno, I. J.; Chisholm, J. A.; Edgington, P. R.; McCabe, P.; Pidcock, E.; Rodriguez-Monge, L.; Taylor, R.; Streek, J.; Wood, P. A *J. Appl. Crystallogr*. **2008**, *41*, 466–470.

122. CrysAlisPRO, Oxford Diffraction, Agilent Technologies UK Ltd, Yarnton, England.

123. Dolomanov, O.V.; Bourhis, L.J.; Gildea, R. J.; Howard, J. A. K.; Puschmann, H. *J. Appl. Cryst*. **2009**, *42*, 339-341.

124. Sheldrick, G.M.; *Acta Cryst.* **2008**, *A64*, 112-122.

125. Sheldrick, G.M.; *Acta Cryst*. **2015**. *A71*, 3-8.

126. Sheldrick, G.M.; *Acta Cryst*. **2014**. C*71*, 3-8.

127. Nardelli, M. *J. Appl. Crystallogr*. **1995**, *28*, 569.

128. Spek, A. L. *Acta Crystallogr.* **2009**, *D65*, 148–155.

129. *Gaussian 09, Revision E.01*, Frisch, M. J., Trucks, G. W., Schlegel, H. B., Scuseria, G. E., Robb, M. A., Cheeseman, J. R., Scalmani, G., Barone, V., Mennucci, B., Petersson, G. A., Nakatsuji, H., Caricato, M., Li, X., Hratchian, H. P., Izmaylov, A. F., Bloino, J., Zheng, G., Sonnenberg, J. L., Hada, M., Ehara, M., Toyota, K., Fukuda, R., Hasegawa, J., Ishida, M., Nakajima, T., Honda, Y., Kitao, O., Nakai, H., Vreven, T., Montgomery, J. A. Jr., Peralta, J. E., Ogliaro, F., Bearpark, M., Heyd, J. J., Brothers, E., Kudin, K. N., Staroverov, V. N., Kobayashi, R., Normand, J., Raghavachari, K., Rendell, A., Burant, J. C., Iyengar, S. S., Tomasi, J., Cossi, M., Rega, N., Millam, J. M., Klene, M., Knox, J. E., Cross, J. B., Bakken, V., Adamo, C., Jaramillo, J., Gomperts, R., Stratmann, R. E., Yazyev, O., Austin, A. J., Cammi, R., Pomelli, C., Ochterski, J. W., Martin, R. L., Morokuma, K.,

Zakrzewski, V. G., Voth, G. A., Salvador, P., Dannenberg, J. J., Dapprich, S., Daniels, A. D., Farkas, Ö., Foresman, J. B., Ortiz, J. V., Cioslowski, J., Fox, D. J. Gaussian, Inc., Wallingford CT, **2009**.

130. *GaussView, Version 5*, Dennington, R., Keith, T. A., Millam, J. M. Semichem Inc., Shawnee Mission, KS, **2016**.
131. Yadav, H. R. and Choudhury, A. R. *J. Mol. Struct.* **2017**, *1150*, 469-480.
132. Yadav, H. R. Understanding the influence of fluorine in crystal packing of organic molecules in the presence and in the absence of other strong/weak hydrogen bonds: A structural analysis, **2017**, Doctoral Thesis, IISER Mohali.
133. Nagarajan, K., Talwalker, P. K., Kulkarni, C. L. *Ind. J. Chem.* **1985**, *24B*, 83−97.
134. Biegler-König, F., Schönbohmand J., Bayles, D. *J. Comput. Chem.* **2001**, *22*, 545–559.
135. Singla, L.; Yadav, H. R.; Choudhury, A. R. *Acta Cryst*, **2020**, *B76*, 604-617.
136. Hirshfeld, F. L. *Crystallogr. Rev.* **1991**, *2(4)*, 169-200.
137. Spackman, M. A.; Brown, A. S. *Annu. Rep. Prog. Chem., Sect. C phys. Chem.* **1994,** *91*, 175-212.
138. Spackman, M. A. *Annu. Rep. Prog. Chem., Sect. C phys. Chem.* **1998**, *94*, 177-207.
139. Koritsanszky, T. S.; Coppens, P. *Chem. Rev.* **2001**, 101 (6), 1583–1627.
140. Low, A. A.; Kunze, K. L.; MacDougall, P. J.; Hall, M. B. *Inorg. Chem.* **1991**, *30(5)*, 1079-1086.
141. Espinosa, E.; Molins, E. *J. Chem. Phys.* **2000**, *113*, 5686.
142. Munshi, P.; Row, T. N. G. *J. Phys. Chem. A* **2005**, *109(4)*, 659-672.
143. Munshi, P.; Guru Row, T. N. *Crystallogr. Rev.* **2005**, *11 (3)*, 199–241.
144. Park, H.; Yoon, J.; Seok, C. *J. Phys. Chem. B* **2008**, *112 (3)*, 1041–1048.
145. Munshi, P.; Jelsch, C.; Hathwar, V. R.; Guru Row, T. N. *Cryst. Growth Des.* **2010**, *10 (4)*, 1516–1526.
146. Hathwar, V. R.; Gonnade, R. G.; Munshi, P.; Bhadbhade, M. M.; Row, T. N. G. *Cryst. Growth Des.* **2011**, *11 (5)*, 1855–1862.
147. Thomas, S. P.; Pavan, M. S.; Guru Row, T. N. *Cryst. Growth Des.* **2012**, *12 (12)*, 6083–6091.

148. Pavan, M. S.; Pal, R.; Nagarajan, K.; Guru Row, T. N. *Cryst. Growth Des.* **2014**, *14 (11)*, 5477–5485.

149. Hathwar, V. R.; Chopra, D.; Panini, P.; Guru Row, T. N. *Cryst. Growth Des.* **2014**, *14* (11), 5366–5369.

150. Chopra, D.; Cameron, T. S.; Ferrara, J. D.; Guru Row, T. N. *J. Phys. Chem. A* **2006**, *110 (35)*, 10465–10477.

151. Singla, L.; Yadav, H. R.; Choudhury, A. R. *Cryst. Growth Des.* **2022**, *22 (3)*, 1604–1622.

152. Sheldrick, G. M. *Acta Crystallogr. Sect. C Struct. Chem.* **2015**.

153. Blessing, R. H. *Acta Cryst*.**1995**, *A51*, 33-38.

154. Farrugia, L. J. WinGX. *J. Appl. Cryst* **2012**, *45*, 849-854.

155. Madsen, A. Ø. *J. Appl. Crystallogr.* **2006**, *39*, 757-758.

156. Mallinson, P. R.; Koritsanszky, T.; Elkaim, E.; Li, N.; Coppens, P. *Acta Cryst*.**1988**, *A44*, 336-343.

157. Zhurov, V. V.; Zhurova, E. A.; Pinkerton, A. A. *J. Appl. Crystallogr.* **2008**, *41*, 340-349.

158. Zavodnik, V.; Stash, A.; Tsirelson, V.; De Vries, R.; Feil, D. *Acta Cryst.* **1999**, *B55*, 45-54.

159. Guillot, B.; Viry, L.; Guillot, R.; Lecomte, C.; Jelsch, C. *J. Appl. Crystallogr.* **2001**, *34* (2), 214–223.

160. Krawczuk, A.; Macchi, P. *Chemistry Central Journal*, **2014**, *8 (68)*, 1-15.

161. Pavan, M. S.; Prasad, K. D.; Row, T. N. G. *ChemComm.* **2013**, *49*, 7558-7560.

162. Hathwar, V. R. and Row, T. N. G. *Cryst. Growth Des.* **2011**, *11*, 1338-1346.

163. Murray-Rust, P.; Glusker, J. P. *J. Am. Chem. Soc.* **1984**, *106* (4), 1018–1025.

164. Shimoni, L.; Carrell, H. L.; Glusker, J. P.; Coombs, M. M. *J. Am. Chem. Soc.* **1994**, *116* (18), 8162–8168.

165. Desiraju, G. R. *Acc. Chem. Res.* **1991**, *24* (10), 290–296.

166. Desiraju, G. R. *Acc. Chem. Res.*, **1996**, *29* (9), 441–449.

167. Steiner, T. *Crystallogr. Rev.* **1996**, *6* (1), 1–51.

168. Desiraju, G. R. *Chem. Commun.* **1997**, *0* (16), 1475–1482.

169. Thakur, T. S.; Kirchner, M. T.; Bläser, D.; Boese, R.; Desiraju, G. R. *CrystEngComm* **2010**, *12* (7), 2079.

170. Dalvit, C.; Invernizzi, C.; Vulpetti, A.. *Chem. - A Eur. J.* **2014**, *20* (35), 11058–11068.

171. Gavezzotti, A.; Presti, L. Lo. *Cryst. Growth Des.* **2016**, *16* (5), 2952–2962.

172. Taylor, R. *Cryst. Growth Des.*, **2016**, *16* (8), 4165–4168.

173. Saha, B. K.; Saha, A.; Sharada, D.; Rather, S. A. *Cryst. Growth Des.* **2018**, *18* (1), 1–6.

174. Turner, M.J.; Mckinnon, J.J.; Wolff, S.K.; Grinwood, D.J.; Spackman, P.R.; Jayatilaka, D.; Spackman, M.A. *CrystalExplorer17;* University of Western Australia, **2017**.

Supporting Information:

The supporting information for the work presented in this thesis is available in the DVD attached at the end of the thesis.

Publications from Thesis

1. **Singla, L.**, Yadav, H. R. Choudhury, A. R. Evaluation of fluorine mediated intermolecular interactions in tetra fluoro tetra hydro isoquinoline derivatives: synthesis and computational studies, *Acta cryst*, **2020**, *B76*, 604-617.
2. **Singla, L.**, Yadav, H. R. Choudhury, A. R. Structural and Computational Analysis of Organic Fluorine-Mediated Interactions in Controlling the Crystal Packing of Tetrafluorinated Secondary Amides in the Presence of Weak C–H···O═C Hydrogen Bonds, *Cryst. Growth Des.* **2022**, *22*(3), 1604-1622.
3. **Singla, L.**, Kumar, A.; Robertson, C. M., Munshi, P. Choudhury, A. R. Understanding of C–F···F–C interactions using experimental charge density analysis. *Cryst. Growth Des.,* **2022** (*Just Accepted*)
4. **Singla, L.**, Yadav, M. K., Choudhury, A. R. The influence of fluorine mediated interactions on the strong hydrogen bonds in a series of "bridge flipped" N,N'-(1,4-phenylene)dibenzamides and N,N'-diphenyldibenzamides. *Cryst. Growth Des.* (*Manuscript Submitted*)
5. **Singla, L.**; Choudhury, A. R. Statistical insight on weak hydrogen bonds involving C=O and C–F groups as hydrogen bond acceptor: A comprehensive database analysis (*manuscript under preparation*)

Other Publications

1. Das, D.; Yadav, M. K.; **Singla, L.**; Kumar, A.; Karanam, M.; Dev, S.; Choudhury, A. R. Understanding of the kinetic stability of cis-isomer of azobenzenes through kinetic and computational studies, *Chemistry Select*, **2020**, *44*(5), 13957-13962.
2. Chauhan, R. S.; Nigam, S.; Ansri, S.; Tyagi, A.; **Singla, L.**; Choudhury, A. R.; Prajapat, C. L. An interesting heterometallic complex [{Ni2(κ2 -SeC5H4N)2(μ-OCH3)CdCl}2] as single source molecular precursor for NiSe/CdSe heterostructure: Consequence of similar Ni-Se and Cd-Se bond distances. *J. Organomet. Chem.* **2021**, *949*, 121955.
3. Thekkeppat, N. P.; **Singla, L.**; Tothadi, S.; Das, P.; Choudhury, A. R.; Ghosh, S. Structureproperty correlation of halogen substituted benzothiazole crystals. *J. Mol. Struct*. **2021**, *1243*, 130765.

4. Mudi, P. K.; **Singla, L.**; Chamuah, A.; Bhattacharya, S.; Choudhury, A. R.; Biswas, B. Schiff base driven denticity-fluctuated structural assortment of zinc-pseudohalide complexes: synthesis, structures and electrical transport properties. *CrystEngComm*. **2022**, *24*, 2418-2428.
5. Kundu, S.; Saha, S.; Das, A.; **Singla, L.**; Choudhury, A. R.; Biswas, B. Methyl group: A potential building block for edge- to-face interlocking of benzimidazole scaffolds in developing blue light emitting molecular aggregates. *J. Mol. Liquids*, **2022**, *347*, 118340.
6. Rani, D.; Singh, A.; Ladhi, R.; **Singla, L.**; Choudhury, A. R.; Bhasin, K. K., Bera, C. Singh, M. Nanochannel mediated electrical and photoconductivity of metal organic nantubes. *ACS sustainable Chem. Engg.* **2022**, *10*(21), 6981-6987.
7. Moorthy, H.; Yadav, M.; Mavileti, S. K.; Tamang, N.; **Singla, L.**; Choudhury, A. R.; Sahal, D.; Rao, N. G. Anti-plasmodial and anti-malarial activity of 3,5-diaryldenetetrahydro—Hpyran-4(3H)-ones via inhibition of PfPyridoxal synthase. *ChemMedChem*, **2022**, e202200411.
8. Singh, S.; Navale, G. Agarwal, S.; Singh, H.; **Singla, L.**; Sarkar, D.; Sarma, M.; Choudhury, A. R.; Ghosh, K. Design and synthesis of ruthenium complexes and their studies on the inhibition of the amyloid β (1-42) peptide aggregation, *Inorg. Chem.*, **2022** (Manuscript Under Review)
9. Sarma, B.; Ranjan, R.; Chauhan, N.; **Singla, L.**; Mukhopadhyay, S.; Choudhury, A. R.; Vyas, K. Highly Active Primary Amine Ligated Ru(II)-Arene Complexes as Selective Catalysts for Solvent-Free N-alkylation of Amines, *Appl. Organomet. Chem.*, 2022 (*Manuscript under review)*
10. Singh, S.; Navale, G. R.; Agrawal, S.; Singh, H. K.; Singla, L.; Sarkar, D.; Sarma, M.; Choudhury, A. R.; Ghosh, K. Design and synthesis of piano-stool ruthenium(II) complexes and their studies on the inhibition of amyloid β (1-42) peptide aggregation, *Int. J. Bio. Macromol.* **2022** (*Manuscript under review).*